The Role of the Transcription Factor Foxn1 in Thymus Organogenesis and Maintenance

Inauguraldissertation

zur
Erlangung der Würde eines Doktors der Philosophie
vorgelegt der
Philosophisch-Naturwissenschaftliche Fakultät
der Universität Basel

von

Angela Jeanne Tamara Bosch
aus Mammern TG

Basel, 2014

Genehmigt von der Philosophisch-Naturwissenschaftlichen Fakultät

auf Antrag von

Prof. Dr. Georg A. Holländer
Dissertationsleiter und Fakultätsverantwortlicher

Prof. Dr. Antonius G. Rolink
Korreferent

Prof. Dr. Giulio C. Spagnoli
Korreferent

Basel, den 20. 5. 2014

Prof. Dr. Jörg Schibler
Dekan der Philosophisch-Naturwissenschaftlichen Faktultät

Summary

The thymus is the primary lymphoid organ responsible for T-cell development and selection, which requires a specialised stromal microenvironment. The thymic stroma consists mainly of thymic epithelial cells (TEC), which can be divided into cortical (c) and medullary (m) TECs, mediating each different functions during T-cell development. The organisation of the thymus compartments is crucial for T-cell development. Therefore it is important to understand the mechanisms behind thymus development as defects in thymus function can lead to immunodeficiency or autoimmunity.

In the context of thymus organogenesis, Foxn1 serves as a master transcription factor essential for TEC development. The loss of Foxn1 constitutes then a molecular cause for athymia as the molecules absence blocks TEC growth and differentiation. Consequently the epithelial cells adapt another cell fate and the thymus rudiment fails to attract lymphoid precursors.

Mice with either a reduced or time restricted Foxn1 expression at the onset of thymus organogenesis displayed a severely disturbed thymus development. Though able to develop into cTEC and mTEC, they remain in an immature state as demonstrated by the absence of mature TEC. Similar as in congenital athymic nude mice, devoid of Foxn1 expression, also common bipotent progenitor TEC were detected. T-cell development was impaired resulting consequently in severe peripheral lymphopenia, which only slightly mitigated with progressive age. Importantly the peripheral T-cells in both mouse models differ from that of nude mice, in that cells with effector and regulatory functions were detected. Furthermore inadequate Foxn1 expression lead to colitis and early death. Bowel inflammation was associated with an increase in Th1 polarised $CD4^+$ T-cells among intraepithelial and lamina propria lymphocytes.

In aggregate this study showed that TEC differentiation and maintenance depends on both a continuous and adequate Foxn1 expression, as short-term or low level Foxn1 expression were insufficient to sustain regular thymus development and function. Inadequate expression of Foxn1 expression resulted consequently in the loss/absence of a regular thymus microenvironment and selection of an autoreactive T-cell repertoire causing auto-immune colitis.

1. Introduction

The thymus is a bilobed organ located anterior to the heart. Although the thymus was already known for centuries[1], its function remained elusive until 1961 when J.F.A.P Miller discovered its contribution to the immune system[2]. Mice that were thymectomised 1-16 hours after birth had underdeveloped lymphoid tissues, the lymph nodes and spleen showed a deficiency of germinal centres and only few plasma cells were detected. Furthermore these mice were more susceptible to infections, however the mortality was reduced when the mice were kept under pathogen-free conditions. By transferring genetically marked cells into thymectomised mice it was finally shown that the antibody-producing cells (B-cells) were derived from the bone marrow whereas thymus derived cells were essential to allow B-cells to respond to antigens[3,4]. The thymus is the primary lymphoid organ responsible for T-cell development, which is critically dependant on thymic stromal cells. The thymic stroma mainly consists of thymic epithelial cells (TEC) which form a three dimensional meshwork where TEC and developing T-cells interact[5,6]. The size of the thymus decreases after puberty, a process called thymic involution[7]. Although the thymic stroma is indispensable for T-cell development, it accounts for less than 1% of the thymic cellularity in the postnatal thymus. The majority of the remaining cells are of hematopoietic origin and consist mainly of thymocytes and to a lesser extent of phagocytic macrophages and antigen-presenting dendritic cells (DC)[7].

1.1. Thymus organogenesis

Thymus development is closely linked to that of the parathyroid. Both organs emerge from a bilaterally positioned organ primordium that arises from the third pharyngeal pouch endoderm[8]. Thymus organogenesis initiates at embryonic day (E) 9.5 with the formation of the pharyngeal pouches and the consequent development of a thymus primordium. At E10.5 a visible thymus-parathyroid anlage is created by the interaction of epithelial cells of the third pharyngeal pouch endoderm and mesenchymal cells[9].

An early descriptive study based on morphological analyses suggested that endodermal and ectodermal germ layers of the third pharyngeal pouch interact at E9.5 with each other to form this primordium[10]. This claim lead to the dual-origin model, proposing that the thymic stroma is derived from both endodermal and ectodermal layers, and that the endodermal layer would

give rise to medullary TEC whereas contributions of the ectodermal layer differentiates into cortical thymic epithelial cells. In parallel N. M. Le Douarin and F. V. Jotereau[11] demonstrated with chick-quail chimeras that the thymus evolves only from the endoderm. This conclusion was drawn from experiments in which pharyngeal endoderm was isolated from quail embryos and transplanted into the body cavity of 3 days old chick-embryos. Using two different species enabled them to distinguish the origin of the cells. The grafted tissue developed into a thymus, the developing T-cells however where of chick origin. The stroma cells inside the graft were shown to be of quail origin, indicating that both cortex and medulla developed from the grafted endoderm. Nevertheless, there was a long standing debate on the contribution of endoderm and ectoderm to the formation of the thymus medulla and cortex[12]. Textbooks favoured to dual-origin model, since the experiments were conducted in mice, whereas the single origin model was derived from an avian model. This debate persisted until Gordon et al. confirmed in 2004 the single origin theory in a mammalian model[13]. They demonstrated the direct contact of the third pharyngeal pouch endoderm and the third pharyngeal cleft ectoderm. However labelling cells form the third pharyngeal ectoderm showed no contribution of ectoderm to the thymus primordium. Transplantation exclusively of E8.5-E9 pharyngeal endoderm under the kidney capsule of athymic mice (also known as nude mice) showed that a functional thymus was generated, including cortical and medullary areas mediating normal T-cell development. To rule out a contribution of the ectoderm, the endoderm was isolated at a developmental stage (E8.5-E9) before the interaction with the ectoderm takes place. Two recent studies using human embryonic stem cells (hESCs) underline the single endodermal origin of the thymus. hESCs were differentiated first into endoderm, then into anterior foregut endoderm, followed by differentiation into ventral pharyngeal endoderm and finally into thymic epithelial progenitor cells (TEPC). The TEPC were transplanted into a nude mice where they were shown to mature into thymic epithelium able to support T-cell development[14,15].

Thymus organogenesis can be divided into distinct steps (Figure 1.1). It starts at E9.5 with the positioning of the pouches a process dependent on several transcription factors. The transcription factors paired box gene 1 (Pax1), paired box gene 9 (Pax9), T-box1 (Tbx1) and eye absent homolog (Eya1) as well as fibroblast growth factor 8 (FGF8) are involved in the early pouch formation. In mice deficient for Pax9 or Fgf8 the thymus is severely reduced in size and develops ectopically[16,17]. The deficiency of Pax1 leads to a hypoplastic thymus with

a reduced frequency of CD4 and CD8 double positive thymocytes[18]. Eya1 was shown to be upstream of Pax1, Tbx1 and Fgf8, as the development of the thymus/parathyroid organ primordia failed in Eya1 deficient mice[19,20]. The homeobox protein a3 (Hoxa3) defines the axial identity of the pouch and is involved together with sine oculis homolog 1/4 (Six1/4) and Pax9 in the initial organ formation and patterning. Hoxa3 and Six1/4 deficient mice are athymic and lack the parathyroid[20,21].

At E11 the outgrowth of the rudiment and patterning begins. At this stage the expression of the transcription factor glial cells missing homologue 2 (Gcm2) is initiated[22]. Shortly after, Foxn1 expression initiates the patterning in two distinct organs. The dorsal part of the primordium expresses Gcm2 and gives rise to the parathyroid[23], whereas the ventral part expresses Foxn1 and gives rise to the thymus[24]. So far it remains elusive what specifies the initial organ fate, Gcm2 and Foxn1 seem to be required only for organ-specific differentiation. In the absence of Foxn1 or Gcm2 the 3rd pharyngeal pouches and later also prospective thymus and parathyroid specific poles are formed but further development is hindered and consequently the organs remain in an early progenitor stage. In the absence of Foxn1 a thymus primordium is formed, but TEC fail to differentiate into cortical and medullary subsets, remain in an early progenitor stage and fail to attract lymphoid precursors[25–27]. As a consequence the three dimensional organisation of the thymus is absent and the thymus degrades into cysts[5,28]. Thus, early thymus development is Foxn1 independent but after organ initiation Foxn1 is required for organ maturation.

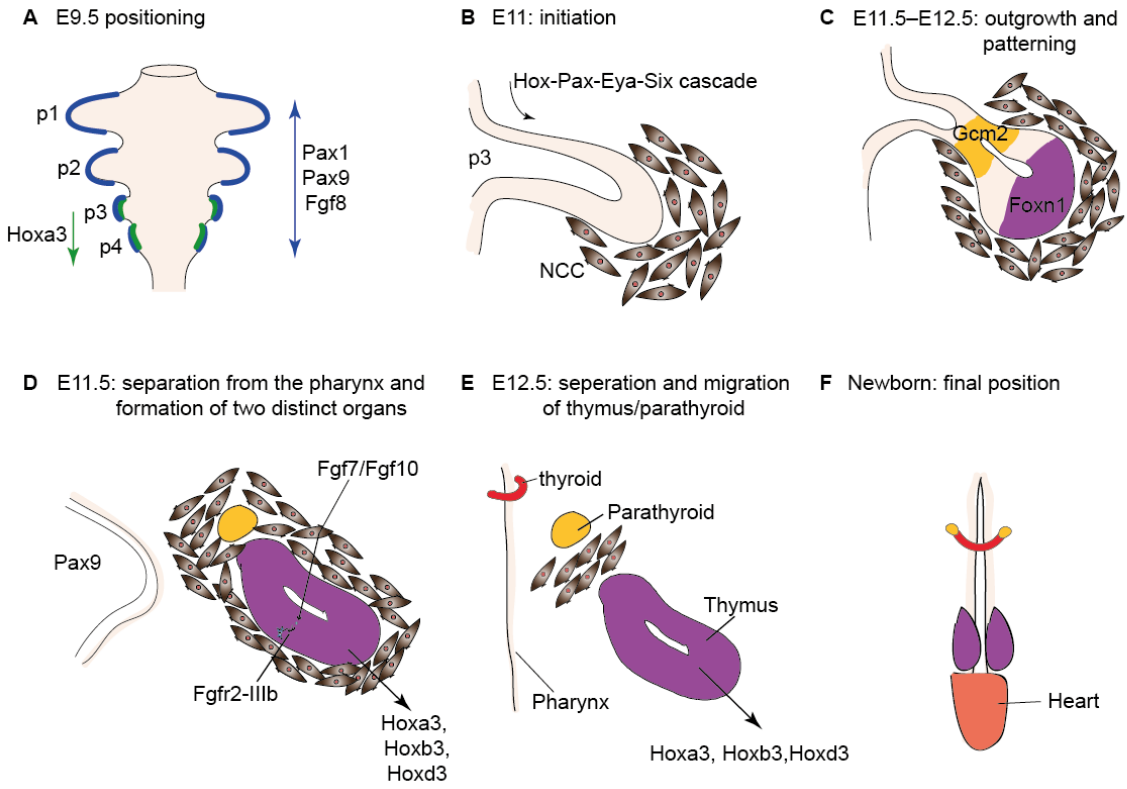

Figure 1.1: Thymus organogenesis. (A) Positioning of the pharyngeal pouches starts at E9.5 and requires expression of Pax1, Pax9 and Fgf8. Expression of Hoxa3 defines the axial identity of the for 3rd pharyngeal pouch. (B) Initiation and rudiment outgrowth begins at E11 and is dependant on the Hox-Pax-Eya-Six cascade. The pouch is surrounded by neural crest cells (NCC), which support development. (C) Between E11.5 and E12.5 the rudiment outgrowth and patterning into parathyroid domain (dependant on Gcm2) and thymus domain (Foxn1 dependant) occurs. (D) At E12 the shared primordium separates from the pharynx and contains two distinct areas. The separation from the pharynx is mediated by apoptotic cell death and requires Pax9. The migration of the shared primordium is controlled by neural crest cells, and is dependant on Hox3 genes. The NCC support TEC differentiation and proliferation by secretion of Fgf7 and Fgf10. (E) At E13.5 the shared primordium is separated in two distinct organs. NCC cells separate the thymus from the parathyroid as they form a wedge between the organs. (F) From E13.5 until birth the thymus and parathyroid migrate to its final position above the heart and beside the thyroid, mediated by NCC. Adapted from Blackburn and Manley 2004[29] and Gordon and Manley 2011[12].

After patterning into two different domains the common primordium detaches from the pharynx by apoptotic cell death[13]. The precise mechanisms controlling this apoptosis mediated detachment are still elusive, however mouse models with absent separation from the pharynx revealed a possible role for neural crest cells (NCC) in this process[30,31]. In Splotch (Pax3) deficient mice the thymus remains attached to the pharynx, these mice display a severe loss of NCC, indicating that the absence of NCC hinders the separation of the thymus from

the pharynx[31]. Between E12.0 and E12.5 the parathyroid and the thymus separate thus forming two distinct organs. This separation process is so far not fully understood. Histological analyses showed that neural crest-derived mesenchymal cells move between the border of the two poles of the shared primordium and help to push them apart[32]. A similar mechanism was described to take place during somitogenesis[33]. A possible role for the mesenchyme in this process is further supported by the finding that mutant mice with NCC specific deficiencies show a disturbed segregation into thymus and parathyroid. Ephrin B2 is required for normal migration of NCC derived mesenchyme and consequently, mice with NCC deficient for ephrin B2 show a delayed segregation of thymus and parathyroid[34]. Pax 3 deficiency lead to a disturbed boundary between thymus and parathyroid domain, identifying a role for NCC cells in the separation of the two organs[31].

With ongoing development the two-dimensional epithelial bilayer converts to a clustered organisation (E12) and finally TEC form a three dimensional meshwork by E13.5[26]. After the separation into parathyroid and thymus at E12.5 the thymus migrates to its final anatomical position above the heart. The mechanisms controlling thymus migration are not fully understood. However there is evidence that migration of the thymus is supported by neural crest-derived mesenchyme. NCC are a migratory population, therefore it is feasible that they pull the thymic lobes to their final position. The separation of the rudiment from the pharynx occurs normally in mice with a NCC specific deletion of ephrin B2, however the thymus does not migrate and is ectopically located in the cervical region. The deletion of ephrin B2 specific in NCC resulted in a reduced motility of NCC, indicating a NCC specific role of ephrin B2 signalling in thymus migration[34]. However, it is still elusive how thymus migration is controlled and which directional clues it follows. It was shown that thyroid migration is dependant on the pharyngeal blood vessels[35]. In hedgehog deficient mice the blood vessels are ectopically positioned, and the thyroid tissue is always located next to this ectopic pharyngeal blood vessel. Furthermore in zebra fish it was shown that ectopic vascular cells are able to redirect thyroid migration[35]. Due to the close proximity of the carotid arteries during migration of the thymus it is feasible that thymus migration is linked to the presence of carotid blood vessels.

1.1.1. Mesenchymal contribution to thymus organogenesis

In addition to the epithelial cells of the third pharyngeal pouch neural crest and mesodermal derived mesenchyme contribute to the formation of a regular thymus. Epithelial-mesenchymal interactions are crucial for the formation of many different organs. The thymus primordium is surrounded by a mesenchymal capsule derived from neural crest cells. Interactions of neural-crest derived mesenchyme and thymic epithelial cells are important for thymus formation, as removal of the mesenchymal capsule showed that the epithelial primordium did not develop into an organ on its own[36]. This is further supported by the absence of a thymus or a reduced thymus size after experimental removal of the pharyngeal NCC in chick embryos[37]. In contrast to these findings, transplantation of pharyngeal endoderm under the kidney capsule of nude mice results in a functional thymus consisting of cTEC and mTEC, thus indicating that the initial organ formation is independent of NCC, since the endoderm was removed before NCC migration takes place[13]. However it cannot be excluded that mesenchymal cells at the transplantation site contribute to organ formation. Further evidence for an NCC independent initial organ pattern is obtained from Pax3 deficient mice. Despite a severe NCC deficiency in these mice, a thymus is present, however the boundary between thymus and parathyroid is disrupted and the organ fails to migrate to its anatomical position, indicating that NCC are dispensable for initial organ patterning, but not for organ migration[31].

The mesenchyme supports TEC proliferation and differentiation via secretion of fibroblast growth factors 7 and 10 (Fgf7, Fgf10), which signal to the Fgfr2IIIb receptor on TEC[38–40]. Evidence for the importance of this signalling pathway came from Fgfr2IIIb deficient mice, in which the outgrowth of the thymic rudiment is arrested after E12.5. A specific role for PDGFR-α^+ mesenchymal cells in regulating TEC development via production of insulin-like growth factor 1 and 2 was demonstrated by grafting fetal thymus devoid of PDGFR-α^+ mesenchyme, the thymus did differentiate however it was reduced in size[41]. NCC derived mesenchyme was shown to contribute to the thymus vascularisation. When Foxn1$^+$ ES cells devoid of vascular endothelial growth factor (VEGF) expression were injected into blastocysts derived from nude mice, the mesenchyme partly restored thymus vasculature, although the branching pattern was altered[42]. By linage tracing experiments these VEGF producing mesenchymal cells were identified as NCC derived[43]. The contribution of neural-crest cell derived mesenchyme to the thymus was believed to decrease once the vasculature is established and epithelial cells support T-cell development[44,45]. However newer studies, in

which NCC were genetically labelled, showed that NCC cells are still contributing to the adult thymus. NCC derived cells were shown to differentiate into pericytes and smooth muscle cells both involved in forming a supportive network for thymic blood vessels[46]. Recently retinoic acid (RA) generated by the thymic mesenchyme was identified as a negative regulator of TEC expansion. Upon adding of a RA antagonist to fetal thymic organ cultures (FTOC) an increase in TEC numbers in particular in cTEC was observed. RA generating mesenchymal cells were also identified in the adult thymus, indicating a role for RA in postnatal TEC homeostasis[47].

1.1.2. Immigration of lymphoid progenitors

The earliest lymphoid progenitor cells arrive at the thymus primordium as early as E11.5[48]. The attraction of the lymphoid progenitor cells is controlled by the expression of the chemokines CCL21 and CCL25[49]. At this early stage of development the thymus does not have a vascularisation[46,49] therefore the progenitors enter the thymus through the capsule[26]. The seeding of the thymus anlage is not a continuous event, rather lymphoid progenitor cells enter the thymus in waves at distinct developmental stages of organogenesis[11,50]. During migration of the thymus no additional progenitors enter the thymus. After the thymus has reached its final anatomical position, the second wave of T-cell precursors arrive[51,52].

The initial patterning of the thymic epithelial compartment, as defined by a differential keratin expression in TEC is independent of the homing of lymphoid cells to the anlage[53]. TEC differentiation in recombination-activating gene 2/common cytokine receptor-chain deficient (RAG2/γc) and Ikaros-deficient mice was normal until E13.5 despite a block in early lymphocyte differentiation. After this stage interactions with developing T-cells (designated thymocytes) are, however crucial for TEC differentiation and the formation of a cortex and medulla[6,54,55]. The regular organisation of the cortex requires crosstalk with thymocytes that have committed to the T-cell lineage[5,6]. Progression in thymocyte development from $CD44^{+}CD25^{-}$ to $CD44^{-}CD25^{+}$ thymocytes has an impact on the development of the thymic cortex including the three dimensional organisation. CD3ε transgenic mice have a block in early T-cell development (do not develop further than $CD44^{+}CD25^{-}$) and as a consequence the thymus displayed large cysts, the normal cortical organisation was missing and a distinct boarder between cortex and medulla was absent. Furthermore the epithelial cells were

organised in a two dimensional fashion and local accumulations of B-cells were observed[56]. However reconstitution of thymopoiesis with bone marrow of WT mice lead only to a rescue of the cortical organisation in fetal mice, but not in adult mice. This result indicates that the induction of a normal cortical organisation takes place only within defined periods in development. The presence of a regular cortex, however, is required for the development of a thymic medulla. In $Rag2^{-/-}$ mice where thymocyte development is blocked at a later $CD44^{-}$ $CD25^{+}$ stage the cortex develops, however the medulla formation is absent. Reconstitution of CD3ε transgenic mice with $Rag2^{-/-}$ bone marrow resulted in cortex formation, cysts were absent and B-cells were also reduced. A second transplantation with wild type bone marrow resulted in a complete reconstitution of the thymic microenvironment[57]. Similar observations were also made in TCR-α deficient mice, in which development is blocked at the $CD4^{+}/CD8^{+}$ double positive stage. These mice displayed a normal cortex but a disorganised medulla[58]. Thus the formation of the medulla is dependent on the presence of single positive thymocytes[59,60].

1.2. T-cell development in the thymus

Thymopoiesis is a temporally and spatially controlled process, which is reflected by separate anatomical compartments each responsible for driving different stages of T-cell development. These are the subcapsular, cortical, cortico-medullary junctional and medullary areas.

The thymus is thought to lack self-renewing hematopoietic precursors securing a continuous generation of T-cells. Consequently a continuous supply of blood-borne lymphoid precursor cells need to access the thymic microenvironment[61,62]. However this concept is challenged by recent reports suggesting that T-cell development can take place even in the absence of such a steady import of progenitor cells, as shown in thymus transplantations into IL-7 receptor deficient hosts[63] or $Rag2^{-/-}\gamma c^{-/-}kit^{W/Wv}$ mutants[64]. Grafting of wild type thymus into $Rag1^{-/-}$ hosts leads to a first wave of emerging T-cells, however grafting into $Rag2^{-/-}\gamma c^{-/-}kit^{W/Wv}$ mutants, completely devoid of T-cell progenitors, resulted in T-cell development that continued for several months. From this experiments the conclusion was made that the thymocyte turnover is dependent on the competition with hematopoietic precursors. Precursors enter the thymus at the cortico-medullary junction (CMJ), where a dense network of endothelial cells with high endothelial venules (HEV)[65] enable both the entry of precursors

and the exit of differentiated thymocytes. Whether after the establishment of the blood circulation the same chemokines are of importance as in early embryogenesis is still unclear. However a study showed a possible role for CCR9 (the receptor for CCL25) in attracting precursors after the establishment of the vasculature[66]. Transplantation of CCR9 deficient bone marrow into lethally irradiated $Rag1^{-/-}$ hosts resulted in a reduced repopulation of the thymus compared to wild type bone marrow, indicating a role for CCR9 in the process of precursor attraction. Hematopoietic precursors do not continuously enter the thymus, it was shown that entrance of precursors is rather a gated and cyclic event[67]. To show this cyclic entrance of precursors mice were intrathymically injected with bone marrow cells to first synchronise the gating event, followed by intrathymically or intravenous injection of congenic BM cells, the degree of chimerism revealed two distinct phases in the thymus. In a first phase an increase in donor thymocytes is observed in the thymus, this phase is followed by a decrease in donor thymocytes, indicating that the influx of new precursors is still prevented, leading to a cyclic entrance of precursors. T cell development can be easily staged by the expression of the co-receptors CD4 and CD8 (Figure 1.2). The earliest thymic progenitors express neither CD4 nor CD8 and are therefore termed double negative (DN). The DN subset can be further divided in the mouse into four consecutive developmental stages according to their expression of CD25, CD44 and ckit (CD117). Since CD44 is also expressed on many nonlymphoid cells, ckit is included to define the developmental steps expressing CD44.

The earliest progenitors DN1 are lineage negative and characterised by the expression of ckit and CD44 in the absence of CD25. These early progenitors still bear the potential to develop into myeloid, natural killer (NK) and dendritic (DC) cells[68–70]. With ongoing development the precursor loose this potential and fully commit to the T-cell lineage. DN1 are located at the cortical-medullary junction where they remain for approximately 10 days[71]. At this early stage Notch signalling mediated by one of its ligands, Delta-like 4, which is expressed on cortical TEC serves the commitment to the T-cell lineage[68–70]. Indeed, deletion of this Notch ligand exclusively on TEC leads to a complete lack in T lineage commitment and hence in a block in T-cell development[72]. Instead the uncommitted T-cell precursors adopt a B-cell fate and regular B-cell development can be observed in the thymus of these mice. DN1 cells eventually migrate into the cortex towards the subcapsular zone and acquire the expression of CD25[73]. Now designated DN2, these cells initiate the rearrangement of TCR-β locus.

Once accessing the area of the subcapsular zone, the T-cell lineage committed thymocytes down regulate the expression of ckit and CD44 and thus acquire the phenotype designated DN3. At this stage, these thymocytes have completed the TCR-β rearrangement. In the event that this rearrangement has successfully resulted in the generation of a productive β-chain a pre-TCR is expressed composed of that rearranged β-chain and an invariant surrogate α-chain, known as the pre-TCR α-chain. Transition from DN3 to DN4 stage defined by concomitant absence of CD44 and CD25 requires the provision of survival signals mediated via the pre-TCR. This process is referred to as the β-selection and constitutes a checkpoint in thymocyte development[74]. Thymocytes that did not successfully rearrange the β-chain fail to produce a functional pre-TCR, and hence lack the necessary signals to survive and are eventually eliminated by apoptosis.

DN4 cells and their progeny reverse the direction of travel and migrate now from the subcapsular zone towards the medulla. In the outer cortex they upregulate CD4 and CD8 expression, which classifies them as double positive (DP) thymocytes. At this stage the α-chain of the TCR rearranges and replaces the pre TCR α-chain, forming a complete and functional α/β TCR on the cell surface of DP thymocytes[75,76]. The survival of DP thymocytes is dependant on the TCR-mediated interaction with self-peptide-MHC complexes presented by cTEC, a process designated thymocyte positive selection. The rearrangement of the TCR result in a great variability in TCR specificities, however not all of the receptors are able to interact with MHC or they even can cause harm. To avoid these T-cell clones selection mechanisms are included. In contrast to B-cells T-cells recognise their antigen in an MHC-restricted fashion, therefore they have to express a TCR specific for self-MHC molecules presenting foreign antigens. DP thymocytes expressing a TCR with intermediate and higher avidity for self-peptide MHC complexes receive sufficient survival signals that allow for the rescue of thymocytes against a default mechanism which initiates programmed cell death 3 to 4 days after the expression of the complete TCR. However, in the instance that this interaction is too weak or absent, DP cells will not be rescued and undergo apoptosis[77,78]. If the interaction between the TCR and its cognate MHC/peptide complex is too strong DP thymocytes will also undergo apoptosis. The selection of immature thymocytes based on their TCR affinity for self/MHC complexes has been named the affinity model. DP cells that have received a selection signal can be distinguished from pre-selection and late post-selection thymocytes by the presence of the early activation marker CD69 and an intermediate

expression of the TCR. Positive selection of DP thymocytes results in a down regulation of both co-receptors CD4 and CD8 ($CD4^{low}CD8^{low}TCR^{intermediate}$), this down regulation is followed by a re-expression of CD4 and shortly after of CD8 ($CD4^{high}CD8^{intermediate}TCR^{intermediate}$)[79]. After this stage the activation of a lineage specific program is induced, resulting in the loss of either CD4 or CD8 expression, dependant on the MHC restriction. Thymocytes with a TCR specific for antigens presented by MHC Class I molecules stop the expression of CD4 and upregulate the expression of the TCR and become CD8 single positive thymocytes defined as $CD8^{high}CD4^{-}TCR^{high}$. However if the TCR recognises an antigen in a MHC Class II dependant context the thymocytes will stop the expression of CD8, upregulate their TCR expression and develop into CD4 positive thymocytes defined as $CD4^{high}CD8^{-}TCR^{high}$.

Following positive selection the single positive (SP) thymocytes migrate into the medulla, where the TCR repertoire is screened for self-reactive specificities, which will be eliminated in a process called negative selection. This process is mediated by mTEC and dendritic cells (DC)[80], which display a diverse set of self-peptides. mTEC are specialised to express sets of genes representing essentially all tissues of the body. This promiscuous gene expression is in part regulated by the autoimmune regulator AIRE[81,82] and ensures central tolerance. SP thymocytes that express a TCR with low affinity for self-peptide MHC complexes will survive, whereas thymocytes with a TCR with a high affinity for self-peptide MHC complexes will be negatively selected and eventually undergo apoptosis. Some CD4 T-cells with an intermediate to high affinity TCR and thus auto-reactive T-cells were shown to escape negative selection by developing into $Foxp3^{+}$ regulatory T-cells[83,84]. The precise mechanism how they escape negative selection is still elusive, however it was shown that the presence of either TGF-β[85] or IL-2[86] could rescue thymocytes from negative selection[87]. A recent study showed that CD27/CD70 interactions rescues developing regulatory T-cells from apoptosis[88]. Mice deficient for either CD27 or CD70 had reduced numbers of regulatory T-cells in the spleen and thymus, whereas all the other subsets were not affected. Adding soluble CD70 to fetal thymic organ cultures increased the regulatory T-cell output, whereas blocking of CD70 lead to a reduction of regulatory T-cells. These findings suggest an important role for CD70, expressed on mTEC, for regulatory T-cell development.

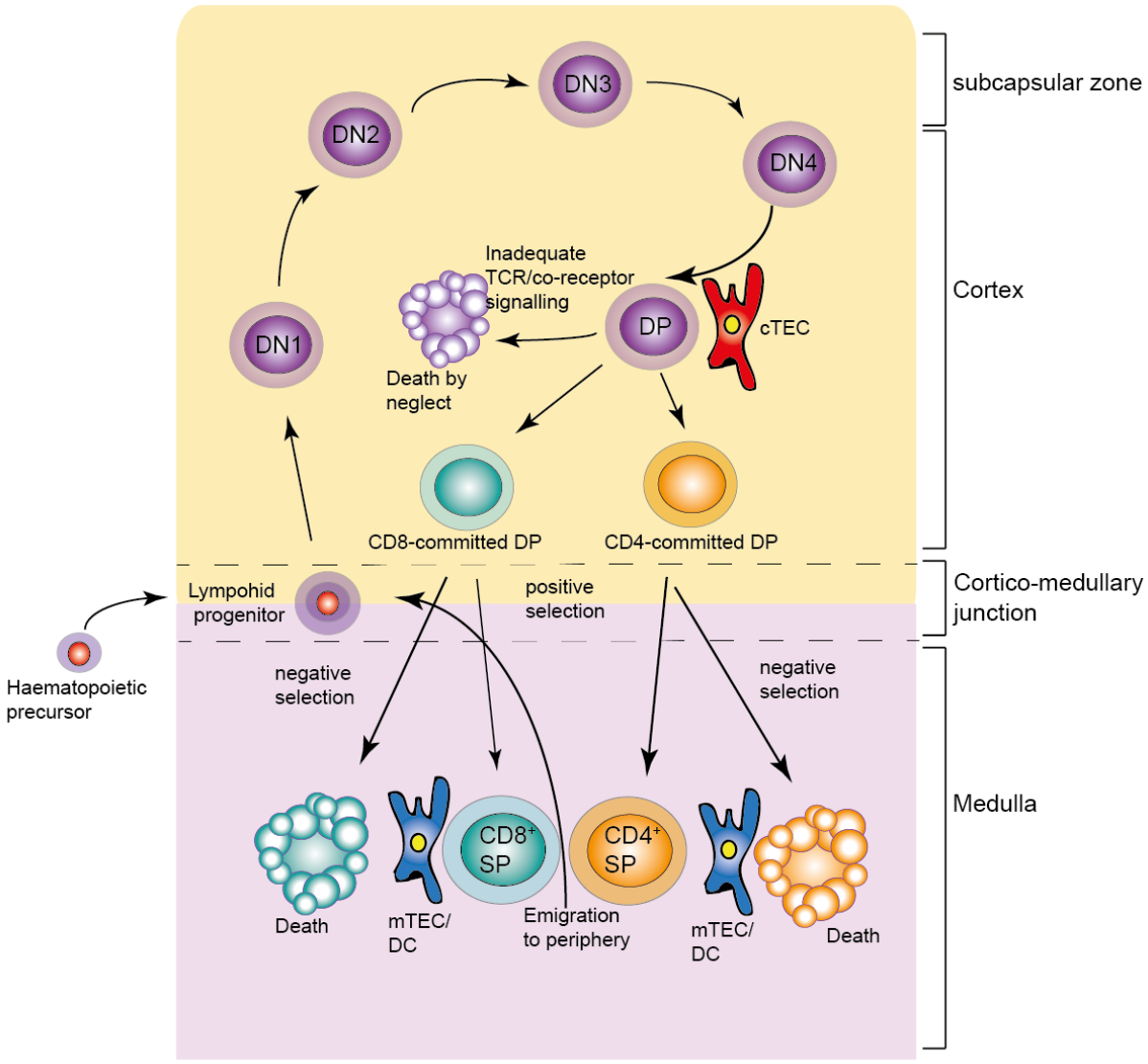

Figure 1.2: T-cell development in the thymus. The thymus is mainly composed of cortex and medulla, each containing distinct thymic epithelial cells. Haematopoietic precursors enter the thymus at the cortico-medullary junction and migrate through the cortex and the subcapsular region, where they interact with stromal cells and develop into $CD4^+CD8^+$ double positive thymocytes. The immature $CD4^-CD8^-$ double negative (DN) thymocytes are divided into four subsets based on the expression of CD25 and CD44. DN1 are $CD25^-CD44^+$, by upregulation of CD25 they become DN2, DN3 have lost expression of CD44 and DN4 are $CD25^-CD44^-$. Interaction of DN4 thymocytes with cortical TEC (cTEC) lead to positively selected $CD4^+CD8^+$ double positive (DP) thymocytes that migrate into the medulla where they finally differentiate into $CD4^+$ or $CD8^+$ single positive thymocytes. Medullary thymic epithelial cells (mTEC) and dendritic cells (DC) mediate negative selection and delete auto-reactive thymocytes. $CD4^+$ or $CD8^+$ single positive thymocytes that have completed differentiation leave the thymus through the cortical medullary junction and migrate into the periphery. Adapted from Germain 2002[89].

Thymocytes that finished the selection process, undergo post selection maturation including the upregulation of the homing receptor CD62L and sphingoisine-1-phosphate receptor 1 (S1P1) required for the egress to the circulation[90].

1.3. Thymic microenvironment

The thymus consists as previously mentioned of a heterogeneous network of specialised stromal cells including TEC, fibroblasts, endothelial cells, neural cells, macrophages and dendritic cells that provide a structural and inductive microenvironment for T-cell development. TECs are characterised by the expression of the epithelial cell adhesion molecule (EpCAM) and can be divided into two main distinct subtypes, namely cortical and medullary TEC. Using cell surface and intracellular markers[91] these subtypes are distinguished according to their function and localisation (Figure 1.3).

Cortical TEC (cTEC) are characterised by the expression of Ly51[91], CDR1[92], ERTR4[93] and the cytokeratins (CK) 8 and CK18[94]. cTEC mediate early T-cell development and positive selection of thymocytes. Different functional subsets can be identified according to the expression of Dll4[72], CD205[95], Cathepsin L[96] and 5t[97]. The endocytic receptor CD205 was shown to facilitate binding and uptake of apoptotic thymocytes[98,99]. However CD205 does not appear to have any role in thymocyte development or selection as demonstrated in CD205 deficient mice[100]. These mice did not show any changes in the thymic microenvironment, all compartments were present and normally distributed, T-cell development and positive selection were not altered. Positive selection by cTEC requires the presentation of self-peptides that have undergone degradation by proteasomes or endosomal/lysosomal compartments. Cathepsin L plays a role in MHC II mediated positive selection of $CD4^+$ T-cells[96,101] as demonstrated in Cathepsin L deficient mice. The thymus specific proteasome catalytic subunit β5t is involved in the generation of peptides from self-antigens that are loaded onto MHC Class I molecules, the ligand for developing T-cells with a MHC Class I restricted T-cell antigen receptor to cause them to develop into single positive $CD8^+$ T-cells. Consequently mice lacking β5t have a reduction in CD8 T-cells[97] and mice lacking Cathepsin L show a reduction in CD4 thymocytes[102].

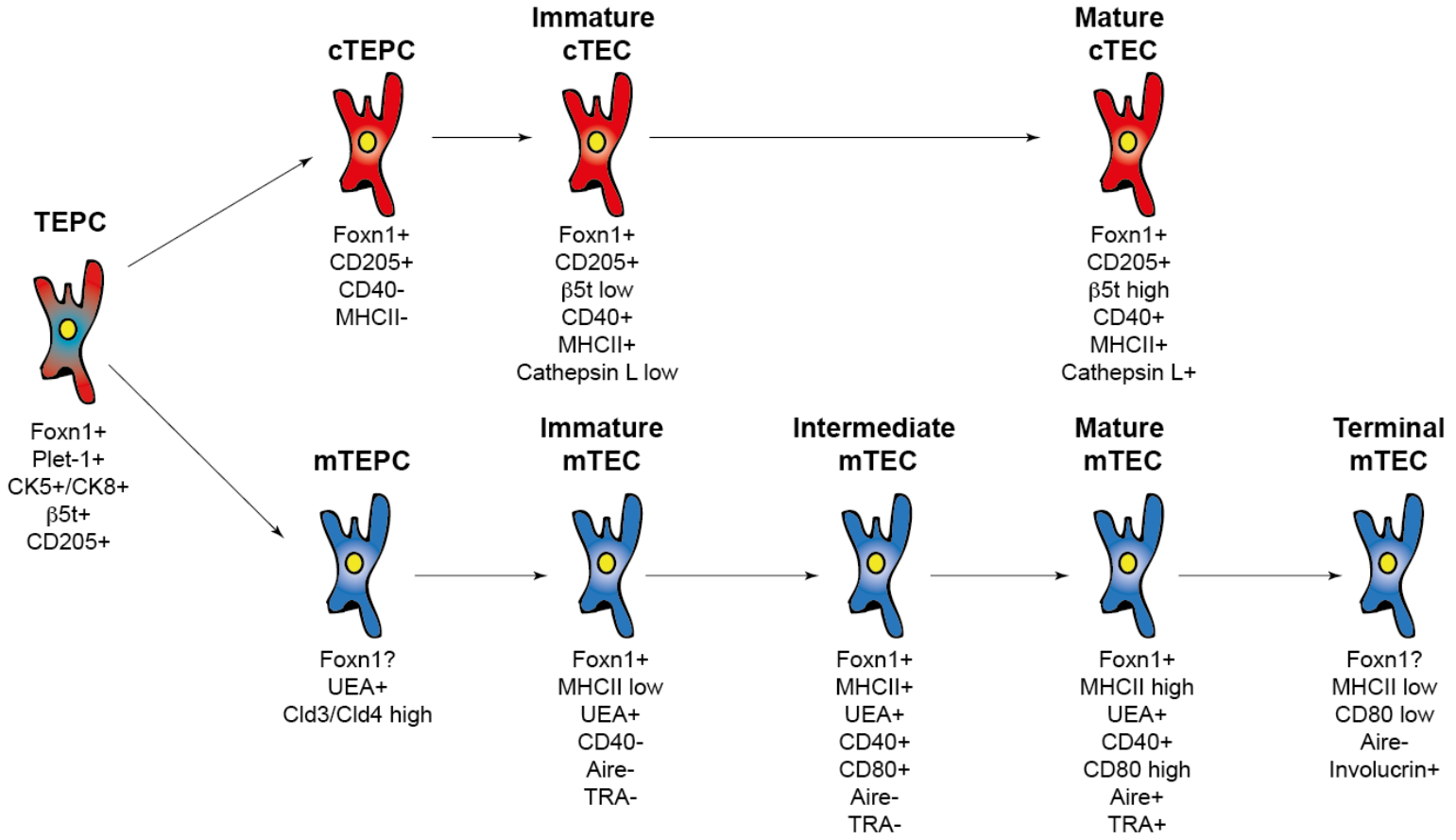

Figure 1.3: TEC development. Bipotent thymic epithelial cell progenitors (TECP) express Foxn1, Plet-1, CK5, CK8[94,103,104] and β5t[105] and CD205[95]. Cortical thymic epithelial progenitor cells (cTEPC) express Foxn1 and CD205 with ongoing maturation they start to up-regulate β5t, MHC II and CD40. Medullary thymic epithelial cell progenitors (mTEPC) express UEA-1 and Claudin 3 and 4. Immature mTEC express low levels of MHCII, intermediate mTEC up-regulate MHC II, CD80 and CD40. Mature mTEC are MHCII high, CD80 high, express CD40, Aire and both Aire-dependent and –independent tissue restricted antigens (TRA). Terminally differentiated mTEC express involcurin and low levels of CD80 and MHCII. Foxn1 is required at all stages of cTEC and mTEC differentiation, though it is not required for initial mTEC lineage progression[106,107].

Medullary TEC (mTEC) are characterised by the expression of the lectin binding Ulex europaeus Agglutinin 1 (UEA1), the cytokeratins CK5 and CK14, CD80, MTS10, ERTR5, Claudin3/4 and Cathepsin S. mTEC are involved in the negative selection of thymocytes, contributing to a self-tolerant T-cell repertoire by effecting the elimination of thymocytes with an autoreactive T-cell antigen receptor. Therefore tissue-restricted antigens are expressed, representing almost all peripheral tissues on mTEC. The promiscuous gene expression[108] is in part regulated by a special subset of MHC II^{high} mTEC expressing Aire. However, not all TRA depend on Aire expression. Indeed a subset of Aire-independent TRA was shown to be regulated by lymphotoxin signalling[109]. Nevertheless, the importance of Aire is shown in Aire deficient mice, which suffer from organ-specific autoimmunity[110–112]. mTEC differentiation can be characterised by different maturation steps. Immature mTECs ($mTEC^{low}$) are MHC $II^{low}CD80^{low}Aire^{-}$ and develop into mature mTEC ($mTEC^{high}$) that are characterised by the expression of $MHCII^{high}CD80^{high}Aire^{+}$ and finally into terminally differentiated mTEC identified as MHC $II^{low}CD80^{low}aire^{low}Involucrin^{+}$[113–116].

1.4. Thymic epithelial cell progenitors

A bipotent thymic epithelial progenitor cell (TEPC) that can give rise to both cortical and medullary TEC has been shown to exist in both the embryonic and the adult thymus[117,118]. The first hint for a bipotent progenitor came from histological studies of nude and wild type embryos. In the absence of Foxn1 TEC are arrested in a progenitor stage characterised by the expression of MTS20 and MTS24[107] and the lack of expression of mature TEC markers including MHC classII[103]. Additional descriptive analysis on histological sections on the expression of CK5 and CK8 showed that TEC in the thymus rudiment are positive for both cytokeratins. With progression of development, in wild type mice, these cells adopt either a $CK5^{+}CK8^{-}$ medullary or a $CK8^{+}CK5^{-}$ cortical TEC phenotype[54,94,119]. Hence these studies suggested that TEC early in development express concomitantly CK5, CK8, MTS20 and MTS24 and may thus represent the so far elusive thymic epithelial precursor cell.

The model of a simple bipotent precursor, giving rise to both cTEC and mTEC is challenged by recent findings, showing that early embryonic bipotent TEPC sequentially co-express the cTEC marker CD205 and respond to RANK stimulation, the latter a feature of mTEC[95]. RANK was shown to control mTEC development in the embryo[113], however so far no

antibodies or reporter mice are available to monitor RANK expression, thus upregulation of the surrogate marker CD40 and MHC Class II are used. The analysis of embryonic TEC identified at E11.5 a small subset of $CD205^+$ TEC, which increases in number and from E13.5 onwards they additionally express CD40. $CD205^+CD40^-$ TEC express a genetic profile associated with cTEC, whereas $CD205^-CD40^+$ TEC are considered as mTEC[120]. Transplantation of reaggregated thymic organ cultures (RTOC) using purified $CD205^+CD40^-$ progenitors gave rise to cortical and medullary thymic areas able to support normal T-cell development [95]. Further evidence for a bipotent precursor expressing cTEC markers comes from lineage tracing experiments, showing that the majority of mTEC are derived from a $\beta5t^+$ progenitor population[105].

In addition to the existence of a bipotent precursor, experimental evidence has been generated that suggests the presence of cTEC and mTEC restricted progenitors. The presence of a direct mTEC progenitor was demonstrated by cell tracing experiments using MHC mismatched chimeras, showing the formation of medullary islets, each of them arising from a single progenitor[121]. Separate progenitors were also described for the cTEC lineage using analysis of differentiation, proliferation and gene expression profiles. The emergence of the cTEC lineage from a bipotent precursors occurs as early as E12 and is dependent on Foxn1, as shown by the absence of CD205 and β5t in Foxn1 deficient mice[120]. The earliest cTEC progenitor was detected on E15 and identified as $EpCAM^+CD205^+CD40^-$.

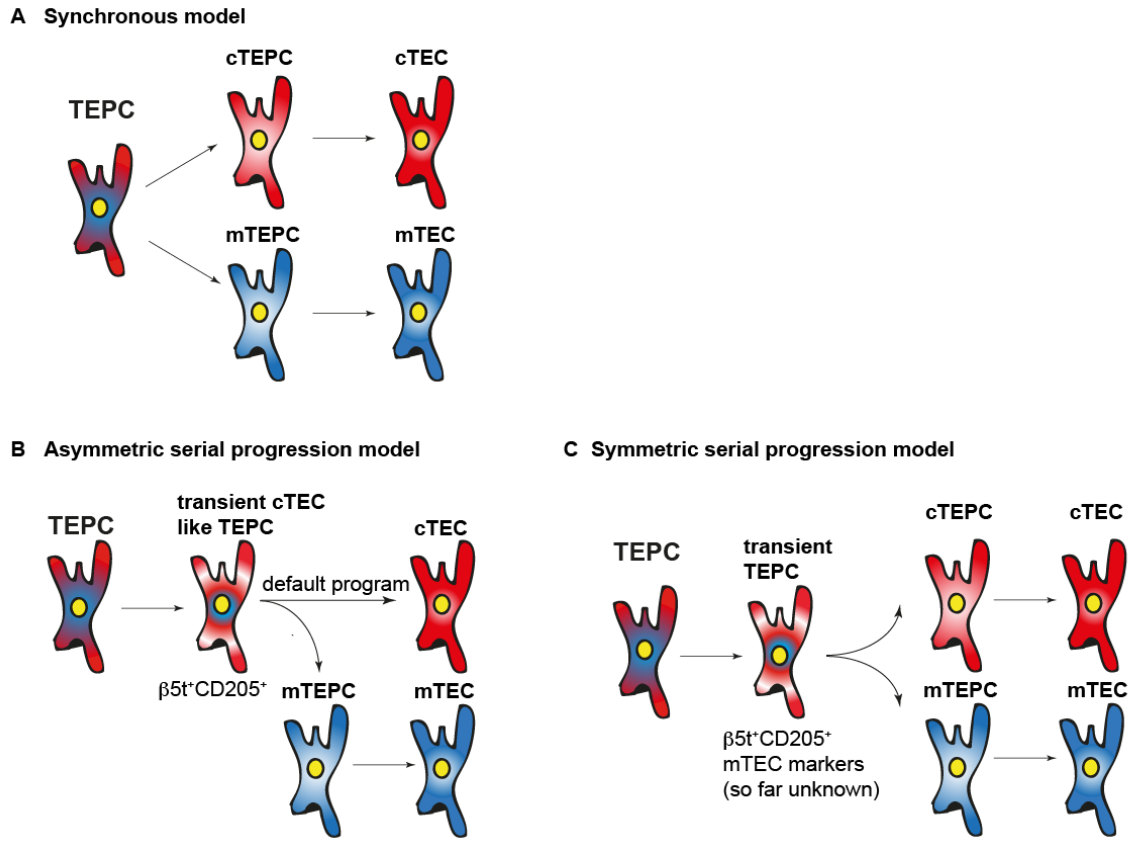

Figure 1.4: Models of thymic epithelial cell development from a bipotent thymic epithelial precursor cell: (A) In the synchronous model a bipotent precursor gives rise to cTEC and mTEC restricted progenitor cells giving rise to cTEC and mTEC. In the asymmetric serial progression model the progenitor develops first into a cTEC like progenitor cell, which develops by default into cTEC, development into mTEC linage requires additional signals. In the symmetric serial progression model TEPC develop into a transient TEPC with cTEC and mTEC marks that gives rise to both cTEC and mTEC.

In summary two different models of thymic epithelial cell development currently exist (Figure 1.4)[122]. In the synchronous model an uncommitted bipotent TEPC gives simultaneously rise to lineage restricted cTEC and mTEC progenitors. In the progression model the development of TEC includes a transitional TEC progenitor stage that expresses phenotypic and molecular features associated with cTECs. The latter model is supported by the latest findings that $Aire^+$ cells originate from β5t expressing cells and that $CD205^+$ precursor give rise to both cTEC and mTEC[95,105]. The progression model includes two different scenarios for the development of TEC. A first one designated as serial progression model suggests the commitment to the cTEC linage constitutes a default program and development into the mTEC lineage requires additional signals. In contrast in the so called symmetric progression TEPC can develop with equal likelihood into either mTEC or cTEC. It

can not be excluded that the transitional thymic epithelial progenitor has not only features of the cTEC lineage but also of the mTEC lineage but the markers are not identified yet[122].

1.5. The transcription factor FoxN1

The Forkhead-box transcription factor N1 (Foxn1 also known as winged helix nude Whn or Hfh11), belongs to the family of winged helix/forkhead transcription factors. They are characterised by a 100 amino-acid monomeric DNA-binding domain that folds into a variant of the helix-turn-helix motif. Because of the characteristic butterfly shape of the motif these transcription factors were named winged helix[123]. Winged helix/forkhead transcription factors are key regulators in embryogenesis and in the maintenance of differentiated cells[124]. The Foxn1 gene consists of two alternative first exons, 1a and 1b, and 8 coding exons. Exons 5, 6 and 7 encode for the DNA binding domain. The transcriptional activation domain is encoded by exons 8 and 9. Using mRNA from mouse thymus and skin, the tissue-specificity of alternative first exon usage was analysed and identified 1a-2 transcripts in both thymus and skin, whereas 1b-2 transcripts were used exclusively in the skin. In addition to the alternative first exons a second type of splicing was observed taking place at the splice acceptor junction in exon 2[125]. The Foxn1 gene is located on chromosome 11 in mouse and chromosome 17 in human[125,126]. Both sequence and function of Foxn1 are highly conserved among rodents and humans[125,127].

Foxn1 serves as the master regulator of the differentiation events that eventually control regular thymus development but also coordinate the normal formation of the hair shafts and the physiology of the mammary gland. Hence Foxn1 is mainly detected in the epidermis, hair follicles, mammary gland and in the thymic epithelium. Mutations in Foxn1 are characterised by defects in the keratinisation of the hair shafts leading to an absence of fur due to the physical breaking of hair at the skin surface[128]. The lack of regular Foxn1 expression also leads to underdeveloped mammary glands and females are not able to lactate their offspring[129]. Finally and functionally most restrictive thymus organogenesis is arrested at an early stage resulting in a primary T-cell deficiency[130,131].

This array of interesting phenotypes was first observed in mice with a spontaneous loss of function mutation of Foxn1. The original description of these mice from 1966 noted a hairless skin, hence the notion “nude”[132]. The precise nature of the complex phenotype was however

only identified 28 years later using sequencing analysis[24]. Despite the complete absence of thymopoietic activity in Foxn1 deficient mice a small population of T-cells can be observed in older animals which are obviously generated extrathymically[133]. Due to their failure in hair follicle formation and the deficiency in T-cell development nude mice are widely used as model for transplantation, immunological, oncological and dermatological studies[133,134].

Foxn1 mRNA is first detected as early as E10.5[135], the protein is first detected at E11.5 in TEC and is robustly expressed at E12.5.[22,136,137]. The induction of the outgrowth of the thymus anlage is Foxn1 independent, however Foxn1 is cell-autonomously involved in patterning and differentiation of immature epithelial cells into functional cortical and medullary TEC[25,107]. This was demonstrated in a chimeric thymus where the presence of wild type TEC did not induce nude TEC to differentiate into cTEC or mTEC.

Foxn1 induction and stabilisation is directed by different genes including Wnt5b and BMP4 that are expressed in the ventral region of the third pharyngeal pouch prior to Foxn1 expression[34,135]. Wnt4 and Wnt5b were shown to induce Foxn1 in cultured TEC lines[135,138]. BMP4 is actively upregulating Foxn1 expression in vivo[139,140], and Foxn1 expression upregulates FgF receptor 2IIIb[140]. Sonic Hedgehog (Shh) is expressed on the dorsal region of the pouch and regulates Gcm2 expression. In the absence of Shh the pouch expresses only BMP4, indicating that Shh negatively regulates Foxn1 expression[141]. FgF8 is also expressed before Foxn1 expression in the prospective thymus region. FgF8 was demonstrated to play a role in the development of the pharyngeal pouch where it signals to the surrounding NCC derived mesenchyme[142]. Immunohistological analysis showed that Foxn1 deficient epithelium was devoid of the Notch ligands Dll1 and Dll4[143]. Experiments taking advantage of mice with different Foxn1 transcript levels showed that Foxn1 directly regulates Dll4, CCL25[144] and paired-box 1 (Pax1) expression. Reductions in the expression levels of Dll4, CCL25 and Pax1 in TEC are proportional to the reduced Foxn1 expression[106]. A comparative analysis of transcriptomes between E12.5 nude and wild type mice identified an additional potential down-stream target of Foxn1, programmed death 1 ligand[145] (PDl ligand). PD1L deficient mice show an enhanced T-cell response and $CD4^+$ T-cells produced more cytokines, when compared to wild type $CD4^+$ T-cells. The corresponding receptor to PDL1, PD1 is expressed on CD4/CD8 double negative thymocytes[146], and is important for self-tolerance as mice deficient for PD-1 develop autoimmune pathologies[147].

The absence of lymphocyte precursors in nude mice is explained by the absence of the cytokines CCL25 and CXCL12, which are involved in haematopoietic precursors homing. Furthermore stem cell factor (scf or kitligand)[148] that is involved in expansion of recent thymic immigrants is absent in Foxn1 deficient mice[149]. The absence of Foxn1 leads also to a block in thymus vascularisation[150]. Endothelial cells fail to accumulate in Foxn1 deficient mice, whereas they increase in numbers in wild type thymus rudiment shortly after TEC start to express Foxn1. VEGF expressed by TEC and mesenchymal cells is involved in thymus vascularisation[42], VEGF was absent in nude thymus.

Deletion of Foxn1 using Cre recombinase under the control of K14 regulatory elements has a larger impact on the skin than on the thymus. These mice showed a defect in the hair follicle formation similar to nude mice, however a thymus was detectable[151]. The thymus was smaller in size when compared to wild type thymus, displayed a disrupted 3-D architecture but nevertheless, T-cell development was present. Deletion of Foxn1 under the control of K14 regulatory elements is only active in cells that are restricted to the medullary lineage. In contrast to the thymus Foxn1 expression in the skin is relatively restricted to the hair cortex and the skin, whereas in the thymus both cortex and medulla express Foxn1. This suggests that Foxn1 in $K14^+$ cells has a crucial role in the skin, whereas its role in the thymus is less important.

Deletion of exon 3 of the Foxn1 gene identified a thymus specific role for the N-terminus, as the skin was not affected. The thymus displayed an aberrant architecture lacking cortical and medullary regions. Nevertheless this thymus was able to support T cell development, although increased frequencies of CD4/CD8 double negative (DN) and reduced percentage of CD4/CD8 double positive (DP) thymocytes were noted[152]. Interestingly DP thymocytes developed without passing through a consecutive DN2 ($CD44^+CD25^+$) and DN3 ($CD44^-CD25^+$) developmental stage[153]. These DP thymocytes were shown to arise from an atypical $ckit^-$ progenitor[154]. According to the expression of ckit and CD24 (HSA) the DN1 compartment can be subdivided into DN1a – DN1e, in which DN1a and DN1b are considered as the canonical hematopoietic progenitors[155]. DN1d and e are devoid of ckit expression, nonetheless they develop into T-cells *in vitro*. Their developmental progression into DP is faster than DN1a, and in contrast to DN1a-d, DN1e express Rag1 and contain rearranged TCRβ chains[155]. The presence of DN1e could explain the absence of DN2 and DN3 stages observed in these mice.

The differentiation into the mTEC linage occurs despite the absence of Foxn1, at least as indicated by the detection of Claudin4^{+} CK5^{+} cells, likely to be early mTEC[106]. Importantly gene dosage experiments showed that the delay in mTEC differentiation correlated with reduced Foxn1 expression[106]. Foxn1 is therefore needed for the initiation of the differentiation into the earliest TEC progenitors and for the subsequent progression into cTEC and mTEC. The presence of early mTEC in the absence of Foxn1 suggests that Foxn1 is not required for the cell fate decision. Low amounts of Foxn1 expression are sufficient for expression of MHC class II but not for inducing T-cell development, suggesting different requirements for Foxn1 in TEC differentiation and their ability to induce thymocyte development[106].

Most of the knowledge on Foxn1 function was gained from experiments on embryonic thymus. Studies on postnatal expression and requirements of Foxn1 started only recently with the generation of inducible knock-in and knock-out models and are not yet fully understood. In the postnatal thymus Foxn1 is required for TEC maintenance. The analysis of different Foxn1 mutants with different Foxn1 expression levels showed that TEC maintenance is sensitive to Foxn1 dosage[156]. The observed phenotypes were closely linked to Foxn1 expression levels, as small changes in Foxn1 levels had large effects on the thymus phenotype. A Foxn1 expression of below 50% of normal Foxn1 mRNA results in a loss of specific TEC subsets and reduced T-cell development. Different TEC subsets require different amounts of Foxn1 mRNA[106,156]. 15% of wild type Foxn1 mRNA is sufficient for the development of mature mTEC, whereas cTEC require higher amounts of Foxn1 for their maturation. Furthermore, different TEC subsets have different amounts of Foxn1 mRNA. Mature mTEC (MHC Class II high) express higher levels of Foxn1 protein and mRNA compared to the mTEC^{low} population. The mTEC^{high} subset was also the most sensitive to experimentally induced down-regulation of Foxn1 expression[156]. Reduction in Foxn1 expression in post natal thymus results in changes in the thymic microenvironment similar to thymic involution[157].

The first Foxn1 mutation in humans was described in 1999 in two sisters from southern Italy[127]. Foxn1 deficiency in humans leads to an alopecia universalis, nail dystrophies and absence of a thymus resulting in a primary T-cell deficiency[158]. Untreated Foxn1 deficient patients rarely survive beyond early childhood due to the T-cell deficiency. There is no cure for Foxn1 deficient patients, however their life can be prolonged by bone marrow[159] and thymus transplantations[160,161]

1.6. Age-related thymic involution

Age-related thymic dangers are characterised by a reduction in thymus size, changes in the composition and organisation of the thymic microenvironment and consequently by a reduced thymopietic activity. Termed in the physiological context as thymus involution these alterations are an evolutionarily conserved phenomenon that can be observed in jawed vertebrates[162]. A main feature of thymic involution is the decrease in thymic epithelial cellularity, a decline in mTEC resulting in a change in the cTEC:mTEC ratio and a particular loss of MHC Class II-high TEC[7] which is accompanied by an expansion of the perivascular space and an increase in adipose tissue[163,164]. The segregation of medullary and cortical compartments is disrupted[163,165] and the complexity of the medullary islets is decreased[166] concomitant with this loss of a regular architecture, areas appear that lack epithelial cells[167]. These changes in the microenvironment lead to a progressive reduction of thymopoiesis, and as a consequence to peripheral lymphopenia with an increased memory T-cell pool displaying signs of oligoclonal expansion[168]. The molecular mechanisms that account for thymic aging and hence involution are only very poorly defined but clinical observations suggest that age-related danger in the biology of hematopoietic stem cells and the presence of hormones, growth factors and cytokine levels contribute to the changes observed. In addition, and of particular relevance for the work presented here, Foxn1 transcripts[169] and protein levels[137] decline with age. However it is unclear whether this decrease is the cause or the consequence of thymic involution. A direct instructive role of Foxn1 for the structural danger observed is suggested by experiments that demonstrate that a reduction of Foxn1 in the postnatal thymus accelerates thymic atrophy[156,170,171] whereas an over-expression of Foxn1 attenuates age-related thymic involution[172]. Independent of the upstream signals operative in changing Foxn1 expression, these results suggest that Foxn1 plays a crucial role in thymic involution.

Aging is also associated with an increased susceptibility for diseases[166,173,174]. In aged mice thymus function is limited, and to compensate the reduced thymic output T-cells proliferate in the periphery acquiring a memory/activated phenotype. The frequency of auto-immune disease is increasing with age, studies comparing young and aged mice showed that the expression of tissue restricted antigens decreases with age[166]. Consequently T-cells emerging from an aged thymus have undergone less stringent selection and include more auto-reactive T-cells, leading to auto-immunity with age.

Thymic aging is coupled with an increase in fibroblasts[175]. Thymic epithelial cells can convert into fibroblasts by epithelial-mesenchymal transition (EMT)[176]. EMT in the thymus was identified by cell tracing experiments, Foxn1$^+$ cells were permanent genetically labelled using LacZ and the phenotype of LacZ positive cells was analysed in 3 month old mice. LacZ$^+$ cells colocalise with fibroblast specific protein-1 (FSP1), a marker for EMT[177], indicating that these cells underwent EMT. In addition these cells are adipogenic. In ghrelin deficient mice transcripts associated with EMT are increased, suggesting that ghrelin maintains the thymic microenvironment by preventing EMT. Thymic involution is enhanced by the metabolic changes in conjunction with obesity, as mice under a high-fat diet accelerate their thymic involution[178]. In contrast mice kept under conditions of caloric restriction display a reduced thymic involution and a restored thymic organisation, possibly due to inhibition of EMT[179]. Mice under caloric restriction were also shown to have a reduction in pro-EMT genes, which prevents the generation of local fibroblasts.

Despite the age related changes in the thymic microenvironment thymopoiesis does not stop completely[180]. The reduced thymic output is not caused by a decrease in hematopoietic precursor attraction, as shown by experiments where both young and aged mice were sub-lethally irradiated and reconstituted with either young or old bone marrow. The absolute numbers of donor cells recovered in the thymus three days after injection was similar, but the numbers increased more rapid in young mice, thus the reduced thymic output is not caused by decrease in attraction but is caused by their impaired survival, proliferation and differentiation in the thymus[181].

1.7. Homeostatic expansion of T-cells in the periphery

A T-cell pool with a broad TCR repertoire of distinct specificities is required for normal immune competence. However during aging the thymic output is reduced, and the size of this peripheral T-cell pool is maintained against a continuous attrition of T-cells by a mechanism of homeostatic T-cell expansion in peripheral lymphoid tissues[182]. Mature thymocytes leaving the thymus receive in the periphery survival signals from self-peptide MHC ligands and cytokines especially IL-7[183]. These interactions provide tonic signals that keep peripheral T-cells alive. The cells remain in the interphase of the cell cycle and hence hardly proliferate[184,185]. However if naïve T-cells encounter a foreign antigen presented by an antigen

presenting cell the TCR signal changes to stimulatory and lead to activation and proliferation, T-cell activation requires costimulation via CD28. The homeostasis of the naïve T-cell pool is regulated by the competition for survival signals, like IL-7 and self-peptide/MHC ligands that are limited under physiological conditions. IL-7 is produced by specialised cells in the secondary lymphoid organs. Mice lacking expression of lymph nodes homing molecules like CCR7 or CD62L show consequently a reduction in naïve T-cells. The common cytokine receptor γ chain is not only used by IL-7 but shared by receptors for the cytokines IL-2, IL-4, IL-9, IL-15 and IL-21, which are all important for generation, survival and homeostasis of lymphocytes[183]. IL-4, IL-15 and IL-7 were shown to enhance homeostatic expansion *in vitro*, however *in vivo* T-cells underwent homeostatic expansion in IL-4 and IL-15 deficient mice, but not in IL-7 deficient mice, suggesting an important role for IL-7 in homeostatic expansion[186]. Under conditions of T-cell lymphopenia the consumption of IL-7 decreases, which lead to an increase in IL-7 availability and consequently IL-7 now acts as a mitogenic stimulus and drives homeostatic expansion. Although IL-2 is able to induce growth, survival or death of conventional T-cells, it is dispensable for the homeostatic expansion of T-cells[187,188]. Though homeostatic proliferation is a slow process normal T-cell numbers are nevertheless restored in the course of weeks given that a sufficient thymic output is still maintained or has returned to normal[189]. Naïve T-cells that undergo homeostatic expansion upregulate CD44, down regulate the expression of the homing molecule CD62L and thus display a memory like phenotype.

In mice that are chronically lymphopenic (e.g. $Rag2^{-/-}$, $TCR^{-/-}$) rapid homeostatic expansion upon adoptive transfer of CD4 T-cells occurs. Beside the normal homeostatic expansion, proliferation is also driven by foreign antigens from the commensal microflora[189,190]. T-cells that proliferate in response to foreign antigens require costimulatory signals through CD28 for their activation and display a upregulation of acute activation marks[180,191]. This antigenic proliferation was reduced when mice were kept in a germ-free environment[192], indicating that the response is directed against the commensal microflora.

1.8. Extrathymic T-cell development

The presence of T-cells in athymic nude mice indicates that T-cell development can also take place in the absence of a functional thymus. Designated extrathymic development, this phenomenon is observed in nude mice particularly in older animals[193]. Nude mice have an abnormal distribution of T-cells in that they have reduced frequency of CD4 T-cells and contain cells that are $Thy1^{pos}$ (a marker for T-cells) but express neither CD4 nor CD8[194]. Extrathymic T-cells were believed to develop in the lymphoid tissues as a function of time. However the anatomical sites where extrathymic T-cell generation occurs are still not well defined and broadly argued upon. There is evidence for extrathymic T-cell development in the gut cryopatches as indicated by the presence of $ckit^{high}$ precurosrs[195], and most importantly mice devoid of gut cryopatches did not harbour extrathymic derived T-cells[196]. In contrast a subsequent study using mice that had GFP under the RAG2 promoter, which allows to follow cells that express the recombinase activation gene (RAG) and are therefore in the process of rearranging their TCR receptor (GFP^{high}) or have recently rearranged their receptor (GFP^{low}), did identify mesenteric lymph nodes and to a lesser extent the Peyer's patches as the site of extra thymic T-cell generation[197]. No GFP expression was detected in the gut cryopatches, indicating that this anatomical site did not contribute to extrathymic T-cells generation. A recent study addressing extrathymic T-cell development after bone marrow transplantation confirmed the mesenteric lymph nodes and Peyer's patches as sites for extrathymic T-cell development. Moreover transplantation of $luciferase^{+}$ preT-cells (DN2 and DN3) showed engraftment in the thoracic and in the abdominal regions. These results are further supported by transplantations into hosts lacking lymph nodes and Payer's patches, which result in a reduced generation of extrathymic T-cells, confirming an important role of the mesenteric lymph nodes and Peyer's patches in extrathymic T-cell generation[198]. In addition, with luciferase assays it was shown that nuclear factor of activated T-cells (NFAT) activation was detected in the mesenteric lymph nodes of nude mice, indicating that similar signalling mechanisms are used in extrathymic and thymic T-cell development[198]. Closer examination of the developmental steps in extrathymic T-cell generation, using mice with GFP under the RAG2 promoter revealed that 97% of the GFP^{high} cells were double positive for CD4 and CD8 showing a similar phenotype as their thymic counterparts, the remaining 3% resemble DN2 and DN3 stages[197,199]. The same study with GFP under the RAG promoter showed that

in euthymic mice GFP^+ cells were absent in the mesenteric lymph nodes, indicating that the extrathymic T-cell generation pathway is supressed under normal conditions and only activated in conditions of lymphocytic depletion or in thymic atrophy, as observed in old mice[197]. The absence of extrathymic T-cell development is not linked to the presence of a thymus, but rather to the presence of αβ-T-cells. This was concluded from a study showing that TCRδ deficient mice did not show extrathymic T-cell development, whereas GFP^+ cells were detected in the lymph nodes of TCRβ deficient mice.

A new option to study extrathymic T-cell development provided the use of oncostatin M (OM) transgenic mice. The thymus of these mice displays hypoplasia and T-cell development is observed only in the lymph nodes and not in the thymus. The OM induced pathway of T-cell generation was found to be totally thymus independent as demonstrated by lethally irradiated nude or thymectomised mice reconstituted with either wild type or oncostatin M transgenic bone marrow. These experiments revealed that extrathymic T-cell development was only present in mice reconstituted with OM transgenic bone marrow, but not in mice reconstituted with wild type bone marrow[199]. Oncostatin M protein was also shown to induce the extrathymic pathway of T-cell generation. Due to the amplification of lymphopoiesis, this model enabled further investigations of extrathymic T-cell development that otherwise is difficult to study due to limited cell numbers. Studies on OM transgenic mice revealed that positive selection in the periphery does not obey the same rules as in the thymus. In the lymph nodes CD8 T-cells are selected on MHC I expressed on hematopoietic cells. Thymectomised wild type mice transplanted with fetal liver cells from OM transgenic mice that were deficient for MHC I did result in a reduction of CD8 T-cells, however CD8 development was not completely abolished, indicating that non hematopoietic cells can also support positive selection although at reduced frequencies[200]. Positive selection is mediated by different sets of MHC-peptide complexes in thymus and lymph nodes, leading to a different repertoire[201]. Negative selection in the thymus is dependant on Aire expression, Aire expression was also detected in lymph nodes although 4 fold reduced compared to expression in TEC[201]. Nevertheless gene chip analysis revealed that genes upregualted by Aire were expressed at similar levels in the thymus and in the lymph nodes[201]. Reporter mice with GFP expression controlled by Aire promoter identified extrathymic Aire expressing cells in the lymph nodes and spleen. Sorting of these cells revealed that they express a different array of self antigens compared to mTEC, nevertheless they were shown to interact and delete autoreactive T-

cells[202]. Extrathymic T-cells display a memory like phenotype ($CD62L^{low}$, $CD44^{high}$), have a rapid turnover and undergo enhanced homeostatic proliferation[203]. They differ in their effector functions when compared to thymic derived T-cells. Extrathymically derived CD4 T-cells expand poorly and fail to provide B-cell help upon viral infections, as demonstrated by the absence of antibodies upon infection with lymphocytic choriomeningitis virus (LCMV) or vesicular stomatitis virus (VSV)[204].

1.9. The mucosal immune system of the gastrointestinal tract

The gastrointestinal tract is the largest mucosal surface. The intestinal epithelium is the interface between the intestinal microbiom and the lymphoid tissues, where it forms a physical barrier against excessive entry of bacteria and other antigens from the intestinal lumen into the circulation. The epithelium also plays a crucial role in shaping the mucosal immune response. The crosstalk between the intestinal epithelial cells, the local immune cells and the intestinal microbes is important for the intestinal homeostasis.

The intestinal epithelium consists mainly of intestinal epithelial cells (IEC), which are connected by tight junctions and promote digestion and absorption of nutrients but also of mucin secreting goblet cells and paneth cells. IEC can produce antimicrobial peptides. Studies showed that IEC are able to discriminate between pathogenic and commensal bacteria. IEC express a wide range of pattern recognition receptors (PRR), recognising bacterial factors like lipopolysaccharide (LPS), lipoproteins or flagellin. Upon triggering of the PRR by microbes, IEC produce proinflammatory cytokines, and alert thereby the immune system[205]. Mice with IEC deficient for single-immunoglobulin-domain-containing interleukin-1 receptor-related protein (SIGIRR), which is a negative regulator of Toll-like receptor (TLR)[206] were more susceptible to intestinal inflammation[207,208], emphasizing the importance of these receptors. Moreover deletion of Toll-like receptor (TLR) 4 or the TLR signalling adaptor protein MyD88 resulted in an impaired immune reaction against bacterial infection[209,210]. Goblet cells, located in the epithelial layer of the small and large intestine, provide additional protection by secreting a mucus layer and factors that play a role in epithelial repair and inflammation[211,212]. Paneth cells, located in the crypts of the small intestine, but not in the colon, contain cytoplasmic secretory granules loaded with antimicrobial proteins like α-defensins[213].

The mucosal immune system of the gastrointestinal tract is composed of several lymphoid organs collectively referred to as gut associated lymphoid tissue (GALT), which allows a rapid and gut restricted immune reaction (Figure 1.5). The GALT consists of secondary lymphoid organs like Peyer's patches (PP) and mesenteric lymph nodes, tertiary organised lymphoid tissues (isolated lymphoid follicles), and diffusely distributed lymphocytes, namely intraepithelial (IEL) and lamina propria lymphocytes (LPL), and dendritic cells. IEL are located above the basement membrane, between the epithelial cells. Underneath the basement membrane located in the intestinal villi are the lamina propria lymphocytes. PP and isolated lymphoid follicles are located within the mucosa. PP are only present in the small intestine, their organisation is comparable to that of lymph nodes, including large B-cell follicles and T-cell areas[214]. M-cells are overlying the PP and transport antigens and bacteria to the underlying immune cells that activate or inhibit immune responses. The formation of PP is dependent on the expression of VCAM1 and the presence of lymphoid inducer cells, but is independent of the intestinal flora[215]. The development of isolated lymphoid follicles is, however, dependant on the intestinal flora, as demonstrated by the absence of these structures in germfree mice and their increase during chronic inflammation[215]. In contrast to PP, isolated lymphoid follicles are distributed along the whole intestinal tract. The lamina propria lymphocytes are composed of conventional T-cells and small populations of unconventional T-cells, i.e. invariant NKT cells and mucosal associated invariant T-cells (MAIT)[216]. Both cell types are characterised by the expression of a semi-invariant TCR-rearrangement. Invariant NKT cells recognise glycolipid antigens presented by CD1d[217], whereas MAIT cells recognise the MHC-related molecule 1 (MR1)[218]. Both invariant NKT cells and MAIT cells are thymus derived. Fetal thymic organ cultures cultured in the absence or presence of MR1 demonstrated the intrathymic origin of MAIT cells[219]. Furthermore, MAIT cells are absent in nude mice, confirming their thymic origin[220]. The presence of MAIT cells is dependent on the colonisation with commensal bacteria, as demonstrated by their absence in germfree mice[221]. IEL are located in the gut mucosa of the small and large intestine and play a crucial role in maintaining the integrity of the gut wall. They regulate the immune responses against pathogens and commensal microbiota. CD8αα IEL act as regulatory T-cells and prevent colitis upon adoptive transfer into T-cell deficient mice[222,223]. They are further involved in immunoregulation at different anatomic sites, as shown in mice which spontaneously develop diabetes (NOD mice). These mice display a reduction in CD8αα IEL, reconstitution with

CD8αα IEL prevents them from diabetes whereas further reduction of CD8αα IEL accelerates the disease[224].

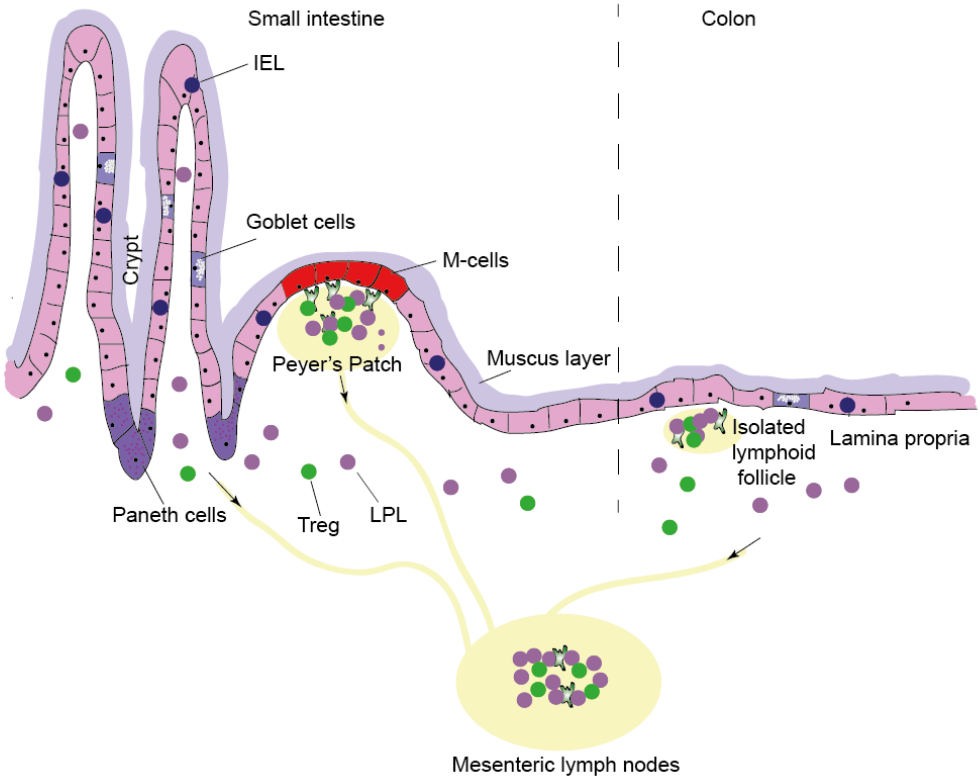

Figure 1.5: The mucosal immune system: The epithelial layer is covered by a layer of mucus secreted by goblet cells, paneth cells secret antimicrobial peptides and protect thereby from bacteria. Intraepithelial lymphocytes (IEL) are located within the epithelial layer. M-cells transport microbes to the Peyer's patches where dendritic cells present the antigens to naïve $CD4^+$ T-cells. Upon activation $CD4^+$ T-cells migrate to the lamina propria.

IEL can be divided into two groups: (i) conventional IEL and (ii) unconventional CD8αα IEL. The first group of IEL are peripheral T-cells that after antigen encounter in Peyer's patches or mesenteric lymph nodes upregulate the expression of α4β7 integrin and CCR9 and home to the gut mucosa[225,226]. These conventional IEL can be either $CD4^+$ or $CD8\alpha\beta^+$. The second group of IEL is specific to the gut wall. They are $CD4^-CD8\beta^-$ but frequently express the CD8αα homodimer. These CD8αα IEL are considered to be part of the innate immune system. In contrast to the conventional IEL the CD8αα T-IEL are not negatively selected as shown by studies using the minor lymphocytes stimulating (Mls) antigen system. In this system the presence of a superantigen in the thymus leads to the deletion of conventional T-

cells expressing a particular Vβ chain. In contrast to conventional T-cells, CD8αα IEL are not responsive to this mitogenic TCR-signal[227]. This tolerance is induced by a mechanism called developmental diversion. Upon receiving a strong TCR signal the cells differentiate into functionally anergeic and coreceptor negative but TCRαβ^{+} thymocytes. These coreceptor negative thymocytes leave the thymus and migrate into the intestine, where they acquire a CD8αα phenotype[228]. Different selection mechanisms were demonstrated for conventional and unconventional IEL using a TCR transgenic system expressing a TCR specific for a male antigen. Conventional T-cells were deleted in male mice, whereas CD8αα IEL with a TCR specific for this male antigen remained detectable. Strikingly, transgene positive CD8αα IEL were absent in female mice, but the conventional T-cell population expressed the transgene[229], indicating that the presence of self-antigens is required for CD8αα development.

CD8αα IEL are distinct from thymus derived T-cells and were therefore believed to be generated directly in the gut wall. This hypothesis was supported by the finding that in primitive vertebrates the adaptive immune system is located in the GI tract. Furthermore, the epithelia of the GI tract and the thymus share a common endodermal origin[230] and genes specific for T-cell development such as Rag, or pTα were detected in lineage^{neg} cells isolated from the gut wall[231,232]. However the finding that CD8αα IEL are 5-10 fold reduced in athymic nude mice and, contrary to euthymic mice, almost all of them express the γδTCR questioned the sole extrathymic origin of CD8αα IEL[233]. Experiments showed that CD8αα IEL are thymus derived because of their reduction following thymectomy in the neonatal. To support this contention, the transplantation of neonatal thymus into thymectomised recipients recovered the pool of CD8αα IEL[234]. While these experiments established that IEL are thymus derived, their differentiation within the thymus still remains incompletely defined. Two different hypotheses exist about the differentiation state of putative IEL leaving the thymus. In the first model, immature precursors leave the thymus before their TCR rearrangement and finish their maturation in the gut. In the second model mature thymocytes that have already rearranged their TCR acquire the CD8αα phenotype after colonialisation of the gut wall[235]. The first model is supported by a study in which wild type thymus was transplanted into Rag/γ_c deficient hosts. The host thymus was found be to colonised by donor-derived wild type Lin^{-}CD44^{+} precursors, that emerged from the wild type thymus. This emigration of early precursors from the thymus is further supported by the localisation of DN1 cells inside the thymus. The DN1 population resides close to the cortico-medullary

junction, where precursors enter the thymus and fully mature T-cells emigrate. In addition, approximately 20% of DNI were shown to express S1P1, a molecule required for thymocyte egress, and these cells also upregulate $\alpha_4\beta_7$ integrin important for gut homing. Furthermore, intravenous injection of $CD44^+$ precursors was shown to reconstitute the CD8αα IEL pool in nude mice[235,236]. The second model is supported by fate mapping experiments, showing that all TCRαβ$^+$CD8αα cells were once double positive during their development[237,238]. Further support comes from anergic coreceptor^{negative} TCR-β^+ thymocytes, which leave the thymus as $CD4^-$ and $CD8^-$ but TCR-β^+ cells and acquire a CD8αα IEL in the gut[228]. However these two models are not mutually exclusive.

1.9.1. Inflammatory bowel disease

Shortly after birth the intestinal lumen is colonised by commensal bacteria. These commensal bacteria take advantage of an environment that is rich in nutrients derived from ingested food and contribute to the digestion of food, provide essential nutrients and prevent propagation of pathogenic microorganisms[239]. The microbiom is species specific and important for proper immune reactions in the gut. Germ-free mice that were colonised with human microbiota were more susceptible to infections, and the T-cell numbers in the small intestine were reduced and comparable to that of germ-free mice. Reconstitution with mouse microbiota, however, was able to restore the intestinal immune compartment and protect the mice from infections[240]. The intestinal immune system has to discriminate between commensal and pathogenic bacteria and mount an immune response accordingly. A disturbed immune response towards components of the normal intestinal flora in the gastrointestinal tract results in inflammatory bowel disease (IBD)[241]. IBD occurs in immunocompetent individuals and is characterised by an infiltration of innate and adaptive immune cells into the lamina propria resulting in increased numbers and activation of these cells in the intestinal mucosa. This leads to locally elevated levels of cytokines and eventually a cytokine driven inflammation of the gut. Regeneration and repair of the epithelium is important for the control and clearance of the inflammatory response to injury. In the case of IBD the inflammatory response result in a constant tissue injury causing erosions, ulcerations and a decrease in the production of protective defensins[242], leading to a further exposure to bacteria and thereby to an amplification of the immune response. Patients with IBD suffer from diarrhoea, rectal bleeding, abdominal pain and weight loss. Two common forms of IBD are Crohn's disease

and ulcerative colitis. Crohn's disease affects both the small intestine and the colon and is associated with an increased production of the cytokines IFN-γ and IL-17[243], whereas ulcerative colitis only affects the colon and is associated with excess of IL-13 production. However both diseases are chronic and relapsing. The colon pathology includes edemas, infiltrations of large numbers of inflammatory cells, erosions and ulcerations. Several factors are identified to contribute to IBD. IBD can be triggered by the immune system itself, by the gut microbiota or by genetic factors, however the disease is mostly an interplay of different factors[244].

Genetic factors can lead to epithelial dysfunction and favour inflammations. Mice deficient for Prostaglandin E receptor 4 (EP4), which is involved in repair and barrier functions, showed increased susceptibility to chemically induced colitis[245]. EP4 was also shown to play a role in humans suffering from IBD[246]. The importance of goblet cells is highlighted in mice deficient for the mucin protein MUC2 which developed intestinal inflammation[247]. In humans, MUC 19 was also associated with IBD[248]. In addition, defects in paneth cells were shown to contribute to human IBD[249].

$CD4^+$ T-cells in the intestine can be divided into effector and regulatory T-cells. The effector T-cells can mount either a Th1, Th2 or Th17 response, all of them were associated with different forms of IBD. In the healthy intestine the regulatory mechanisms are controlling the effector T-cells, however if this equilibrium is disturbed inflammation will occur (Figure 1.6). There are several regulatory lymphocytes mediating tolerance in the intestine. These mechanisms involve not only the reduction of inflammation but also enhancing the integrity of the intestinal barrier. These regulatory cells can also interact with IEC and enhance thereby their barrier function. The two main key players in providing tolerance in the gut are IL-10 and TGF-β, both factors can induce regulatory T-cell populations[250]. IL10 is a potent suppressor of macrophage and T-cell function. Mice deficient for IL-10 develop colitis, however in specific pathogen-free conditions these mice display only a local inflammation, indicating that IL-10 is an immunoregulator in the intestinal tract[251]. Experiments with IL-10 deficient mice that were also deficient for B-cells showed that the colitis was induced only by $CD4^+$ T-cells[252]. In animal models injection of recombinant IL-10 rebuilt the intestinal homeostasis, furthermore the addition of IL-10 inhibits colitis in adoptive transfer model[253,254]. TGF-β is another regulatory molecule involved in colitis induction. TGF-β receptor II deficient mice die because of inflammation triggered by T-cells[255,256]. The

development of NKT cells and $CD8^+$ T-cells as well as maintenance of peripheral Foxp3-expressing regulatory T-cells depend on TGF-β signalling. TGF-β plays also an important role in the homeostasis of the epithelium as demonstrated by TGF-β receptor II specific deletion in goblet cells, which results in colitis[257].

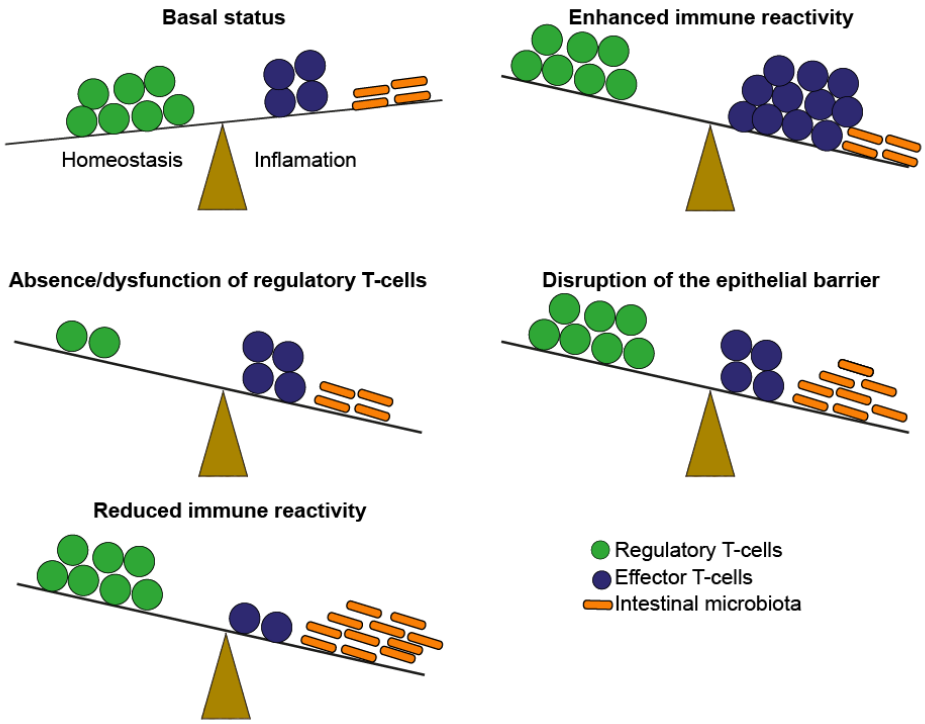

Figure 1.6: Pathways to mucosal inflammation: In the basal status the regulatory mechanism protect from colitis. However if this balance is disrupted colitis occur. Reasons for colitis can be an enhanced immune reactivity, or the absence of regulatory T-cells. Furthermore the disruption of the epithelial barrier and also a reduced immune reactivity can lead to an increase in proinflammatory stimuli and result in colitis. Adapted from Izcue et al 2009[258]

A hyperreactivity to the normal microbiom is observed in various animal models such as IL-2 or IL-10 deficiency[259]. However IBD is not observed in germfree mice, indicating that the microbiom drives the inflammation of the mucosa. This is further confirmed by crossing of IL-10 deficient mice with MyD88 deficient mice, which results in the absence of colitis, indicating that microbial components are required for IBD[260]. Colitis is therefore the result of a dysfunctional interaction between the bacterial microflora and the gut mucosal immune system. Changes in the microflora, either in numbers or in the composition of the microorganisms can cause the loss of tolerance. However a defect in the mucosal immune

system can also cause colitis, either by a defective effector T-cell population, which overreacts, or by defective or absent regulatory T-cells.

2. Aim of the project

Foxn1 is the key transcription factor for thymus development and TEC differentiation. In the absence of functional Foxn1 TEC fail to differentiate and remain in an immature common progenitor stage.

The aim of this project was to establish whether Foxn1 expression is required only at the onset of thymus organogenesis, or alternatively whether Foxn1 expression is also critical during the postnatal thymus for regular TEC biology. Furthermore it was investigated whether reduced Foxn1 expression suffices for TEC development, and weather different TEC subsets have different requirements for Foxn1. To assess these questions novel experimental models were created that control the expression of Foxn1 in a time sensitive-fashion or the extent of transcription, respectively. Specifically I wished to assess whether Foxn1 expression is required in the post natal thymus. It was hypothesised that Foxn1 expression at the onset of thymus organogenesis would rescue thymus development, as in the adult thymus Foxn1^{negative} TEC were detected expressing both Dll4 and CCL25[137]. This would indicate that Foxn1 is no longer required after initial organ formation as TEC develop and maintain the expression of Dll4 and CCL25 in the absence of continuous Foxn1 expression, still allowing the attraction of precursors and their development into the T-cell lineage. The second aim was to assess whether cTEC and mTEC display a differential Foxn1 dependence and weather a reduced Foxn1 expression result in thymus development.

The following questions were investigated:

- The effect of reduced Foxn1 or Foxn1 withdraw for TEC and thymus development
- T-cell development in the altered microenvironment
- Functionality of the T-cells and their subsets

3. Materials and methods

3.1. Mice

Conditional Foxn1$^{fl/fl}$ mice were designed and generated in our laboratory by Marcel Keller and Thomas Boulay.

In brief a Foxn1 targeting vector was constructed from a PGKneoF2L2DTA backbone (kindly provided by Philippe M. Soriano New York USA), the 5' homology arm contained parts of exon 6 and 3' homology arm parts of exon 9. Exons 7 and 8 encoding for the DNA binding domain were inserted at a SmaI restriction site and flanked by loxp sites. The construct included a neomycin resistance cassette, for positive selection flanked by FRT sites and diphtheria toxin A (DTA) cassette as a negative selection marker. Electroporation of ES cells with the targeting vector and mouse generation was done external by inGenious Targeting Laboratory Inc. (New York, USA). The received mice were on a 129 x C57Bl/6 mixed background and crossed to C57Bl/6 mice in our facility. This mouseline was designated as Foxn1loxneo. The mice were crossed to Flp deleter mice (129S4/SvJaeSor-Gt(ROSA)26Sor$^{tm1(FLP)Dym/j}$) obtained from The Jackson Laboratory. The resulting line was named Foxn1floxed. Foxn1$^{fl/fl}$ mice were crossed to Foxn1-Cre mice [Zuklys at al. 2009] to achieve TEC specific deletion of Foxn1. C57Bl/6 nu/nu and C57Bl/6-Ly5.1 [B6.SJL-Ptprc^{a}/BoyJiTac] mice were purchased from Taconic. B6 Rag 2$^{-/-}$ mice were obtained from the Jackson Laboratory.

For developmental staging, the day of vaginal plug was considered as embryonic day (E) 0.5. Mice were housed at the center for biomedicine animal facility in accordance with institutional guidelines and cantonal review board.

3.2. Cell suspension and cell counting

Cell suspensions of lymph nodes and spleen were obtained by placing the organs between two wet meshes, 70-100 µm pore size and rub gently with a plunger or forceps until most cells are squeezed out. The resulting cell suspensions were washed in PBS+2% FCS (fetal calf serum) and centrifuged 5 minutes at 4°C, 1500 rpm, or alternatively in 1minute at 4600rpm (1.5ml Eppendorf tube). Red blood cells of the spleen were lysed in ACT (Ammonium Chloride – Tris buffer; 1 ml per 30x10^{6} cells), after two minutes the reaction was stopped by adding

IMDM (Iscove's Modified Dulbecco's Medium) plus 2% FCS, centrifuged and resuspended in PBS plus 2% FCS (FACS buffer). Staining and cell counting was performed in PBS plus 2% FCS.

Cells were counted using a Z1 Coulter particle counter from Beckman Coulter. 20µl of cell suspension and three drops of zap-oglobin II lytic reagent from Beckman Coulter, Inc. (Beckman Coulter, Inc. , Fullerton, CA, USA) were added to 10 ml Isoton II.

3.2.1. TEC isolation

For thymic epithelial cell isolation, thymi were pooled and digested at 37°C using 1mg/ml Collagenase D + 50µg/ml DNase I in FACS buffer. After 10 minutes of incubation on a thermomixer (Eppendorf) at 700 rpm the thymi were pipetted up and down around 20 times. If still clumps were visible the thymi were incubated another five minutes before pipetting again, until all clumps were dissolved resulting in a single cell suspension. The cells were washed and resuspended in PBS plus 2% FCS.

3.2.2. Tissue lymphocyte analysis

The entire intestine of wild type, Foxn1$^{neo/neo}$, Foxn1$^{lox/lox}$::Foxn1-cre and C57Bl/6 nu/nu mice were isolated and faeces were removed. The Peyer's patches were removed from the small intestine. A small piece of the colon and small intestine was frozen for histological analysis. The colon and small intestine were first cut longitudinally and then into small pieces of 0.5-1 cm length. The pieces were incubated twice 10 minutes at room temperature in 10 ml IMDM + 10 % FCS + 1mM DTT on a shaking platform (200 rpm) to remove debris. The fragments were washed and resuspended in 10 ml IMDM+10%FCS. Intraepithelial lymphocytes (IEL) were isolated by vortex (2x 4 minutes, in 10ml each). For lamina propria lymphocytes (LPL) isolation the fragments were incubated 45 minutes at 37°C in 5ml IMDM + 10% FCS + 1mg/ml Collagenase IV. After isolation IEL and LPL were washed, resuspended in FACS buffer, counted and stained.

3.2.3. Bone marrow isolation

The femur was isolated, cut above the knee and placed open end down in a 5 ml Falcon tube which was equipped with a cut-off tube and 300µl media. The tubes were centrifuged at 2000 rpm 5 minutes, the tip containing the bone was removed and the samples were proceed to staining.

3.3. Antibodies, flow cytometric analysis and sorting

Staining was performed in PBS+2%FCS on ice, antibodies were added at optimized dilutions and incubated for 30 minutes. Depending on the amount of cells, either 5 ml or 10 ml Falcon (BD, Franklin Lakes, NJ, USA) or 1.5 ml Eppendorf (Hamburg, Germany) tubes were used. In case of biotin-conjugated antibodies, a second staining step with fluorochrome labelled streptavidin was performed. Prior to analysis DAPI was added to a final concentration of 0.1 ng/µl. Before acquisition the cells were filtered through a 40µm mesh. Acquisition and sorting of TEC, CD4 T-cells and regulatory T-cells were performed using FACS ARIA (BD Bioscience), controlled by FACS Diva software, and analysis was carried out using FlowJo 9.4 (Tree Star).

Antibodies used:

FITC labelled: CD24 (clone: M1/69; BioLegend), CD25 (clone: PC61; BioLegend), CD62L (clone: Mel-14; BioLegend), TCR Vβ2 (clone: B20.6; BioLegend), TCR Vβ6 (clone: RR4-7; BD), TCR Vβ8 (clone: F23.1; BD), TCR Vβ14 (clone: 14-2; BD), CD44 (clone: IM7; BioLegend), TCR-β (clone: H57-597 ; BioLegend), CD8β (clone Ly-3; BioLegend), Sca1 (clone: D7; ebioscience)

PE labelled: TCR-β (clone H57-597 ; BioLegend), CD44 (clone: IM7; BioLegend), FoxP3 (clone: FJK-16; ebioscience), Foxp3 (clone: 150D; BioLegend), TCR-γδ (clone: GL3; BioLegend), TNF-α (clone: MP6-XT22; BioLegend), TER 119 (clone TER119; BD), CD19 (clone ID3; BioLegend)

APC labelled: CD117 (c-kit) (clone: 2B8; BioLegend), Nrp1 (clone: 761705; R&D Systems)

Cy5 labelled: CD25 (clone: PC61; self made), CD19 (clone: ID3; self made)

Alexa 647: CD3 (KT3; selfmade), Helios (clone: 22F6; BioLegend), IL-17 (clone: TC11-18H10.1; BioLegend), CD8 (clone: 53.67; self made), B220 (clone: RA3-6B2; self made),

APC-Cy7 labelled: CD4 (clone: GK1.5; BioLegend).

PerCPCy5.5 labelled: CD25 (clone: PC61; BioLegend), EpCAM (clone: G8.8; BioLegend), Il10 (clone: JES5-16E3; BioLegend).

PE-Texas-Red labelled: CD19 (clone: 6D5; Molecular Probes), CD45 (clone: 30-F11; Molecular Probers)

PECy7 labelled: CD8 (clone: 53-6.7; BioLegend), CD45 (clone: 30-F11; Biolegend), Ly5.1 (clone: A20; BioLegend), IFN-γ (clone: XMG12; BioLegend), B220 (clone: RA3-6B2; BioLegend), CD44 (clone: IM7; BioLegend), CD62L (clone: Mel-14; BioLegend)

A-700 labelled: CD8α (clone: 53-6.7; BioLegend), CD45 (clone: 30-F11; BioLegend), CD62L (clone: MEL14; BioLegend), TCR-β (clone: H57-597; BioLegend)
Biotin: CD3 (clone: KT3; selfmade), CD4 (clone: GK1.5; selfmade), CD8 (clone: 53-6.7; BioLegend), CD11b (clone: M1/70; BioLegend),
CD11c (clone: N418; BioLegend), B220 (clone: Ra3-6B2; BioLegend), CD19 (clone: ID3; selfmade), CD45 (clone: M1/9.3.4HL2; selfmade), EpCAM (clone: G8.8; selfmade), TCRγδ (clone: GL3; ebioscience), F4/80 (clone: BM4; BioLegend), Pan NK (clone: DX5; BioLegend), NK1.1 (clone: PK136; Biolegend)
Streptavidin: PE (BioLegend); PECy7 (BioLegend), PerCpCy5.5 (BioLegend), PE-Texas-Red (Molecular Probes).

3.3.1. Intracellular staining

3.3.1.1. Foxp3 staining

For Foxp3 staining the cells were fixed and permeabilized using Foxp3 staining kit from eBioscience, according to the manufacturers protocol. Unspecific staining was blocked using 10% normal mouse serum and 15% 2.4G2 supernatant (self-made). For Foxp3 staining in combination with Helios the Foxp3 staining kit and antibody from BioLegend was used, according to the manufacturers protocol.

3.3.1.2. Cytokine staining

For cytokine staining the cells were stimulated using 1µg/ml Brefeldin A (Sigma), 0.5µg/ml Ionomycin (Sigma) and 0.05µg/ml PMA (Sigma) 4 hours at 37°C. The cells were fixed and permeabilized using cytofix/cytoperm kit from BD, according to the manufacturers protocol.

3.3.2. Cell depletion

Prior to sorting of regulatory T cells and CD4 T cells cell suspensions were enriched for $CD4^{pos}$ cells. The isolated cells were labelled with biotinylated CD4 antibodies and incubated for 20 minutes on ice, followed by a washing step and resuspended at $100*10^6$ cells/ml. 50µl of anti-biotin microbeads (Miltenyi Biotec) were added. The cells were incubated 15 minutes in the fridge, washed and filtered. The cells were then applied to an AutoMACS separator (Miltenyi Biotec), where labelled cells were enriched. The CD4 enriched cells were further stained and analysed or sorted. Alternatively for some T-cell analysis $B220^{pos}$ cells were depleted using dynabeads. In brief cells were labelled using RA3-6B2 antibody 30 minutes,

washed and incubated with dynabeads (life technologies) 15-20 minutes, B220 positive cells were removed by magnetic separation.

3.4. Histology

3.4.1. Tissue embedding

Pieces of colon, small intestine, thymus lobes and whole embryos (E11.5, E12.5, E13.5) were embedded in OCT compound (Medite) in Cryomolds (Tissue-Tek; Biosystems). Tissues were frozen using 2-Methylbutane (Sigma) in combination with dry ice and then stored at -80°C until cutting.

3.4.2. Cutting

Sections of 6-8µm thickness were cut using a cryostat (Roche). Sections of embryos were cut, stained with toluidine blue and inspected under the microscope. As soon as the thymus was reached the sections were collected. The sections were mounted on superfrost plus slides (Menzel-Gläser, Thermo Scientific) and air dried over night. The following day the sections were either stained directly or wrapped in aluminium foil and stored at -80°C until usage.

3.4.3. H&E

Sections were fixed 45'' in Delaunay fixation (100ml ethanol, 100ml acetone and 0,2 ml 1M TCA), rehydrated in gradient ethanol solutions (100%, 96%, 70% and 50% ethanol) 45'' each and then H_2O. Afterwards stained 2 minutes with Hematoxyline, washed 3 times 1 minute in warm H_2O, counterstained in 1% aqueous Erythrosine B solution and washed 3 times 1 minute in H_2O. The tissue was dehydrated in gradient ethanol solutions (50%, 70%, 96% and 100% ethanol), finally the coverslips were mounted using Pertex. Imaging was done using a Nikon Eclipse E600 microscope (10x/0.3 NA Plan-Flour objective. The pictures were taken using a Nikon DXM 1200F camera controlled by Nikon ACT-1 software (Nikon instruments, Europe).

3.4.4. Histological analysis and colitis score

Colon slices were frozen in OCT, and sections of 7 µm were cut and stained with Haematoxylin and Erythrosine B. The tissues were graded from 0 to 4, according the following features: grade 0, no changes observed; grade 1, mild cell infiltrations and slight epithelial cell hyperplasia; grade 2, pronounced epithelial cell hyperplasia, significant cell

infiltrations in mucosa as well as submucosa and mild depletion of goblet cells; grade 3, marked epithelial cell hyperplasia, extensive cell infiltrations in mucosa, submucosa as well as tunica muscularis and significant depletion of goblet cells; grade 4, marked epithelial cell hyperplasia, extensive cell infiltrations and substantial depletion of goblet cells (>50%). Each section was rated twice at different days, the grade indicated was the mean of both ratings.

3.4.5. Immunohistochemistry

6-8µm thick tissue sections were fixed in cold Acetone (-20°C) 10 minutes at RT. The tissue sections were encircled with Pap pen (Biosystems) and dried 2 minutes, rehydrated twice 10 minutes in PBS and incubated 20 minutes with 5% goat serum in PBS to block nonspecific binding. Staining with primary antibodies, diluted in goat serum was preformed. After 1 hour of incubation the slides were washed twice 5 minutes in PBS and the secondary antibodies were added. After 45 minutes incubation time the slides were washed twice 5 minutes in PBS. Prior to mounting DAPI was added for 5 minutes, the slides were washed again and the coverslips were mounted using Hydromount (National Diagnostics). Images were acquired using Zeiss LSM 510 confocal microscope and Zeiss LSM 510 acquisition software, version 3.2 (Carl Zeiss) or a Leica DMI 4000 microscope using AF 6000 software. All pictures were processed and assembled using Image J (http://rsbweb.nih.gov/ij/).

3.4.5.1. Antibodies used:

Rabbit anti-CK5 (Covance), mouse anti-CK8 (Progen), mouse anti-CK18 (Progen), rat anti-ERTR7 (provided by W. van Ewijk, Utrecht, Netherlands), Aire (clone: 5H12; provided by S. Hamish, Adelaide, Australia), CD31-FITC (clone 390; ebioscience), rabbit anti-β5t (MBL, Japan), Rabbit anti-Foxn1 (provided by T. Amagai, Japan), CD4 (clone H129; self made), CK14 (Covance)

As secondary antibodies Alexa Fluor-conjugated anti-IgG antibodies (life technologies) and SA-Cy3 (BioLegend) were used.

As negative controls only the secondary antibodies were applied.

3.4.5.2. Antigen retrieval

For Foxn1 protein detection an antigen retrieval was performed. Thymus or embryos were collected and fixed in 4%PFA in PBS for 4 hours (thymus) or over night (embryos) at 4°C. The tissue was placed in 20% sucrose in PBS prior to cryopreservation in OCT compound.

For antigen retrieval the slides were boiled in 10mM NaCitrate (pH 6), then left on the bench 20 minutes and boiled again. The slides were cooled down and the staining protocol was proceeded starting with the blocking step.

3.5. In vitro T-cell activation and proliferation assays

Freshly sorted CD4 T cells were washed in PBS and labelled with 2.5µM CFSE for 7 minutes at room temperature and washed twice with media. Sorted CD4 T cells were activated using 1µg/ml anti-CD3ε (self made) in the presence of irradiated B6 $Rag2^{-/-}$ splenic accessory cells (AC) in a 1:1 ratio. The cells were co-cultured for 72 hours in 96 well plates round bottom (Falcon). The proliferation index was calculated using flow jo software. Suppression assays were set up using CFSE labelled effector T-cells and Tregs in a 1:1 ratio in the presence of anti-CD3ε and accessory cells in a 1:1 ratio.

3.6. Adoptive transfer of T cells

CD4 and regulatory T cells were sorted, washed and re-suspended in HBSS and finally injected intravenously into the tail vein of B6 $Rag2^{-/-}$ mice. Injection was preformed with 100'000 CD4 cells isolated from either wild type, $Foxn1^{neo/neo}$, $Foxn1^{fl/fl}$::Foxn1-Cre or nude mice. The mice were controlled and weighed every second day. If the weight loss constituted more than 20% of the maximal bodyweight the mice were analysed.

3.7. RNA isolation and quantitative reverse-transcribed polymerase chain reaction analysis

3.7.1. RNA isolation

RNA of sorted cells was isolated using the micro RNeasy kit from Qiagen (Qiagen, CA, USA). RNA isolation was performed according to the manufacturers protocol. TECs were sorted directly into RLT lysis buffer (provided by the kit) and stored at -80°C until they were further processed. Thymus isolated on embryonic day 12.5 were collected and cultured on a filter until genotyping was performed. Then they were digested as described previously. The pellet was resuspended in lysis buffer and stored at -80°C until they were further processed.
In short the samples were mixed with an equal volume of 70% ethanol and applied to a RNeasy micro column and centrifuged (15 seconds, 10000rpm). Then 350µl of RW1 buffer

was added and centrifuged (15 seconds, 10000rpm) to bind total DNA. To digest DNA the samples were incubated 15 minutes with 80µl DNase1 incubation mix afterwards 350µl of RW1 buffer was added and centrifuged (15 seconds, 10000rpm). To wash 500µl RPE buffer was added and centrifuged (15 seconds, 10000rpm). In a next step 500µl 80% ethanol was added and centrifuged (2 minutes at 10000rpm). Then the samples were dried by centrifugation at maximal speed for 5 minutes. By adding 12 µl of RNase free water the RNA was eluted 1 minute at maximum speed. The samples were stored at -80°C until further processing to cDNA.

3.7.2. cDNA synthesis

For cDNA synthesis 12µl of total RNA were transferred into 0.6 ml tubes (genuine Axygen Quality, CA, USA) and mixed with 1µl dNTP (10mM), 1µl random hexamere (500ng/µl, Sigma, St. Louis, Mo, USA) and 1µl dT20 (1µM/µl, Mycrosynth, Balgach, Switzerland). The samples were denatured 5 minutes at 65°C followed by 1 minute on ice. Then 4.5 µl 5x first strand buffer, 1µl DTT (10mM, Invitrogen, Carlsbad, CA, USA), 1µl RNase Out (20u/µl, Ambion, Foster City, CA USA) and 1µl Superscript III (RT 200U7µl, Invitrogen) were added. The samples were incubated at 25°C for 5 minutes, followed by 50°C for 60 minutes. The reaction was finally inactivated at 70°C for 15 minutes and cDNA was stored at -20°C.
dNTPs: Are a mixture of dATP, dGTP, dCTP and dTTP 10 mM each at neutral pH.
5x first strand buffer: Consists of 250mM Tris-HCl (pH 8.3 at room temperature), 375 mM KCL and 15 mM $MgCl_2$ (Invitrogen).

3.7.3. qPCR- Quantitative PCR

qPCR was performed using the SensiMix dT Kit (Quantace Ltd, London, UK).
The reaction mix contained: 6.25µl Sensimix 2x+50x (Quantance), 0.375 µl forward primer (10mM), 0.375µl reverse primer (10mM) and 2.75µl H_2O. Finally 2.75 µl of cDNA was added into 0.1 ml strip tubes from Corbett Research (Corbet Research, Sydney, Australia).
qPCR was performed in duplicates using a Rotor-gene RG-3000A (Corbet research) and the following program:
95°C for 10 minutes, followed by 50 cycles of 95°C 10 seconds (denaturing), 60°C for 15 seconds (annealing) and 72°C 20 seconds (elongation) and melting from 72°C to 95°C. Data analysis was performed using Rotor gene 6 software. PCR specificity was controlled by analysing the melting curves. The data was exported as Microsoft Excel file. Expression

levels of specific mRNA were normalised to GAPDH expression by calculating $2^{-\Delta CT}$ whereas ΔCT is defined as the CT of the gene of interest- the CT of housekeeping gene. Mean values were compared between wild type and mutant mice using a Mann-Whitney U test (two-tailed).

Primers used:

Foxn1:

(forward primer): TCT ACA ATT TCA TGA CGG AGC ACT

(reverse primer): TCC ACC TTC TCA AAG CAC TTG TT

CCL21:

(forward primer): AGC TAT GTG CAA ACC CTG AGG A

(reverse primer): TTC CAG ACT TAG AGG TTC CCC G

CCL25:

(forward primer): GTT ACC AGC ACA GGA TCA AAT

(reverse primer): GGA AGT AGA ATC TCA GAG CA

CCL19:

(forward primer): CCT GGG TGG ATC GCA TCA TCC G

(reverse primer): AGA GCA TCA GGA GGC CTG GTC CT

CXCL12:

(forward primer): AAA TCC TCA ACA CTC CAA AC

(reverse primer): GCT TTC TCC AGG TAC TCT TG

GAPDH:

(forward primer): GGT GAA GGT CGG TGT GAA CG

(reverse primer): ACC ATG TAG TTG AGG TCA ATG AAG G

EpCAM:

(forward primer): TGA GGA CCT ACT GGA TCA TC

(reverse primer): TAT CGA GAT GTG AAC GCC TC

3.7.4. Genotyping of mice

The mice were numbered and genotyped by toe clipping. A small piece of toe was digested in 500µl lysis buffer containing Proteinase K at 56°C in a Thermomixer shaking at 750 rpm (Eppendorf). PCR was performed either directly from the lysate or if necessary further purification was done. To purify undigested tissue was pelleted 10 minutes at maximum speed and the supernatant was poured into an equal amount of isopropanol. The tubes were inverted and DNA precipitate was formed, after 5 minutes the precipitates were centrifuged

10 minutes at maximum speed and washed in 70% ethanol. The supernatant was discarded and the DNA pellet was air dried approximately 30 minutes and resuspended in 200µl TE buffer. The tube were incubated at 56°C on a thermomixer shaking at 750µm for 2 hours until the pellet was resuspended. The DNA was stored at +4°C until PCR analysis.

PCR reaction mix

2.5µl 10x buffer

0.5µl dNTP's (2.5mM)

1.0µl forward primer

1.0µl reverse primer

19.4µl H_2O

0.1 µl Taq polymerase

0.5 µl DNA template

Total Volume 25 µl

PCR conditions

94°C 4 minutes initial denaturation

followed by 33 cycles 30 seconds at 94°C (denaturation), 30 seconds at 58°C (annealing) and 40 seconds at 72°C (elongation).

And final elongation 10 minutes at 72°C.

For genotyping the following primers were used:

forward primer: CCCTGTCTCGAAAAACCAAA

reverse primer: GGCTCTAGGTCTGGGGATTC.

For verification of Foxn1 deletion the following primer pair and PCR conditions were used:

Forward primer: 5' CCC TGT CTC GAA AAA CCA AAC 3'

Reverse primer: 5' CTT TTC CCA GCT TTG TCA GAT3'

94°C 4 minutes initial denaturation

followed by 33 cycles 30 seconds at 94°C (denaturation), 30 seconds at 58°C (annealing) and 60 seconds at 72°C (elongation).

And final elongation 5 minutes at 72°C.

3.7.5. Agarose gel electrophoresis

1.3 g agarose (Invitrogen) were dissolved in 100ml 1xTAE buffer in a microwave-oven under heating. The gel was cooled down and poured into an electrophoresis chamber. 2µl of 6x loading dye including gel red (Biotium, Hayward, CA) were added to 10µl of the PCR products and to the marker. Per sample 10µl were loaded on the gel. The gel was run for at least 45 minutes at 75V. 10µl of a 1 Kb plus DNA ladder (Invitrogen) was used as a standard to determine the size of the PCR products. The gels were finally analysed using a Gel Doc XR system controlled by Quality One 4.6.2 software from Bio-Rad.

3.8. Enzyme-linked immunosorbent assay (ELISA)

3.8.1. IL-2 ELISA

IL-2 concentrations were determined in the supernatant of activated T-cells on day 3 of the proliferation assay performing an ELISA (IL-2 ELISA kit, ebioscience) according to the manufactures protocol.

3.8.2. Detection of anti-ssDNA autoantibodies in serum

Blood was extracted from the mouse heart and transferred into Microtainer SST tubes (BD). After at least 30 minutes incubation at room temperature the coagulated blood was spun down at maximal speed 1 minute. The serum was collected and transferred into a fresh tube and stored at 4°C until further analysis. To detected anti-single-stranded DNA autoantibodies a flat bottom 96 ELISA well plate (Corning) was coated with 100µl/well PBS containing 2.5 µg/ml of heat-denatured calf thymus-ssDNA (pH7.2; Sigma) and incubated over night at 4°C. The next day the plate was washed 3 times with ELISA washing buffer and 150µl/well blocking buffer was added. After 2 hours of incubation at RT the plate was washed 3 times before 100µl of sample was added. The serum samples were diluted 1:100 in ELISA blocking buffer. After 2 hours of incubation the plate was washed 3 times in ELISA washing buffer and 100µl of the secondary antibody IgG2 alkaline phosphate labelled (BD Pharmingen) was added. After 1 hour of incubation the plate was washed 6 times in ELISA washing buffer and developed with 50µl of the alkaline phosphatase substrate DNPP (Sigma) dissolved in substrate buffer. After 15 minutes the reaction was stopped by adding 50µl 1M NAOH and the absorption was measured at a wave length of 405 nm.

3.9. Anti-nuclear antibodies analysis

The serum of mice was diluted in FACS buffer in a starting dilution of 1:100. The serum was incubated 30 minutes on a kidney section isolated from a $Rag2^{-/-}$ female mouse. Afterwards the sections were washed twice 10 minutes in PBS before staining with anti-mouse IgG-Alexa 488 (life technologies) for 30 minutes at room temperature in the dark. Then the slides were washed again twice 10 minutes in PBS followed by 5 minutes of DAPI staining and washed in PBS for another 10 minutes. Finally the coverslips were mounted using hydromount. The samples were analysed using a Leica DMI 4000 microscope. Pictures were taken with a Leica DFC345 FX camera, the system was running by Leica AF 6000 software. ANA positive sera were further titrated 1:500, 1:1000 and 1:2000.

3.10. Solutions

IMDM medium:	500 ml (Gibco-BRL, Gaithersburg, USA) + 10% FCS (Hyclone, Perbio, Erembodegem, Belgium) + 5 ml Kanamycin sulfate (Gibco-BRL) +0.5 ml 2-mercapto-Ethanol (50MM, Gibco-BRL)
1x PBS (sterile):	Dulbeco's phosphate buffered saline (Sigma) without $CaCl_2$ and $MgCl_2$ Mili-Q water Filter sterilised (0.22µm cellulose acetate, bottle top filtered, Coroning, NY, USA)
HBBS:	500 ml (Gibco-BRL) without $CaCl_2$ and $MgCl_2$
FACS-buffer:	2% FCS in PBS
AutoMACS running buffer:	FACS-buffer + 2.5mM EDTA (Gibco)

ACT:	0.16 M NH_4Cl (Sigma) 2.06g Trizma®base (Sigma) in 90ml dH^2O pH 7.65 fill to 100ml
6x Loading buffer:	0.25% Bromophenol blue (Fluka, Buchs, Switzerland) 0.25% Xylene cynol FF (Fluka) 15% Ficoll (Type 400; Sigma) Add to 50 ml ddH_2O
DNA ladder:	Ready-load 1Kb Plus DNA ladder (Invitrogen)
50x TAE:	242g Trizma®base (Sigma) 57.1ml Glacial Acetic Acid (Fluka) 100ml EDTA (0.5M, pH 8.0; Sigma)
Collagenase D:	Roche diagnostics
Dnase:	Roche diagnostics
Collagenase IV:	Worthington
DAPI:	Invitrogen
Toluidine blue:	0.25 g per 50ml miliQ H_2O (Sigma)
PFA:	4%; dissolved at 55°C for 2 hours. (Merck)
Sucrose:	20% (Fluka)
Acetone:	Sigma
Blocking:	5% normal goat serum in PBS (Gibco-BRL)
Tail lysis buffer:	100mM Tris pH8.5 (Sigma) 5mM NA-EDTA (Sigma) 0.2% SDS (Fluka) 200mM NaCl (Fluka) Fill up to 1L with H_2O

Proteinase K was freshly added to a final concentration of 100µg/ml ()

Cell counting:	Isoton II solution (Beckman Coulter, USA)
	Zap-oglobin™ II lytic reagent (Beckman Coulter, USA)
ELISA wash buffer:	0.1% Tween20 in PBS (Fluka)
ELISA blocking buffer:	2% BSA in PBS (Fluka)
Dinitrophenylphosphate:	100mg/ml in dH_2O (Sigma)
ELISA Substrate buffer:	0.1mg/ml $MgCl_2$ x $6H_2O$ (Fluka)
	2% 1M NaN_3 (Fluka)
	10% Diethanolamine (pH 9.8) (Merck)
	Fill up with H_2O

3.11. Statistical analysis

P values were calculated using Mann-Whitney U test (two-tailed), each experimental group was compared independently to wild type mice and to congenital nude mice in an independent analysis. Analysis was performed using GraphPad Prism 6 software (GraphPad Software Inc., La Jolla, CA, USA). P values of <0.05 were considered as significant.

4. Results

4.1. Mouse models for TEC targeted loss of Foxn1 function

Two mouse models that differ in the degree of a decrease of Foxn1 expression and its timing were used to investigate the role of Foxn1 in thymus organogenesis and maintenance. The two mouse strains specifically differ in the amount and timing of Foxn1 expression. Mouse model 1, designated $Foxn1^{neo/neo}$ has been generated to study the effect of reduced Foxn1 expression during and after ontogeny on thymus development and function. The second mouse model designated $Foxn1^{fl/fl}$::Foxn1-Cre allows a tissue-specific and time-controlled deletion of Foxn1 expression. This strain was used to investigate whether Foxn1 expression is continuously needed throughout life, or alternatively whether a functional thymus can be formed under the conditions that Foxn1 is only expressed during the start of thymic ontogeny but not later. The basic principle of the experimental models to be investigated are displayed in Figure 4.1.

All TEC express Foxn1 during embryogenesis, however in the postnatal thymus both $Foxn1^{+}$ and $Foxn1^{-}$ TEC were detected, expressing both Dll-4 and CCL25[137]. Foxn1 was shown to regulate the expression of Dll-4 and CCL25[143,144], their expression is absent in Foxn1 deficient mice, however in postnatal thymus their expression seems to be Foxn1 independent. Lineage tracing experiments showed, that the $Foxn1^{-}$ TEC are descendants from $Foxn1^{+}$ TEC[261]. Therefore the question was addressed whether Foxn1 expression is required in the adult thymus. TEC are a heterogeneous population consisting of cTEC and mTEC, with each different Foxn1 expression levels. Foxn1 is higher expressed in cTEC than in mTEC[106], and in $mTEC^{high}$ Foxn1 expression is higher when compared to $mTEC^{low}$[157]. In the aged thymus Foxn1 expression decreases[169]. Therefore the influence of reduced Foxn1 expression on thymus organogenesis and on the different subsets was studied.

Foxn1 expression in wild type mice starts at embryonic day E11.25, and is strongly detected at E12.5[136]. In $Foxn1^{neo/neo}$ mice the expression of Foxn1 is decreased when compared to wild type expression, but stably expressed. However in $Foxn1^{fl/fl}$::Foxn1-Cre mice, Foxn1 expression will start normally, but will be switched off once Cre recombinase is present (Fig. 4.1). Since the cre recombinase is under the Foxn1 promoter, Foxn1 will be deleted immediately after it was activated.

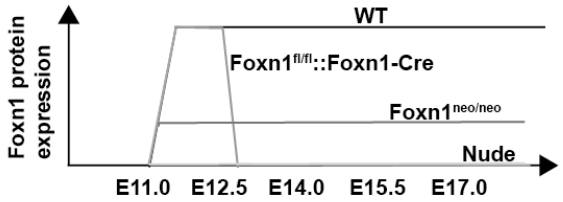

Figure 4.1: Mouse models displaying differences in Foxn1 expression. Schematic representation of expected Foxn1 protein expression in wild type (WT), Foxn1$^{neo/neo}$, Foxn1$^{fl/fl}$::Foxn1-Cre and nude mice.

Both mouse models were compared to wild type mice and congenital nude mice, using histology the thymic microenvironments of all four mouse strains was assessed and compared. Thymocyte development and peripheral T-cells were analysed using flow cytometry.

4.1.1. Generation of Foxn1$^{neo/neo}$ mice

To achieve conditionally deficient mice that allows for tissue and time restricted loss of regular gene expression, we targeted the Foxn1 locus such, that a loxP site was introduced each 5' of exon 7 and 9. The Foxn1 gene targeting vector was constructed using the PGKneoF2L2DTA backbone (kindly provided by Philippe M. Soriano, Mount Sinai Hospital, New York, USA). The homology arms of the targeting sequence contained 5' parts of exon 6 and 3' parts of exon 9 . Exons 7 and 8 encoding in part for the DNA binding domain were inserted at a SmaI restriction site flanked by loxP sites (Fig. 4.2). The targeting construct included a neomycin resistance cassette used for positive selection, flanked by FRT sites. A diphtheria toxin A (DTA) cassette was included for negative selection. Electroporation of ES cells with the targeting vector was done external by inGenious Targeting Laboratory Inc. Targeted ES clones were screened by PCR for homologous recombination and injected into blastocysts.

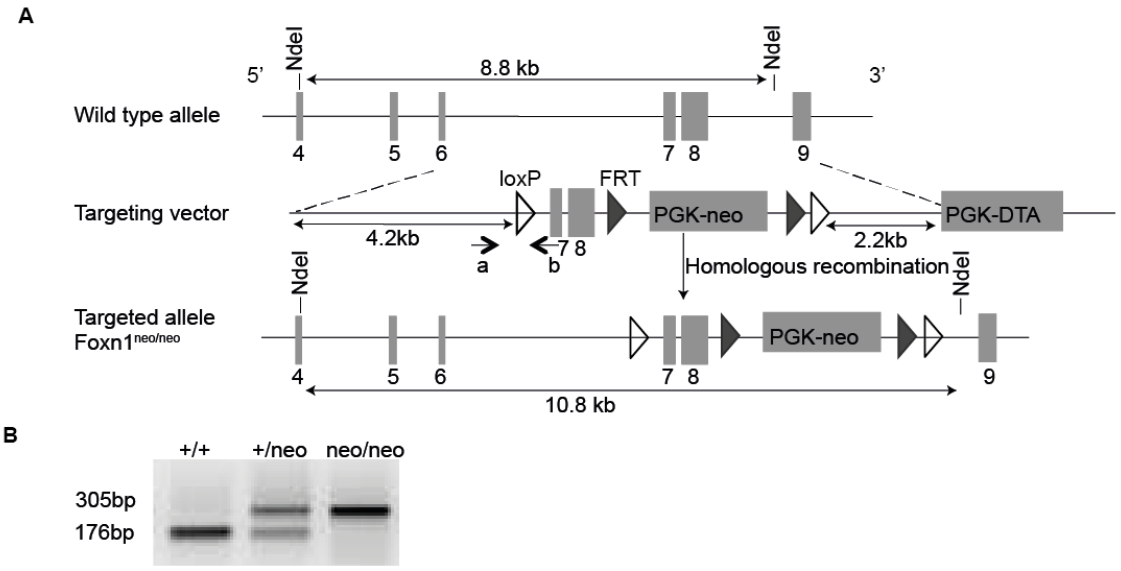

Figure 4.2: Generation of Foxn1$^{neo/neo}$ mice (A) Wild type Foxn1 genomic locus, targeting vector and structure of targeted Foxn1 allele (designated as Foxn1$^{neo/neo}$). Exons are numbered. a and b indicate primers used for genotyping. The restriction site Nde1 was used to verify correct homologous recombination. (B) PCR of wild type, Foxn1$^{+/neo}$ and Foxn1$^{neo/neo}$ locus using primers detailed in panel A.

The neomycin cassette in its intronic position impaired the transcription of Foxn1, which resulted in a decrease in Foxn1 expression. The relative amounts of Foxn1 transcripts were five-fold reduced in Foxn1$^{neo/neo}$ mice when compared to wild type mice (Fig. 4.3). The phenomenon that the PGKneo cassette can interact with locus control regions is well known and explained by a cryptic splice acceptor site between the PGK and the neomycin[262,263]. The persistent presence of the PGK-neomycin cassette between exons 8 and 9 generated a hypomorphic Foxn1 allele, allowing to study the impact of a reduced Foxn1 expression on thymus organogenesis and function. Heterozygous Foxn1$^{neo/+}$ mice did not show any defects in thymus and thymocytes development (Appendix I), suggesting that the presence of only one wild type Foxn1 allele result in thymus development and TEC differentiation. This is expected as mice heterozygous for the spontaneous Foxn1 mutation display a normal thymus and are able to support T-cell development at frequencies comparable to wild type thymus.

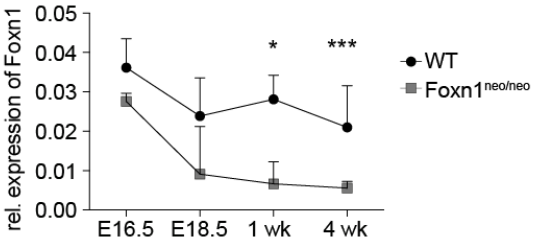

Figure 4.3: Reduced Foxn1 expression in Foxn1$^{neo/neo}$ mice. Quantification of Foxn1 transcripts in sorted wild type (WT) and Foxn1$^{neo/neo}$ TEC at different ages normalised to GAPDH. The data shows mean values ± Standard derivation, from three independent experiments. Statistical significance was calculated using Mann-Whitney test *p < 0.5, ** < 0.01, *** < 0.001.

4.1.2. Foxn1 deletion in Foxn1$^{fl/fl}$::Foxn1-Cre mice

To study the consequences of Foxn1 deletion early in organogenesis, conditional knock-out mice were generated (Fig. 4.4 A). The Foxn1$^{neo/neo}$ mice described in the previous section were crossed with mice expressing the recombinase flippase under the transcriptional control of the Gt(ROSA)26Sor promoter[264] to excise the neomycin cassette. The resulting line was breed to homozygosity and designated Foxn1$^{fl/fl}$. In contrast to Foxn1$^{neo/neo}$ mice with reduced Foxn1 transcripts, Foxn1 transcripts were normal in homozygous Foxn1$^{fl/fl}$ mice and thymus organogenesis proceeded normally (Appendix II). Homozygous Foxn1$^{fl/fl}$ mice were crossed with Foxn1-Cre mice[136]. Foxn1-Cre mice express the Cre recombinase under the control of the Foxn1 promoter, leading to a TEC and skin specific deletion of Foxn1. Cre specific recombination in Foxn1-Cre mice can be detected as early as E11.5 as shown by crossing Foxn1-Cre mice with Rosa26^{loxPlacZ} reporter mice[136]. However at this early time point β-galactosidase expression is limited to only a few epithelial cells when compared to Foxn1 protein expression, whereas at E12.5 both Foxn1 and β-galactosidase were broadly expressed, suggesting that β-galactosidase expression is approximately one day behind Foxn1 expression. This delay can be explained by the fact that Cre mediated loxP excision requires time, Cre transcription starts at E11.25, initiated by the Foxn1 promoter, this lead to formation of mRNA and finally to the protein and consequently loxP excision. Therefore there is a gap between the onset of Cre expression and the effect of Cre mediated exicision[263], which leads to a short one day window of Foxn1 expression before exon 7 and 8 are excised and Foxn1 transcripts cannot be generated anymore.

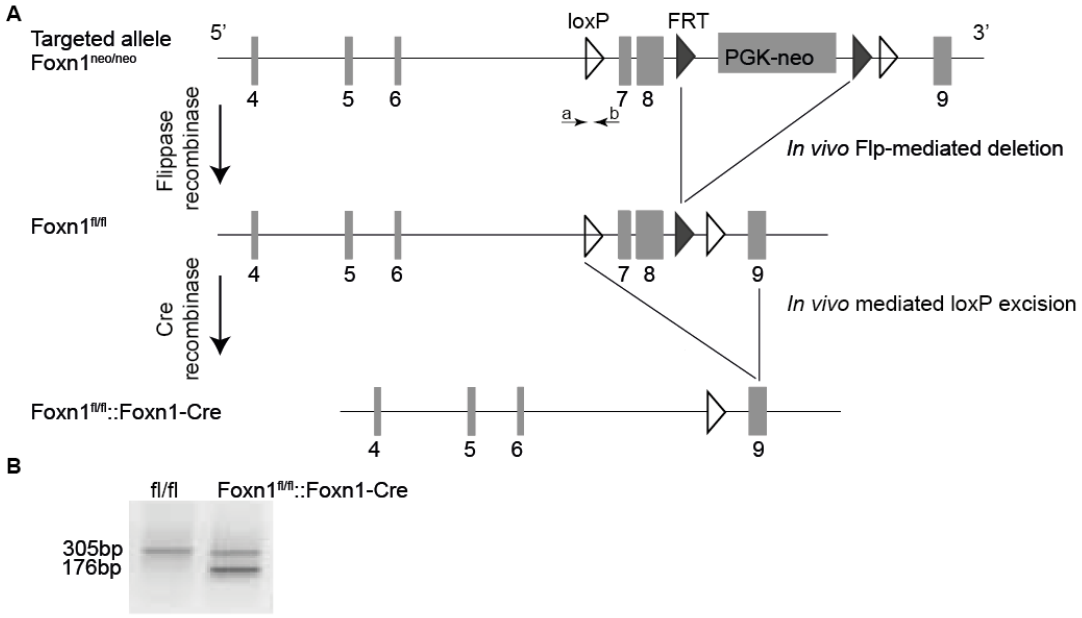

Figure 4.4: Generation of Foxn1$^{fl/fl}$::Foxn1-Cre mice. (A) In vivo removal of the neomycin cassette by crossing Foxn1$^{neo/neo}$ mice to mice expressing the recombinase flippase under the transcriptional control of Gt(ROSA)26Sor promoter. Foxn1$^{fl/fl}$ mice were subsequently crossed to Foxn1-Cre mice, to delete exons 7 and 8 in TEC and skin. (B) Genotyping of Foxn1$^{fl/fl}$ and Foxn1$^{fl/fl}$::Foxn1-Cre mice, using primer a and b indicated in Figure 4.2 A. The Foxn1 transgene result in a wild type Foxn1 band (at 176 bp) present in Foxn1$^{fl/fl}$::Foxn1-Cre mice beside the recombined Foxn1 allele (at 305bp).

To construct mice that express the recombinase under the Foxn1 promoter, designated Foxn1-Cre, a Foxn1 transgene was integrated into chromosome 15 using a P1 artificial chromosome (PAC) targeting vector. The expression of this transgene was shown to parallel the expression of the endogenous Foxn1 expression[136]. This Foxn1 transgene was also detected in Foxn1$^{fl/fl}$::Foxn1-Cre mice, as indicated by the presence of two bands, the wild type band (176 bp) resulting from the Foxn1 transgene located in chromosome 15 and the floxed allele (305bp) whereas in Foxn1$^{fl/fl}$ mice only the floxed allele was detected (Fig. 4.4 B).

Foxn1$^{fl/fl}$ females were bred with Foxn1$^{fl/fl}$::Foxn1-Cre males, as Foxn1$^{fl/fl}$:Foxn1-Cre females are typically unable to lactate due to Foxn1 ablation. The litter size was comparable to that of wild type mice. Female nude mice were shown to have a reduced fertility, due to lower serum levels of estradiol, progesterone and thyroxine[265]. In concordance with this report, female Foxn1$^{fl/fl}$::Foxn1-Cre mice showed reduced fertility, as demonstrated by the observation that pregnancies could not be achieved despite mating for 12 months.

4.2. Efficacy of Foxn1 deletion

To determine the efficacy of Foxn1 deletion in embryonic E16.5 Foxn1$^{fl/fl}$::Foxn1-Cre mice, RNA and DNA were isolated from sorted TEC collected at different time points (Fig. 4.5). The size of the PCR product demonstrated that TEC from E16.5 Foxn1$^{fl/fl}$::Foxn1-Cre mice had successfully recombined, as a very dominant band of the expected 184 bp size could be detected. However the Foxn1 locus remained unaltered in non-epithelial stroma cells of the same mice thus confirming the TEC-specific deletion. In TEC from Foxn1$^{fl/fl}$::Foxn1-Cre mice a faint WT band was detected, this does not necessarily mean that the recombination was not complete, rather this WT Foxn1 band results from the Foxn1 transgene that was shown to parallel endogenous Foxn1 expression. The Foxn1 locus was unaltered in sorted wild type TEC (Fig. 4.5 B).

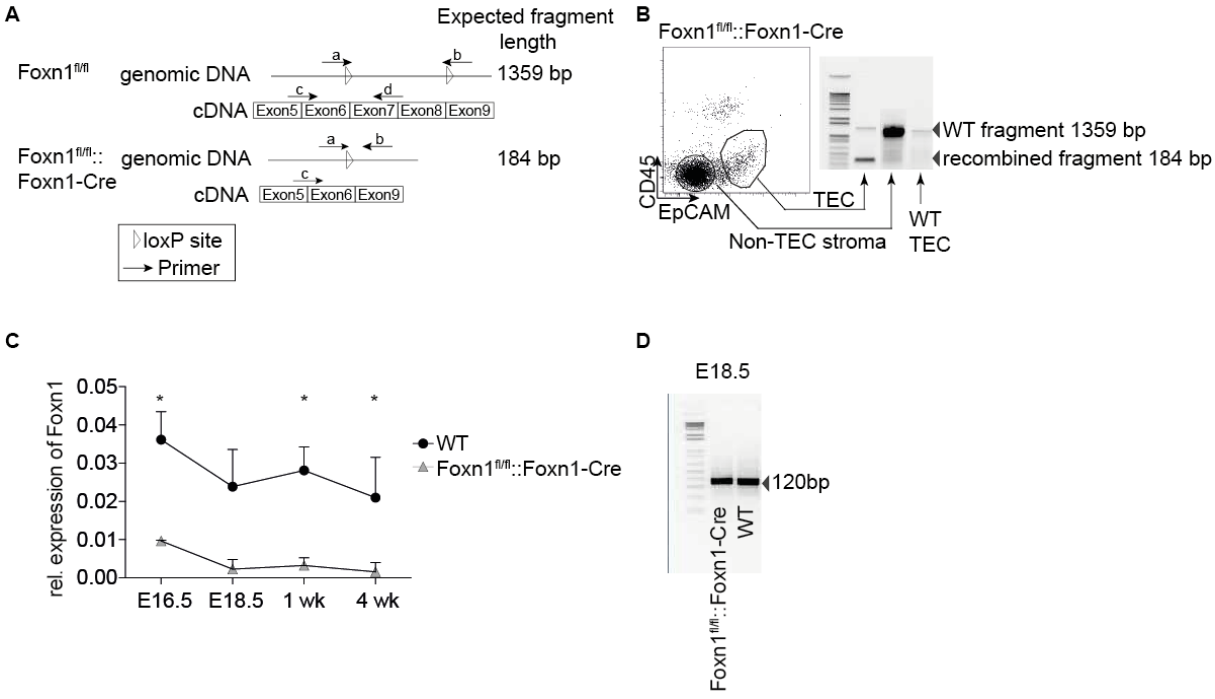

Figure 4.5: Conditional deletion of Foxn1 in Foxn1$^{fl/fl}$::Foxn1-Cre mice. (A) Illustration of primer choices (a-d) for PCR of Foxn1 sequences in genomic and complementary DNA for the detection of Foxn1 exon 7 to 8 deletions. (B) Genomic deletion of exons 7 and 8. This was verified on sorted TEC defined as EpCAM^{pos} CD45^{neg} isolated from E 16.5 thymic lobes. (C) Quantification of Foxn1 transcripts in sorted TEC from mice of indicated ages using primers c and d (see panel A). (D) Size of Foxn1 qPCR product from E18.5 WT and Foxn1$^{fl/fl}$::Foxn1-Cre TEC. The expression was normalised to GAPDH. The data shows mean values ± SD of three independent experiments. Statistical significance was calculated using Mann-Whitney test *p < 0.5, ** < 0.01, *** < 0.001.

To further characterize the experimental system and to document the change of Foxn1 transcripts in Foxn1$^{fl/fl}$::Foxn1-Cre TEC after Cre mediated excision of exons 7 and 8, TEC were isolated from Foxn1$^{fl/fl}$::Foxn1-Cre mice at various ages and analysed by qPCR for the relative Foxn1 transcript copy number (Fig. 4.5). The relative amount of Foxn1 transcripts in TEC from Foxn1$^{fl/fl}$::Foxn1-Cre mice was significantly reduced when compared to age-matched wild type mice. Though the locus was deleted efficiently as early as E16.5, Foxn1 transcripts could still be detected as late as 4 weeks after birth. In contrast, Foxn1 protein could not be detected as early as E12.5 in Foxn1$^{fl/fl}$::Foxn1-Cre mice using immunohistochemistry. These consistently detected transcripts are Foxn1 transcripts from exon 6 and 7 as demonstrated by the size of the amplicon. These Foxn1 transcripts result from the Foxn1 transgene inserted into chromosome 15, encoding the Cre recombinase under the Foxn1 promoter, these transcripts did not translate into protein, since after the ATG the coding sequence for Cre recombinase was inserted. In congenital nude mice Foxn1 protein was not detected in E12.5 embryos. To identify the epithelial cells of the thymus cytokeratin 8 was included. Using immunohistochemistry, the Foxn1 protein could not be detected in Foxn1$^{fl/fl}$::Foxn1-Cre mice even when analysed as early as E12.5. Foxn1$^{neo/neo}$ mice displayed at the same embryonic stage in comparison to wild type fewer Foxn1 positive TEC. These TEC were not equally dispersed but rather clustered in specific areas. In new born Foxn1$^{neo/neo}$ mice, thymic Foxn1 protein could still be detected, although the signal intensity was significantly reduced when compared to wild type mice.

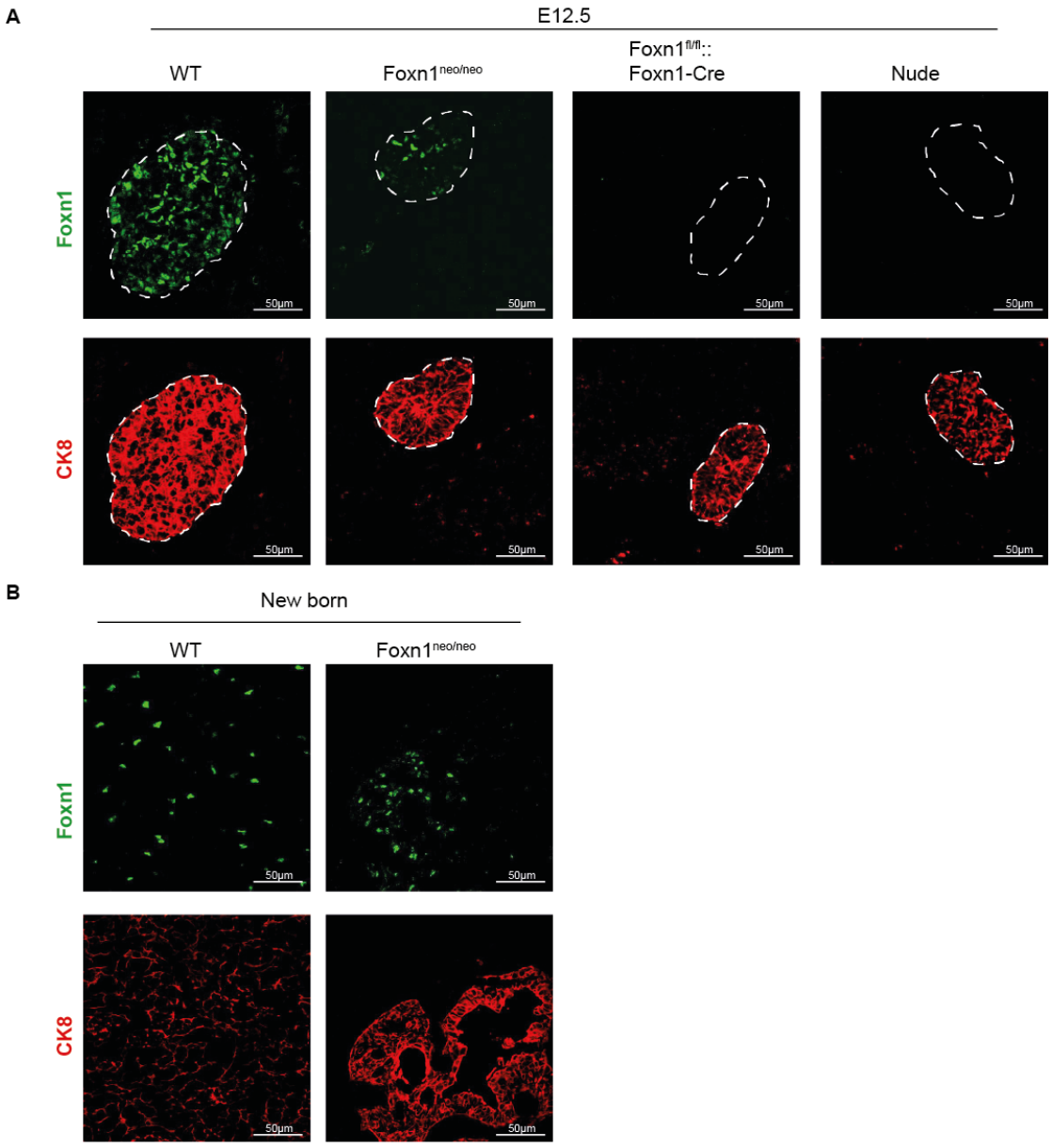

Figure 4.6: Foxn1 protein is undetected in Foxn1$^{fl/fl}$::Foxn1-Cre mice as early as E12.5. Sections of embryonic day 12.5 (A) and new born (B) thymic tissue were stained for Foxn1 protein (green) and cytokeratin 8 (red). Representative microphotographs of 8 independent experiments.

The conditional deletion of *Foxn1* in Foxn1$^{fl/fl}$::Foxn1-Cre TEC was complete and TEC specific. Targeting the neomycin cassette to intron 8 of the *Foxn1* locus resulted in lower concentrations of Foxn1 transcripts and consequently reduced Foxn1 protein, whereas Foxn1 ablation in TEC resulted in the absence of Foxn1 protein as early as E 12.5. Hence two separate novel mouse models were generated that differ in the kinetic and in the amount of Foxn1 expression. These two mouse models now allowed to probe whether Foxn1 expression

is required after early thymus organogenesis, whether Foxn1 expression is required throughout TEC differentiation, whether physiological TEC development is still possible despite a reduced Foxn1 expression level and finally, weather different TEC subsets require different Foxn1 expression levels for their development.

4.3. Foxn1$^{fl/fl}$::Foxn1-Cre and Foxn1$^{neo/neo}$ mice show a skin phenotype and reduced weights

Foxn1 is important for hair follicle formation, since its absence results in impaired keratinization of the hair shafts and, consequently, to short and bent hair unable to efficiently penetrate the epidermis, thus resulting in alopecia[128,132,266]. Therefore the coat phenotype of Foxn1$^{neo/neo}$ and Foxn1$^{fl/fl}$::Foxn1-Cre mice was analysed. In concordance with reports on spontaneous Foxn1 mutations[132], Foxn1$^{fl/fl}$::Foxn1-Cre mice displayed a generalised alopecia identical to that observed in congenital nude mice (Fig. 4.7). In contrast and reflecting residual Foxn1 protein expression, Foxn1$^{neo/neo}$ mice had a hair coat that was less dense when compared to wild type mice (Fig. 4.7). In addition Foxn1 protein is also expressed in the whisker pads[128] and its absence resulted in whiskers that were curled and shortened, indistinguishable to those of nude mice, whereas the whiskers in Foxn1$^{neo/neo}$ mice were unaffected.

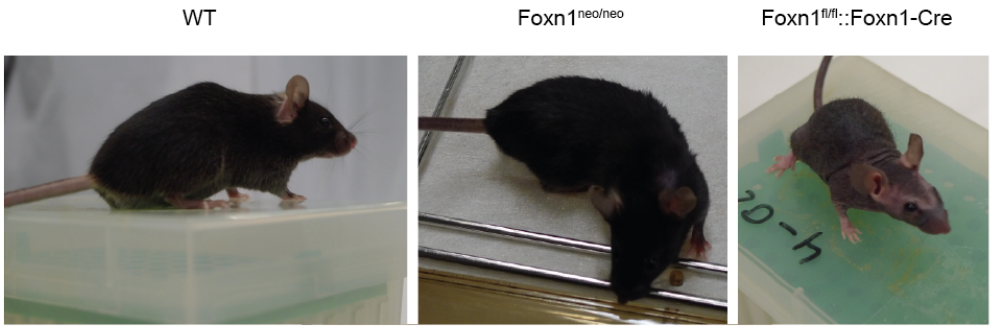

Figure 4.7: The nude phenotype is improved in Foxn1$^{neo/neo}$ mice Representative pictures of 6 week old wild type (WT), Foxn1$^{neo/neo}$ and Foxn1$^{fl/fl}$::Foxn1-Cre mice.

Foxn1$^{neo/neo}$ and Foxn1$^{fl/fl}$::Foxn1-Cre mice appeared macroscopically smaller in size when compared to wild type littermates as determined by direct comparison of littermates. To further quantify the perceived size difference, the weight of the animals was measured over a time period of 40 weeks. The weights of Foxn1$^{neo/neo}$ and Foxn1$^{fl/fl}$::Foxn1-Cre mice were significantly lower independent of gender when compared to wild type litter mates (Fig. 4.8).

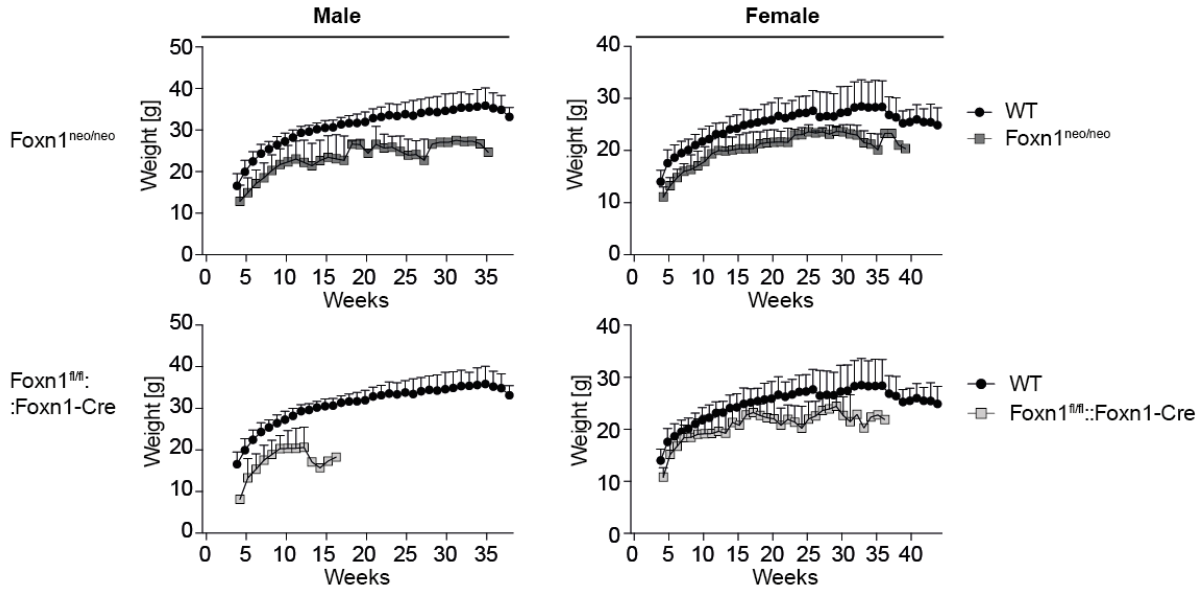

Figure 4.8: Reduced weight in Foxn1$^{neo/neo}$ and Foxn1$^{fl/fl}$::Foxn1-Cre mice. Weight curves of male and female Foxn1$^{neo/neo}$ (-■-), Foxn1$^{fl/fl}$::Foxn1-Cre (-□-) and wild type (WT) (-●-) mice. For each time point and group at least 3 and as many as 13 mice were investigated. The data displayed provides mean values ± SD. Only three Foxn1$^{fl/fl}$::Foxn1-Cre males were analysed, they were all died within 15 weeks.

In summary Cre mediated deletion of exon 7 and 8 of the Foxn1 gene on the onset of thymus organogenesis results in the nude phenotype whilst only a reduction of Foxn1 expression caused a mild decrease in coat thickness but normal whiskers. Furthermore a reduction or complete loss of Foxn1 protein, resulted in mice with reduced weight and size, which might be explained by a faster metabolism due to absence of fur.

4.4. Foxn1$^{neo/neo}$ and Foxn1$^{fl/fl}$::Foxn1-Cre mice display severe thymus hypoplasia

Foxn1 is mainly expressed in skin and thymic epithelial cells. In the latter Foxn1 serves as a master transcription factor orchestrating thymus organogenesis with the exception of the formation of the thymus primordium[25]. In the absence of Foxn1 a rudiment develops, however after early organ formation the thymus fails to attract lymphoid precursors and degrades into cysts. To investigate the consequences of an early loss or reduction of Foxn1 protein expression during thymus organogenesis I first analysed the thymus cellularity in Foxn1$^{neo/neo}$, Foxn1$^{fl/fl}$::Foxn1-Cre and wild type mice at embryonic days 16.5 and E18.5, on postnatal days 1 and 7 and in 5 week old animals. For the latter two time points, thymic tissues from nude mice were used in addition for comparison. E12.5 Foxn1$^{neo/neo}$ and

Foxn1$^{fl/fl}$::Foxn1-Cre thymi were macroscopically indistinguishable from wild type organs (data not shown) suggesting that early thymus development is independent of Foxn1 expression. At E16.5 the difference in macroscopic size of Foxn1$^{neo/neo}$ and Foxn1$^{fl/fl}$::Foxn1-Cre thymus was already significant and progressively with time (Fig. 4.9 A). The thymi of the mutant mice were hypoplastic and typically displayed multiple cysts of different sizes. The thymi from Foxn1$^{neo/neo}$ and Foxn1$^{fl/fl}$::Foxn1-Cre were despite these similarities clearly distinguishable in appearance from those of nude thymus. For example, the fatty tissue surrounding the thymus was different in colour and appearance. Because the thymus in all mutant mouse strains was positioned similarly to wild type animals along the carotid arteries, an absence or reduction of Foxn1 did apparently not influence thymus migration. Hence, this observation confirms that the migration of the thymus anlage during embryonic organ development is Foxn1 independent.

Parallel to the reduced macroscopic size, thymic cellularity in E16.5 Foxn1$^{neo/neo}$ and Foxn1$^{fl/fl}$::Foxn1-Cre mice was significantly reduced to 26’528 ± 8869 and 20’216 ± 11697 cells respectively whereas age-matched wild type mice had a thymus with a cellularity of 1’803’750 ± 649’697 cells. This reduction increased over time (***$p<0.05$) but was comparable to that of nude mice (Fig. 4.9 B). Hence, both an initial normal but subsequently absent or only reduced Foxn1 expression resulted in a severely hypoplastic thymus, that was indistinguishable in size and cellularity from that of nude mice which never express Foxn1. Therefore only a short term or overtime reduced Foxn1 expression do not allow for the regular outgrowth of the thymus rudiment and the significant presence of lymphoid precursors.

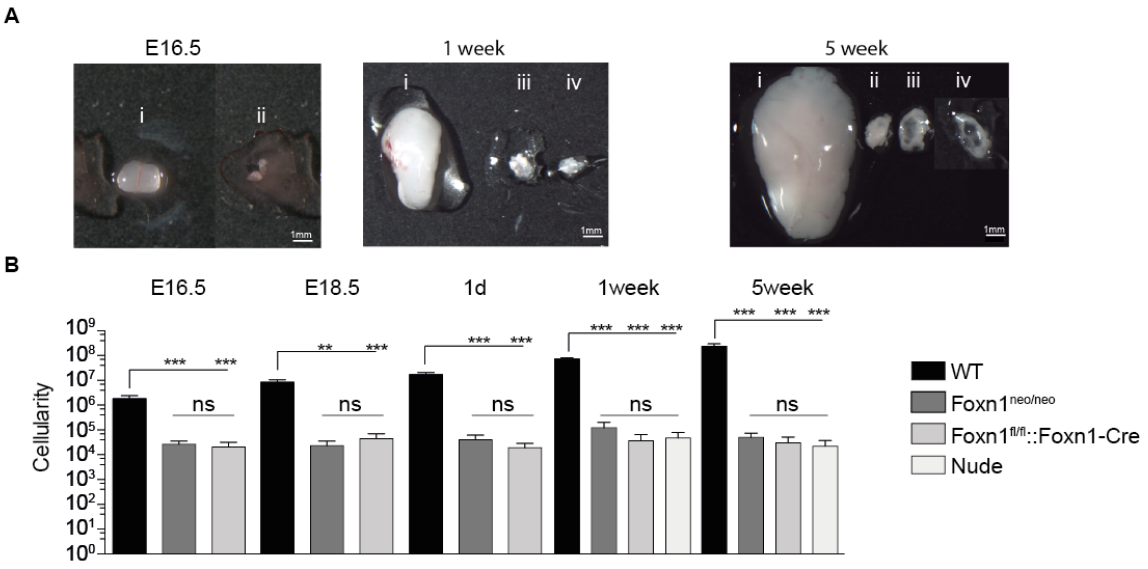

Figure 4.9: Both reduction and deletion of Foxn1 cause severe thymic hypoplasia. (A) Representative photomicrographs of thymic lobes isolated from (i) wild type (WT), (ii) Foxn1$^{neo/neo}$, (iii) Foxn1$^{fl/fl}$::Foxn1-Cre and (iv) nu/nu mice at E16.5, 1 week and 5 weeks of age. (B) Thymic cellularity at E16.5, E18.5, 1day, 1 week and 5 weeks of age. WT (■) Foxn1$^{neo/neo}$ (■), Foxn1$^{fl/fl}$::Foxn1-Cre (□) nu/nu (□) mice. Values were indicated as mean plus standard derivation, from at least three independent experiments. Statistical significance was calculated using Mann-Whitney test *p < 0.5, ** < 0.01, *** < 0.001.

This result indicates that the skin is less sensitive to Foxn1 reduction compared to the thymus, however the fur of Foxn1$^{neo/neo}$ mice is less dense indicating that the rescue is not complete.

4.4.1. The Chemokines required for thymocytes attraction are reduced in Foxn1$^{neo/neo}$ and Foxn1$^{fl/fl}$::Foxn1-Cre mice.

The colonisation of the early thymus anlage is controlled by the expression of the chemokines CCL19, CCL21, CCL25 and CXCL12[49,148], with the chemokines CCL25 and CXCL12 directly dependant for their transcription on Foxn1 expression[144]. To elucidate whether the reduced thymus cellularity resulted from a defect in precursors attraction, secondary to changes in the chemokine expression I analysed the transcription of the above mentioned chemokines in TEC purified from Foxn1$^{neo/neo}$, Foxn1$^{fl/fl}$::Foxn1-Cre mice and wild type mice. The expression of all four chemokines was severely reduced in both embryonic E16.5 and adult TEC of the mutant mice compared to wild type animals (Fig. 4.10). The cytokine expression was similar in Foxn1$^{fl/fl}$::Foxn1-Cre and Foxn1$^{neo/neo}$ mice, despite the presence of reduced Foxn1 transcripts. Hence, reduced Foxn1 expression does not induce the presence of cytokines. It might be that Foxn1 expression is too weak to drive cytokine expression.

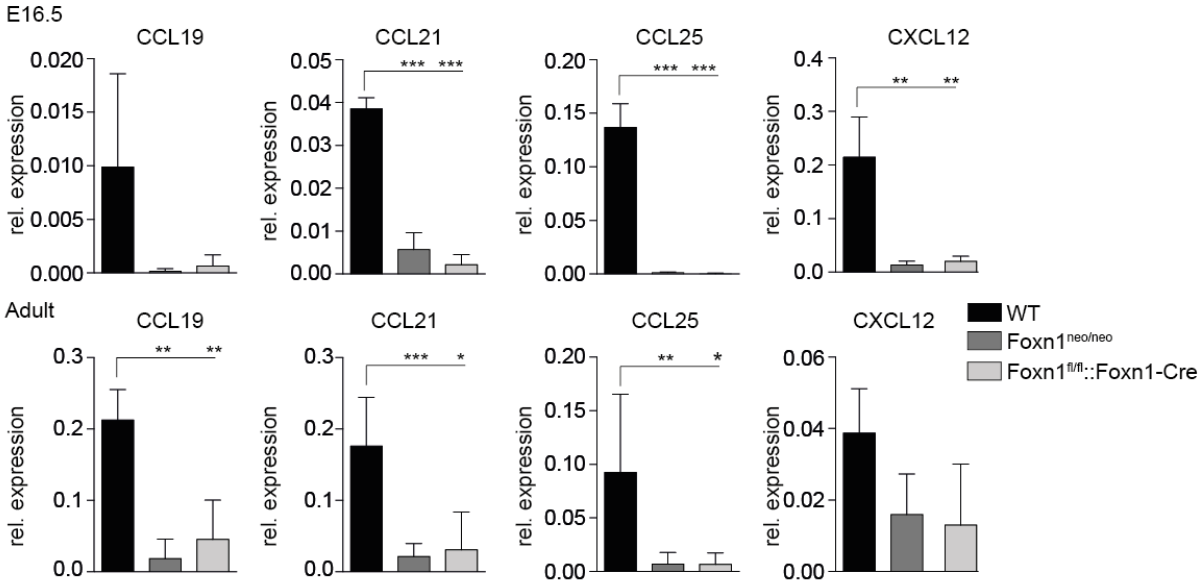

Figure 4.10: Reduced transcription of chemokines that are involved in T-cell precursor homing to thymus. Quantification of CCL19, CCL21, CCL25 and CXCL12 transcripts in sorted EpCAM^{+}/CD45^{-} TEC of WT (■), Foxn1$^{neo/neo}$ (■) and Foxn1$^{fl/fl}$::Foxn1-Cre (■) mice at E16.5 and adult age normalised to GAPDH. Pooled data from 3 independent experiments, values indicate mean ± SD. p values were determined by Mann-Whitney test, *p <0.05, ** < 0.01, *** < 0.001.

This result suggests that reduced Foxn1 expression or short term Foxn1 expression does not suffice to maintain regular chemokine expression and that therefore the recruitment of T-cell precursors into Foxn1$^{neo/neo}$ and Foxn1$^{fl/fl}$::Foxn1-Cre thymus is reduced or absent. This result is in concordance with the reduced thymic cellularity in Foxn1$^{neo/neo}$ and Foxn1$^{fl/fl}$::Foxn1-Cre mice that is indistinguishable from nude thymus, which lack T-cell precursors.

4.4.2. Foxn1$^{neo/neo}$ and Foxn1$^{fl/fl}$::Foxn1-Cre thymus are vascularised

After the entry of the first progenitor cells, the thymus vascularisation is established in a Foxn1-dependant fashion[150]. Both TEC and mesenchymal cells can produce vascular endothelial growth factor (VEGF), which is essential for blood vessel formation in the thymus[42]. In the absence of Foxn1 PDGFRβ^{+} mesenchymal cells cannot migrate into the thymus and the vasculature is not established. CD31^{+} endothelial cells are detected in the wild type thymus as early as E12.5, interestingly both CD31^{+} endothelial and PDGFRβ^{+} mesenchymal cell were absent in nude thymus. A lack of thymus vascularisation might therefore contribute to the small thymus size observed in Foxn1$^{neo/neo}$ and Foxn1$^{fl/fl}$::Foxn1-

Cre mice, as T-cell precursors would fail to enter the thymus, precluding of the crosstalk between thymocytes and TEC necessary for the regular development, differentiation and architectural organisation of the thymic stromal compartment and thus also eventually favouring the formation of cysts. To study to consequences of only short term normal or continuously reduced Foxn1 expression on thymus vascularisation sections of thymus tissue isolated from one and six week old mutant and wild type mice were analysed for the detection of the endothelial cell marker CD31. This marker was absent in the thymus of nude mice, at one and six weeks of age. This was a thymus organ autonomous finding as $CD31^{+}$ cells could be detected outside of the thymus rudiment in the surrounding adipose tissue. In contrast, intrathymic vessels could be identified in the $Foxn1^{fl/fl}$::Foxn1-Cre, and $Foxn1^{neo/neo}$ mice. In six week old $Foxn1^{fl/fl}$::Foxn1-Cre mice the vascularisation was different from vascularisation of $Foxn1^{neo/neo}$ mice as the thymus was less vascularised and most of the vessel were detected in the adipose tissue, similar as observed in nude mice (Fig. 4.11). This result implies that short term or reduced Foxn1 expression suffices for the establishment and maintenance of thymic vascularisation, further suggesting that the limited thymus size and reduced precursor seeding are not directly coupled to the vascularisation of the thymus. However this analysis was only descriptive, the quality of the blood vessel was not assessed.

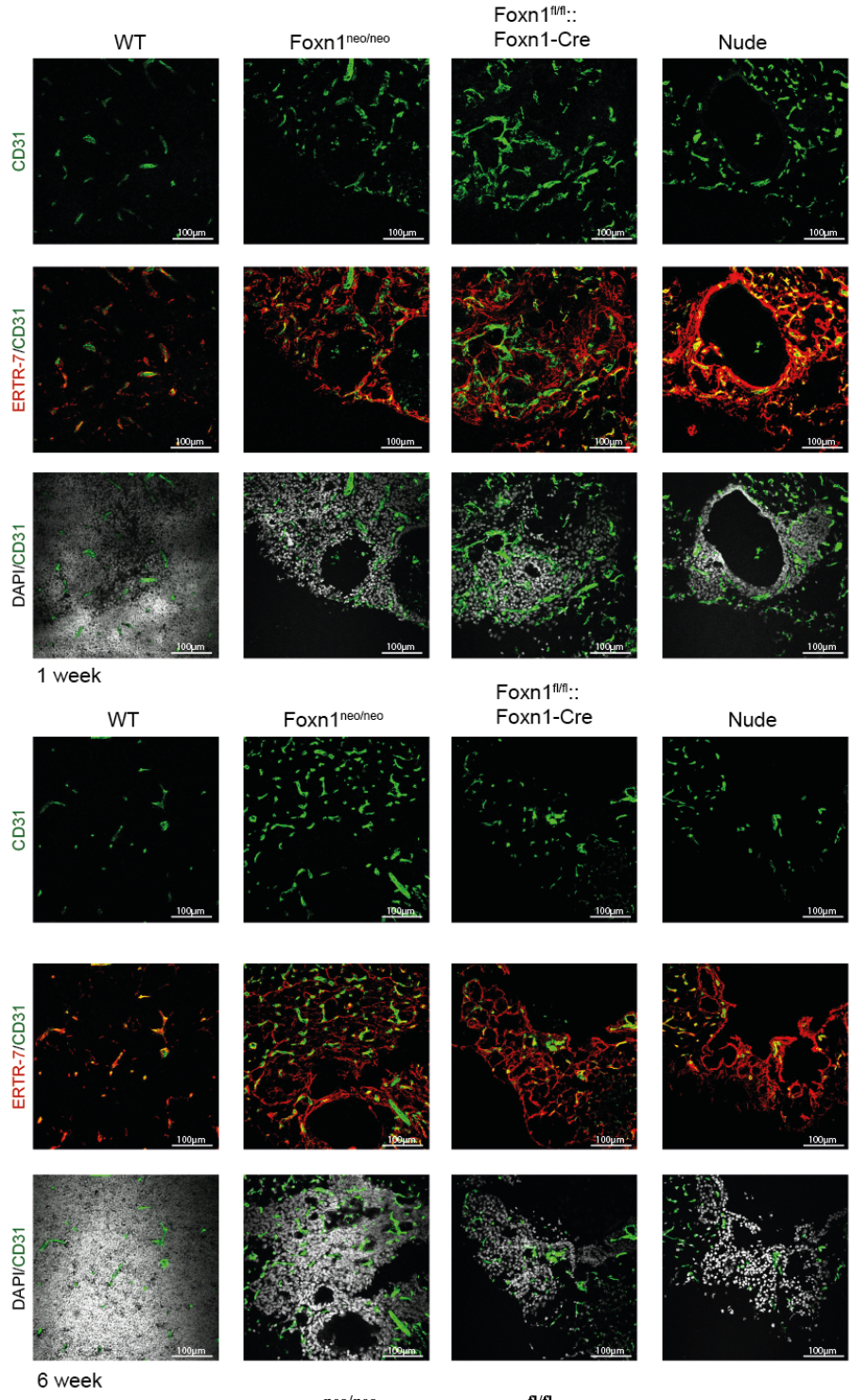

Figure 4.11: Vascularisation in Foxn1$^{neo/neo}$ and Foxn1$^{fl/fl}$::Foxn1-Cre mice was not impaired. Photomicrographs of thymic tissue sections analysed in confocal microscopy of 1 week and 6 week old wild type (WT), Foxn1$^{neo/neo}$, Foxn1$^{fl/fl}$::Foxn1-Cre and nu/nu mice stained for ERTR-7 (red), CD31 (green) and DAPI (grey).

4.5. Architecture and composition of the thymus

TEC in nude mice remain in an early progenitor stage[107] underscoring the importance of Foxn1 for regular TEC development and their differentiation into medullary and cortical subpopulations[25]. In addition, for the formation of a cortex and medulla interactions with developing thymocytes are essential[5,54]. The cellularity of Foxn1$^{neo/neo}$ and Foxn1$^{fl/fl}$::Foxn1-Cre thymus was drastically reduced, and chemokines involved in precursor homing were reduced in TEC isolated from Foxn1$^{neo/neo}$ and Foxn1$^{fl/fl}$::Foxn1-Cre mice, both indicators for a reduced or absent precursors homing. Because the absence or reduction of T-cell precursor homing and their subsequent expansion and regular differentiation will influence the composition and architectural organisation of the cortex and medulla, I analysed and compared the stromal epithelial compartment of mutant and wild type mice. Darker (i.e. cell dense) cortical and lighter medullary zones are typically observed when tissue sections are stained with haematoxylin and eosin (H&E). This segregation is however not observed in thymi with only an early but normal Foxn1 protein expression (i.e. Fonx1$^{fl/fl}$::Foxn1-Cre) or with a subnormal expression following regular Foxn1 transcripts (Fig. 4.12). This can be explained by the absence or large reduction of T-cells in the thymus. With increasing age the only epithelial cells, identified by cytokeratin (CK) 5 and 8 expression, in Foxn1$^{neo/neo}$ and Foxn1$^{fl/fl}$::Foxn1-Cre thymic tissue, were restricted to the lining of the cysts, similar to the findings in nude thymus (Fig. 4.12). The epithelial stromal network was interspersed in both mutant mice already at 1 week of age with adipocytes. A previous study suggested that cyst formation is a default pathway of the TEC development in the absence of thymocytes, as the presence and expansion of thymic cysts inversely correlated with the presence of thymocytes[28]. The observation that cyst formation is dependant on the absence of thymocytes is in accordance with the cyst formation in the nude thymus, where thymocytes are absent. The cysts and the absence of cortex and medulla segregation observed in Foxn1$^{neo/neo}$ and Foxn1$^{fl/fl}$::Foxn1-Cre thymus imply a strong reduction or complete absence of thymocytes in Foxn1$^{neo/neo}$ and Foxn1$^{fl/fl}$::Foxn1-Cre mice, which is further corroborated by their low chemokine expression level for T-cell precursors.

Epithelial cells are polarised cells forming a two dimensional structure, however the TEC are special as they form a three dimensional network. In the absence of the thymic crosstalk the three dimensional network of the thymus is disrupted and TEC consequently adopt a two

dimensional organisation and cysts appear[5]. The cysts observed in Foxn1$^{neo/neo}$ and Foxn1$^{fl/fl}$::Foxn1-Cre mice would suggest that the three dimensional architecture of the thymus is absent resulting in epithelial cells which form mainly a two dimensional architecture.

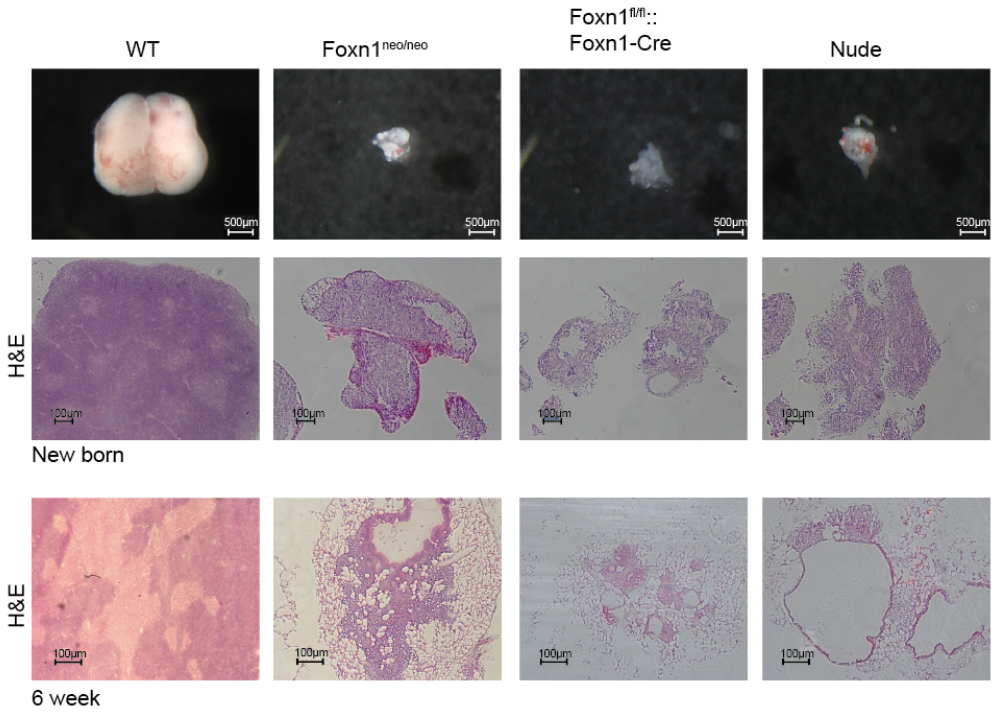

Figure 4.12: Loss of regular thymic architecture in Foxn1$^{neo/neo}$ and Foxn1$^{fl/fl}$::Foxn1-Cre thymic tissue. Hematoxylin and Eosin staining of thymic tissue sections of new born (middle rows) and 6 week old mice (lower row).

Next, immunohistochemistry was performed to further investigate the composition of the thymic microenvironment, and to identify whether the epithelial cells remained in an early CK5 and CK8 double positive progenitor stage as observed in nude mice[53,267] or whether their development proceeds. In a first step the cortical marker CK8 (green) and the medullary marker CK5 (red) were used to characterize the TEC specific cytokeratin expression pattern. Specifically I tested whether TEC were double positive, a phenotype typically observed in nude mice or alternatively whether separate cortical and medullary TEC subpopulations had formed each expressing either CK5 or CK8. In contrast to the impression gained from H&E stainings, distinct cortical and medullary areas were appreciated in Foxn1$^{neo/neo}$ and Foxn1$^{fl/fl}$::Foxn1-Cre mice both at 1 and 6 weeks of age (Fig. 4.13 A). However these distinct cortical and medullary areas were restricted to small islets in comparison to wild type thymi.

This segregation was not complete as an increase in CK5 and CK8 double positive cells was also detected, $CK5^{+}CK8^{+}$ TEC are typically detected at the cortico-medullary junction and under conditions where thymocytes are missing or are grossly reduced as in CD3ε transgenic mice where T-cell development is blocked at an early stage[94]. In aggregate, these results likely suggest furthermore that T-cell development must be very comprised in both $Foxn1^{neo/neo}$ and $Foxn1^{fl/fl}$::Foxn1-Cre thymi.

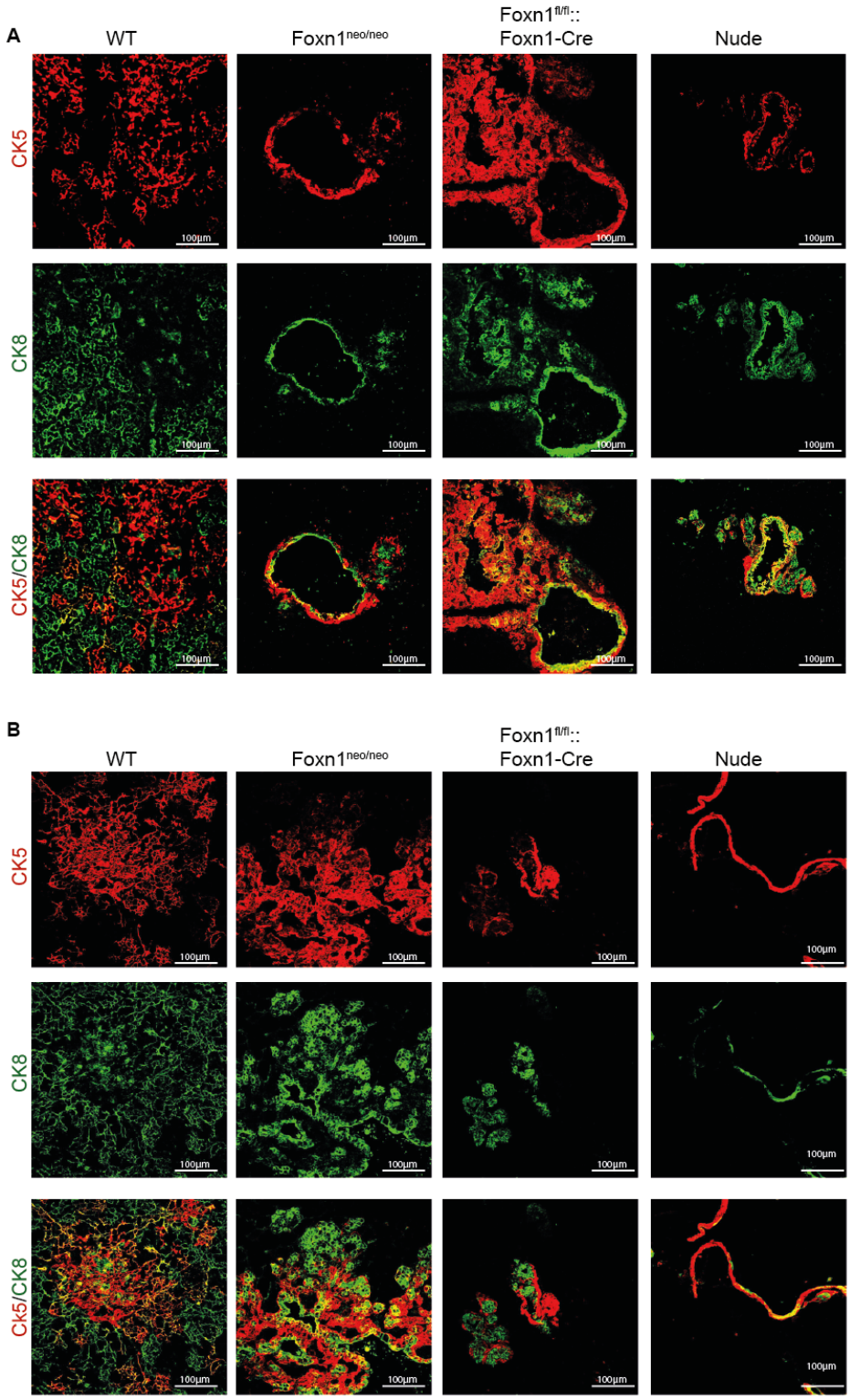

Figure 4.13: Changes in thymic microenvironment in Foxn1$^{neo/neo}$ and Foxn1$^{fl/fl}$::Foxn1-Cre mice. Confocal microscopy of thymic tissue sections of 1 (A) and 6 (B) week old mice stained for the epithelial markers CK5 (red) and CK8 (green).

Because TEC are replaced during thymic involution by fibroblasts, possibly at least in part via the process of epithelial-mesenchymal-transition[176] I analysed the presence of these cells in thymus sections of mutant and wild type mice using the fibroblast marker ERTR-7. In six week old Foxn1$^{neo/neo}$ and Foxn1$^{fl/fl}$::Foxn1-Cre thymi, the epithelial cell compartment was replaced by fibroblasts and TEC were restricted to small islets, surrounded by fibroblasts. The increase in fibroblasts correlates with the age of the mice (data not shown). An increased number of fibroblasts compared to wild type thymi was also observed in nude thymi (Fig. 4.14). The increase of fibroblast would argue that a premature thymic involution causes the phenotype observed in Foxn1$^{neo/neo}$ and Foxn1$^{fl/fl}$::Foxn1-Cre mice or alternatively the absence of T-cell precursors and therefore a lack of regular TEC development causes the phenotype observed.

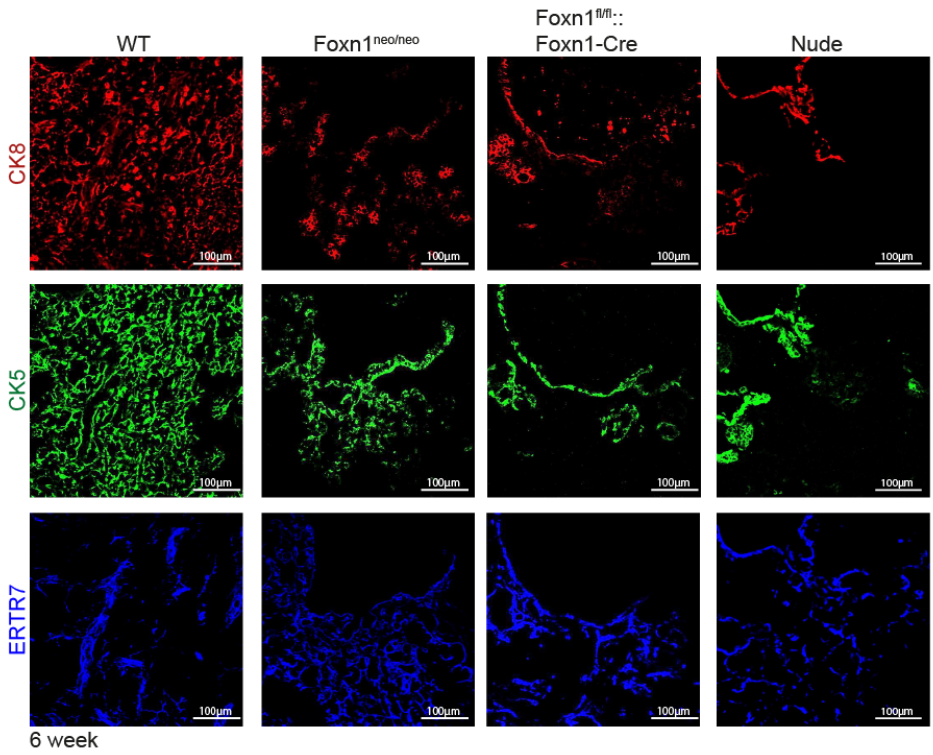

Figure 4.14 Increase in fibroblasts in Foxn1$^{neo/neo}$ and Foxn1$^{fl/fl}$::Foxn1-Cre mice. Confocal microscopy sections of 6 week old wild type (WT), Foxn1$^{neo/neo}$, Foxn1$^{fl/fl}$::Foxn1-Cre and nude mice stained for the epithelial markers CK8 (red), CK5 (green) and the fibroblast marker ERTR-7 (blue).

In summary these results showed that the thymic architecture is severely disturbed, with the formation of cysts and a loss of a three dimensional epithelial network and architecture. Thus thymic architecture is not induced with short term or reduced Foxn1 expression. Segregation

into cortex and medulla was incomplete and with age the only epithelial cells present were lining the cysts, whereas the remaining space was filled by fibroblasts. However TEC can develop into distinct cTEC and mTEC, which is not observed in nude TEC, suggesting that T-cell precursor entry is not completely abrogated.

4.5.1. Foxn1$^{neo/neo}$ and Foxn1$^{fl/fl}$::Foxn1-Cre mice lack hallmark of cortex and medulla

I next analysed the expression of β5t in the thymus cortical areas of Foxn1$^{neo/neo}$ and Foxn1$^{fl/fl}$::Foxn1-Cre mice, since β5t is only expressed in mature cTEC. β5t expression is directly or indirectly dependant on Foxn1 expression, since nude mice fail to express β5t[268]. Specifically, I wished to know whether expression of β5t requires continuous and regular Foxn1 expression for cTEC to acquire normal β5t expression. This protein was expressed in wild type thymic tissue as early as E12.5 in TEC, but could never be detected in E12.5 Foxn1$^{fl/fl}$::Foxn1-Cre mice (Fig. 4.15 A). A short term expression of Foxn1 does therefore not suffice to initiate β5t expression. In Foxn1$^{neo/neo}$ mice β5t expression was present in a quarter of the E12.5 embryos analysed, indicating a dosage effect (Fig. 4.15 B). Since in Foxn1$^{neo/neo}$ mice Foxn1 expression is reduced by a hypomorphic allele, which is the result of the neomycin cassette, the expression of Foxn1 varies between different embryos. Embryos with more Foxn1^{+} TEC expressed β5t, whereas in embryos with less Foxn1^{+} TEC β5t expression was absent. In one and six week old Foxn1$^{neo/neo}$ thymus β5t protein was absent, although Foxn1 mRNA was still present. However Foxn1 protein was reduced in 1 week old Foxn1$^{neo/neo}$ mice. These results showed that β5t is dependent on a stable and adequate Foxn1 expression.

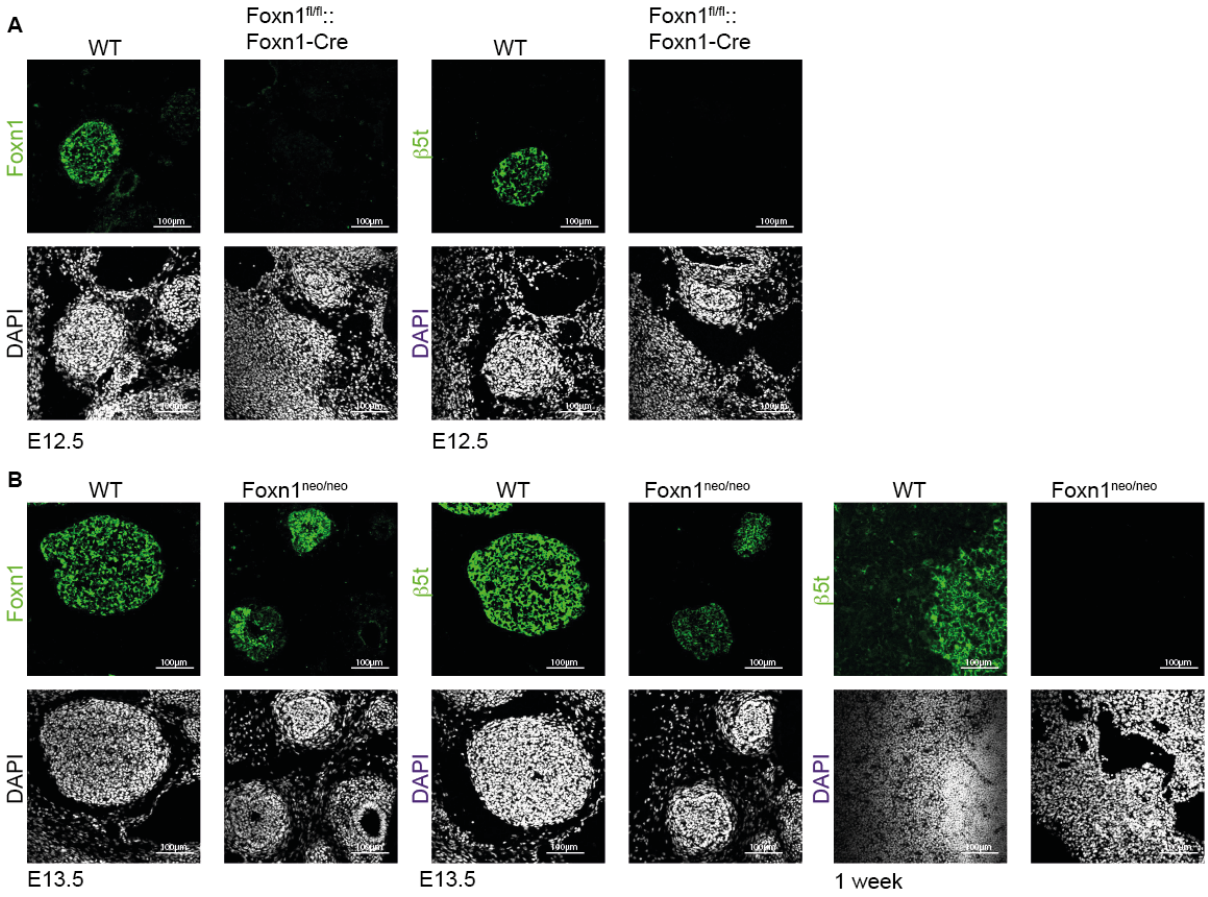

Figure 4.15: β5t expression is absent in Foxn1$^{fl/fl}$::Foxn1-Cre and 75% of Foxn1$^{neo/neo}$ mice. Photomicrographs of thymus tissue sections analysed in confocal microscopy. (A) E12.5 wild type (WT) and Foxn1$^{fl/fl}$::Foxn1-Cre thymus section stained for Foxn1 (green) and Dapi (grey) or β5t (green) and Dapi (grey). (B) E13.5 WT and Foxn1$^{neo/neo}$ mice stained for Foxn1 (green) and Dapi (grey) or β5t (green) and DNA (grey), and 1 week old mice stained for β5t (green) and Dapi (grey).

To further characterise the thymic medulla of Foxn1$^{neo/neo}$ and Foxn1$^{fl/fl}$::Foxn1-Cre mice and the expression of the autoimmune regulator (Aire) was determined. During embryogenesis the maturation of Aire^{-} mTEC into Aire^{+} mTEC is promoted by the presence of RANKL[269]. RANKL is expressed by lymphoid inducer cells[113] and by positively selected SP thymoyctes[269]. Because the thymic cellularity is significantly reduced in Foxn1$^{neo/neo}$ and Foxn1$^{fl/fl}$::Foxn1-Cre mice, I investigated whether the medulla contained Aire^{+} mature TEC. Using immunohistochemistry Aire protein could not be detected in the medulla of Foxn1$^{neo/neo}$ and Foxn1$^{fl/fl}$::Foxn1-Cre and nude mice of both one and six weeks of age (Fig. 4.16). Hence, a reduced or a short term expression of Foxn1 only was incompatible with a regular induction of Aire expression in mTEC, most likely via an indirect mechanism that involves the absence of sufficient cells providing Aire-inducing signals[269–273]. As a consequence of this absence of

mTEC known to be essential for the induction of several immunologic tolerance[111,112,273], autoimmunity may be the consequence of an incomplete or ineffective thymocyte selection.

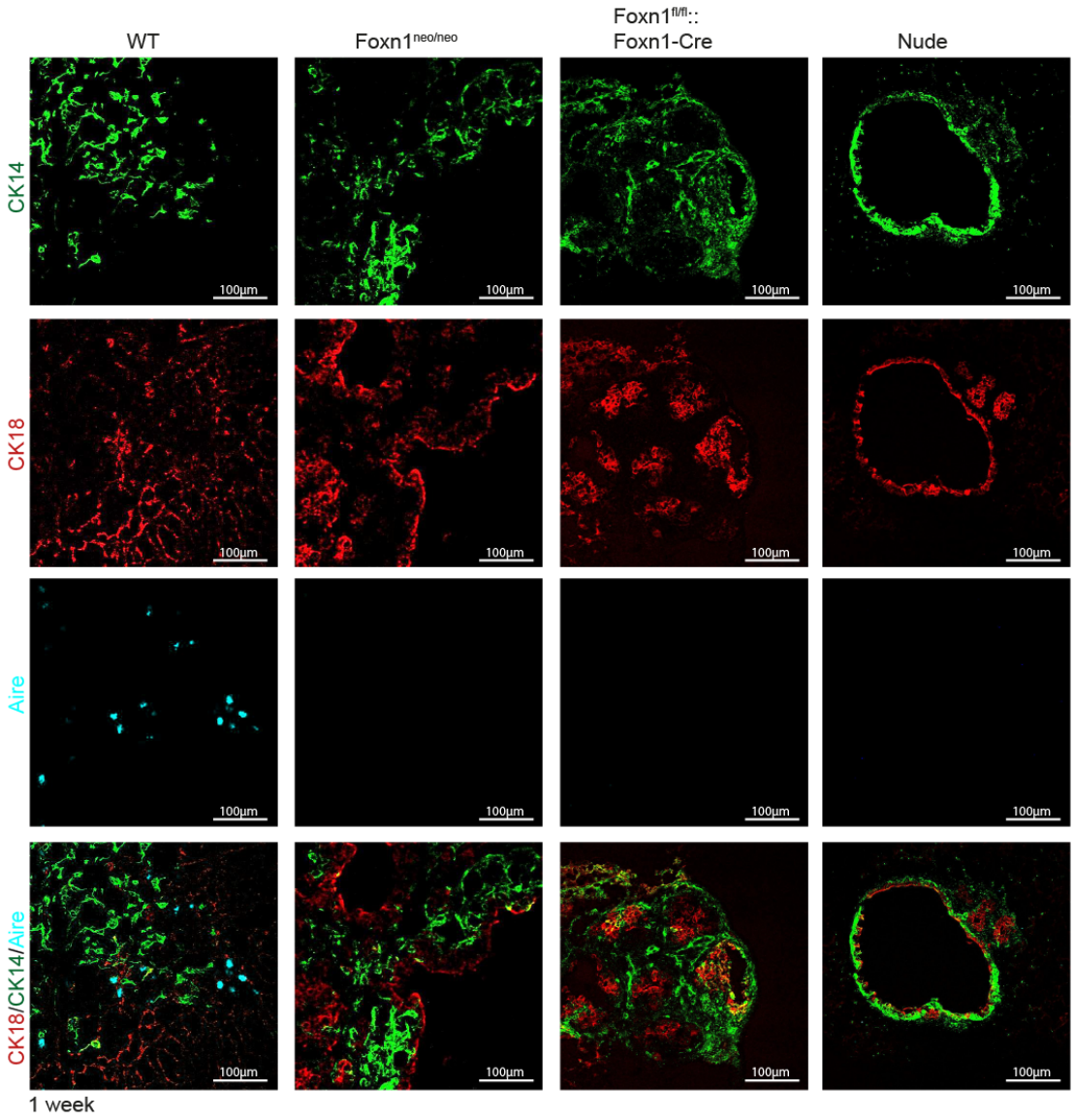

Figure 4.16: Aire expression is absent in Foxn1$^{neo/neo}$ and Foxn1$^{fl/fl}$::Foxn1-Cre thymi. Photomicrographs of thymus tissue sections of 1 week old wild type (WT), Foxn1$^{neo/neo}$, Foxn1$^{fl/fl}$::Foxn1-Cre and nude mice analysed in confocal microscopy stained for K14 (green), K18 (red) and Aire (blue).

4.6. Severely impaired T cell development in Foxn1$^{neo/neo}$ and Foxn1$^{fl/fl}$::Foxn1-Cre thymus

A regularly structured thymic stromal environment is essential for the normal differentiation of T-cells[94,261,274,275]. Given the significant structural changes in the thymus of Foxn1$^{neo/neo}$ and Foxn1$^{fl/fl}$::Foxn1-Cre mice I next investigated the T-cell development of these mutant animals and compared them to wild type controls at distinct stages of embryonic and postnatal development (Fig. 4.17 A). c-kit positive early thymic precursors were detected in both Foxn1$^{neo/neo}$ and Foxn1$^{fl/fl}$::Foxn1-Cre mice. Their development to maturational stages beyond DN1 was yet completely blocked as thymocytes with a double positive phenotype (i.e. $CD4^+CD8^+$ cells) could not be detected at E16.5 when already 15.5% of lymphoid cells display this phenotype in age-matched wild type controls (Fig. 4.17 B, left). Two days later in embryonic development double positive thymocytes were present in some but not all mice albeit at reduced frequency (<10%), when compared to wild type animals (>80%) (Fig. 4.17 C), though a canonical progression beyond the DN1 stage was still not detected in these animals without regular Foxn1 expression. Whether T-cell development follows normal differentiation but occurs below the detection limit of FACS or, alternatively whether T-cell development follows a non-canonical pathway remains to be determined. The latter explanation has been identified in Foxn1$^{\Delta/\Delta}$ mice[152,154] where DP thymocytes develop from ckit^{negative} progenitor cells directly into DP thymocytes without passing through the DN2 and DN3 stages of maturation. In one week old and adult Foxn1$^{neo/neo}$ and Foxn1$^{fl/fl}$::Foxn1-Cre mice, lymphoid cells beyond the DN stage could not be detected (Fig. 4.17 D, E), providing a phenotype appearance comparable to that of nude mice where an absence of effective T-cell development is characteristic. These results indicate that the thymus may be functional early in embryogenesis, though the T-cell development was clearly severely altered in the absence of regular Foxn1 expression.

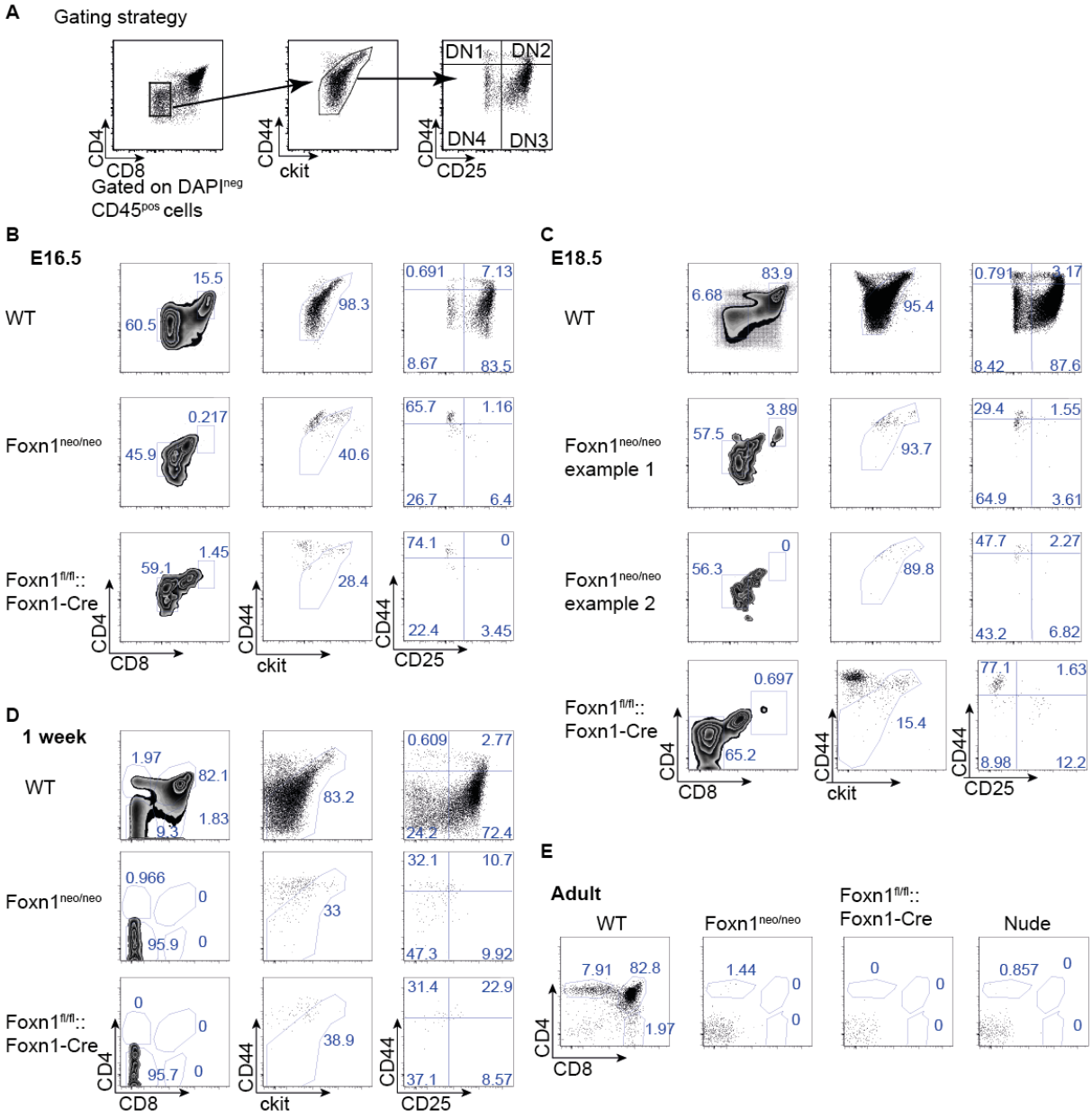

Figure 4.17: Severely impaired T-cell development in Foxn1$^{neo/neo}$ and Foxn1$^{fl/fl}$::Foxn1-Cre mice.
(A) Gating strategy: Cells were stained for CD4 and CD8 and double negative T-cells were further analysed for DN1 to DN4 subsets using CD44, c-kit and CD25 expression. T-cell development in E16.5 (B), E18.5 (C), 1 week (D) and adult (E) mice. Representative FACS plots from at least three independent experiments.

4.6.1. Hematopoietic progenitors in bone marrow are not affected by Foxn1 expression in Foxn1$^{neo/neo}$ and Foxn1$^{fl/fl}$::Foxn1-Cre mice

To exclude the possibility that the transgenic construct used influenced the developmental potential of T lymphoid cells, the frequency of Lineage^{neg}, Sca-1^{pos} and ckit^{pos} (LSK) was investigated. Since the thymus lacks self-renewing hematopoietic precursors it depend on a continuous supply of blood-borne lymphoid precursor cells identified in the bone marrow as LSK cells[276–279]. The frequency of LSK cells was compared to wild type and nude controls increased in both Foxn1$^{neo/neo}$ and Foxn1$^{fl/fl}$::Foxn1-Cre mice (Fig. 4.18 A). LSK cells expressing L-selectin (CD62L) are considered as a bone marrow homologue of the early T-lineage progenitor in the thymus [280,281], there was no significant difference in the frequency of CD62L^{high} LSK precursors between wild type and mutant mice (Fig. 4.18 B). Thus, the genetic approach chosen to alter correct Foxn1 expression did not inadvertently reduce the frequencies of T-cell precursors in the bone marrow and thus did not account for the observed phenotype. However, a significant increase in the frequency of LSK cells was appreciated, which may be caused by the residual expression of Foxn1. Overexpression of Foxn1 was shown to increase the LSK pool in the bone marrow of aged mice[282]. Therefore this increase in LSK could be attributed to a short term or reduced Foxn1 expression in combination with a reduced precursor attraction, resulting in an increased LSK pool.

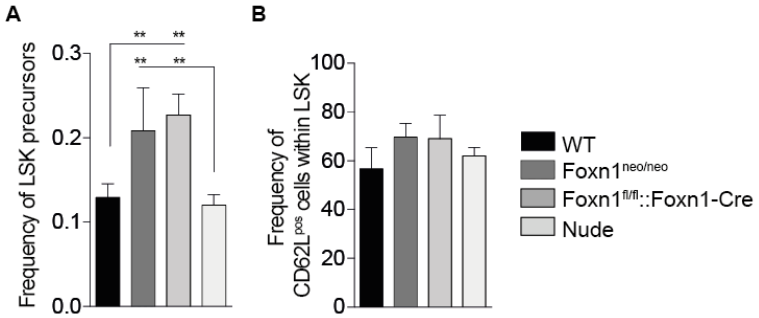

Figure 4.18: Increased frequencies of hematopoietic progenitors in the bone marrow of Foxn1$^{neo/neo}$ and Foxn1$^{fl/fl}$::Foxn1-Cre mice. (A) Frequency of lineage^{neg}Sca1^{pos}ckit^{high} (LSK) precursor cells in the bone marrow of wild type (WT; ■), Foxn1$^{neo/neo}$ (■) Foxn1$^{fl/fl}$::Foxn1-Cre (■) and nude mice (□). (B) Frequency of CD62L^{pos} cells within LSK pool. Pooled data of 2 independent experiments, values indicate mean +SD, n = 3 per experimental group. p values were determined by Mann-Whitney test *p < 0.05, ** < 0.01, *** < 0.001.

4.7. T-cells are detected in the periphery of Foxn1$^{neo/neo}$ and Foxn1$^{fl/fl}$::Foxn1-Cre mice

The consequences of a time-controlled loss or reduction of Foxn1 in TEC on the peripheral T-cell pool was assessed next. Despite the striking absence of an overt thymus in nude mice T-cells can be detected in the periphery. These T-cells are, however, extrathymically derived and their frequency increases with age[193]. I therefore examined and compared the periphery of Foxn1-target mouse mutant to specifically evaluate the consequences of a Foxn1 reduction or a TEC specific loss of Foxn1 after a short period of correct expression levels of Foxn1. As expected, a significant decrease in absolute T-cell numbers was observed in lymph nodes of Foxn1$^{neo/neo}$, Foxn1$^{fl/fl}$::Foxn1-Cre and nude mice at one week of age (Fig. 4. 19 A), which continued to be reduced in 10 week old mutant mice (96-99%) when compared to age-matched wild type animals. On closer examination, there was however a significant but in absolute cell number very small increase in T-cells in Foxn1$^{neo/neo}$ mice when compared to nude controls, which was at 5 weeks 10-fold and at 10 weeks 40-fold higher. Similar, but less prominent was the expansion of peripheral T-cells in Foxn1$^{fl/fl}$::Foxn1-Cre (13-fold) when compared to nude mice (Fig. 4.19 A).

CD8 T-cells are preferentially generated in the peripheral lymphoid compartments of nude mice[194]. To further discriminate T-cells present in Foxn1$^{neo/neo}$ and Foxn1$^{fl/fl}$::Foxn1-Cre mice from those of nude mice, T-cells were also investigated for CD4 and CD8 expression. The absolute number of CD4 T-cells was significantly reduced in both mutant strains at all ages when compared to wild type animals but increased in comparison to nude mice i.e. 870-fold in Foxn1$^{neo/neo}$ and 48-fold in Foxn1$^{fl/fl}$::Foxn1-Cre in one week old animals (Fig. 4.19 B). The difference continued to be observed for as long as I followed these mice (10 weeks), though the fold differences clearly changed between the different mouse strains compared. A different picture emerged for the detection of CD8^{+} peripheral T-cells. At 1 week of age CD8 T-cells were 2000-fold reduced in Foxn1 mutant mice in comparison to wild type animals. By 10 weeks of age, the frequency of CD8 T-cells was comparable for Foxn1$^{fl/fl}$::Foxn1-Cre and nude mice, whereas that in Foxn1$^{neo/neo}$ mice was even increased by 12-fold vis-à-vis nude animals (Fig. 4.19 C). The difference between Foxn1$^{fl/fl}$::Foxn1-Cre and Foxn1$^{neo/neo}$ mice might result from the continuous but reduced Foxn1 expression in Foxn1$^{neo/neo}$ mice.

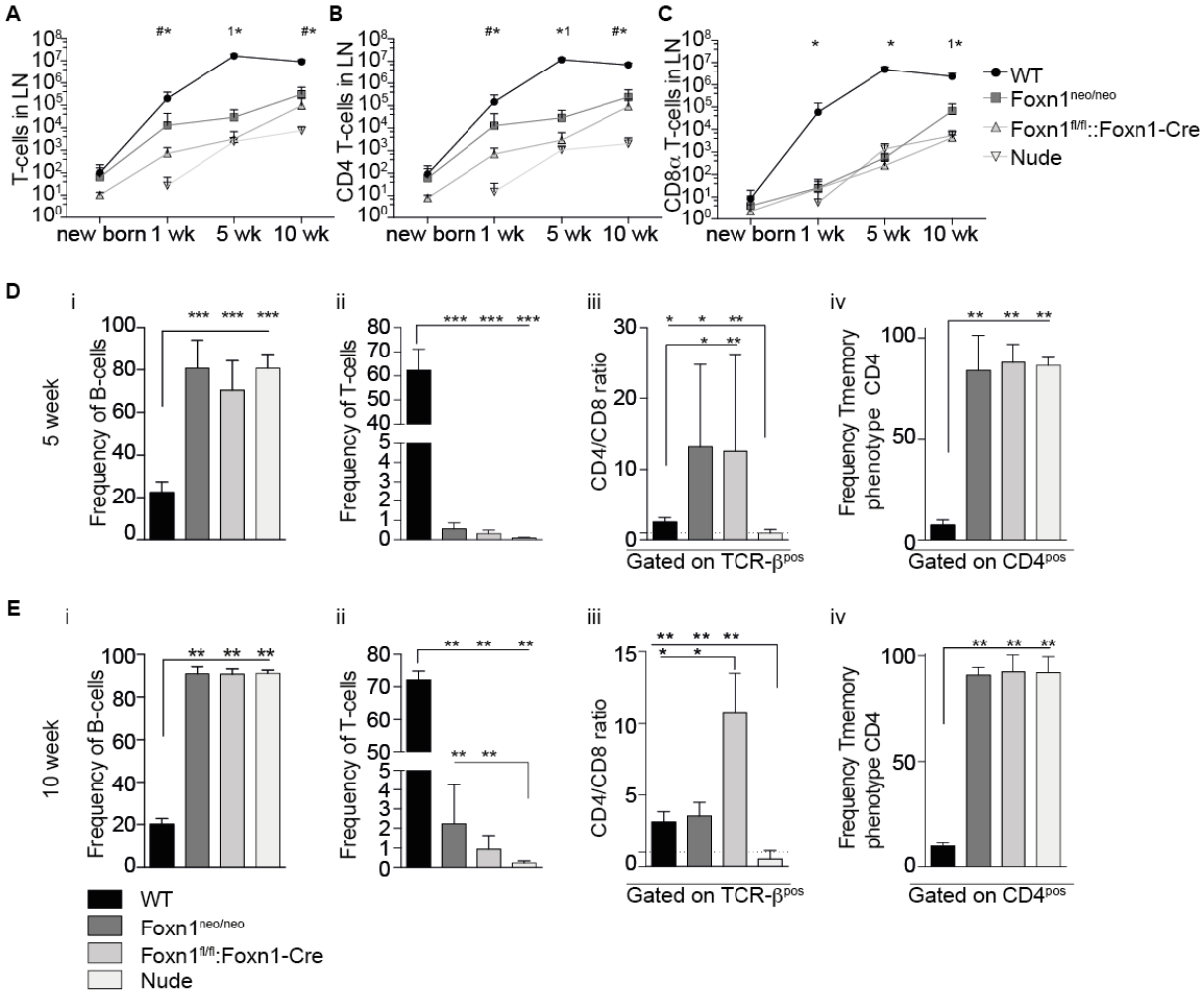

Figure 4.19: T-cells are present in the lymph nodes of Foxn1$^{neo/neo}$ and Foxn1$^{fl/fl}$::Foxn1-Cre mice.
Absolute numbers of T-cells (A), CD4 T-cells (B) and CD8 T-cells (C) in lymph nodes isolated from wild type (WT; –●–), Foxn1$^{neo/neo}$ (–■–), Foxn1$^{fl/fl}$::Foxn1-Cre (–△–) and nude mice (–▽–) at the indicated ages. Significance is indicated as * for WT cells against all other groups; # for nude cells significantly different from that of all other groups analysed and ^{1} for Foxn1$^{neo/neo}$ cells significantly different from that of Foxn1$^{fl/fl}$::Foxn1-Cre and nu/nu mice respectively. Detailed analysis of the T-cell compartment of WT (■) Foxn1$^{neo/neo}$ (▬), Foxn1$^{fl/fl}$::Foxn1-Cre (▬) nude mice (▭) of five weeks (D) and 10 weeks (E) of age. All panels report pooled data from 2-3 independent experiments: values indicate mean +SD, n ≥ 3. p values were determined using Mann-Whitney test. *p < 0.05, ** < 0.01, *** < 0.001

The relative frequency of B-cells in the lymph nodes of Foxn1$^{neo/neo}$, Foxn1$^{fl/fl}$::Foxn1-Cre and nude mice was 4-fold increased compared to wild type mice (Fig. 4.19 Di and Ei), which is likely explained by the absence of T-cells, since absolute B-cell number in wild type and mutant mice were not altered (data not shown). The frequency of TCR-β^{+} cells was 100-fold reduced in Foxn1$^{neo/neo}$, Foxn1$^{fl/fl}$::Foxn1-Cre and nude mice compared to wild type mice (Fig. 4.19 D ii). However after 10 weeks their frequency was significantly increased in Foxn1$^{neo/neo}$

(2.21% ± 2%) and Foxn1$^{fl/fl}$::Foxn1-Cre mice (0.93% ± 0.68%) when compared to nude mice (0.22% ± 0.1%; Fig. 4.19 E ii). Analysing the ratios of CD4 to CD8 T-cells revealed that in Foxn1$^{neo/neo}$ and Foxn1$^{fl/fl}$::Foxn1-Cre mice more CD4 than CD8 T-cells were present (Fig. 4.19 D iii and E iii), whereas the ratio was reversed in nude mice. More than 80% of the CD4 T-cells in Foxn1$^{neo/neo}$ and Foxn1$^{fl/fl}$::Foxn1-Cre mice expressed a memory-like phenotype (Fig. 4.19 D iv and E iv), indicating that these cells had undergone homeostatic expansion or had undergone specific antigen-driven activation.

In aggregates these analyses suggest that the peripheral T-cell pool in Foxn1$^{neo/neo}$ and Foxn1$^{fl/fl}$::Foxn1-Cre mice has a composition different from that of nude mice: Foxn1$^{neo/neo}$ and Foxn1$^{fl/fl}$::Foxn1-Cre mice had an increased frequency of CD4 T-cells particularly those with a memory like phenotype compatible with limited thymic output.

4.7.1. Composition of the TCR Vβ repertoire among T-cells of Foxn1$^{neo/neo}$ and Foxn1$^{fl/fl}$::Foxn1-Cre mice

Given a dramatically altered thymic microenvironment, T-cell selection may be affected in Foxn1$^{neo/neo}$ and Foxn1$^{fl/fl}$::Foxn1-Cre mice, thus altering the TCR-Vβ repertoire of peripheral T-cells. Because Foxn1$^{neo/neo}$ and Foxn1$^{fl/fl}$::Foxn1-Cre mice are severely lymphopenic, only the four most common Vβ (Vβ2, 6, 8 and 14) were analysed by immunostaining and flow cytometric analysis. This collection of Vβ allowed to investigate around 50% of the Vβ repertoire. Foxn1$^{neo/neo}$ mice showed changes in the repertoire when compared to wild type lymph nodes (Fig. 4.20), Vβ2 (3.61% ± 1.85% and 6.09% ± 0.75%, respectively) and Vβ6 (9.48% ± 0.41% and 9.98% ± 13.94%, respectively) were significantly reduced when compared to wild type mice. The relative frequency of Vβ 8 was increased in Foxn1$^{neo/neo}$ mice 35.06% ± 35.6% when compared to wild type mice 20.84% ± 0.57% and Vβ14 was reduced in Foxn1$^{neo/neo}$ mice compared to wild type mice (4.87% ± 5.53 and 7.36% ± 0.53%, respectively). Although the values were not statistical significant the repertoire composition varied between the different mice analysed, as some Vβ clones were preferentially used. The variety in the different mice analysed was apparent indicating that the repertoire was not polyclonal.

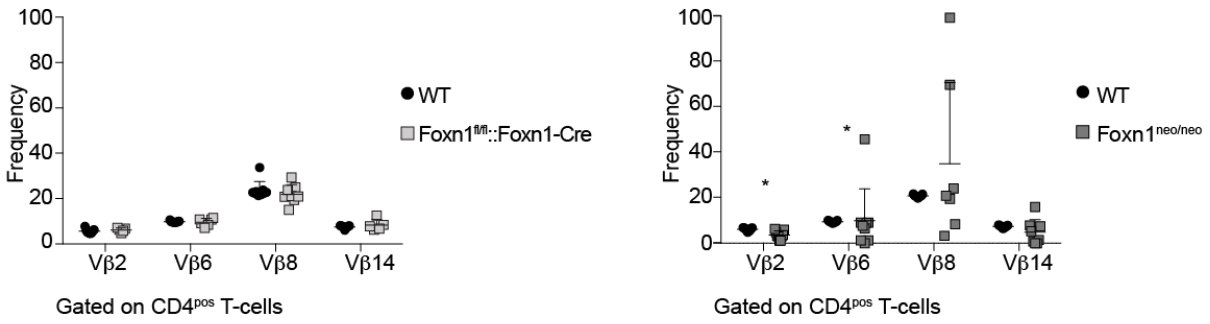

Figure 4.20: Vβ repertoire frequency in Foxn1$^{fl/fl}$::Foxn1-Cre, Foxn1$^{neo/neo}$ and wild type mice. Frequency of Vβ2, Vβ6, Vβ8 and Vβ14 was tested in lymph nodes isolated from wild type (WT; ●) Foxn1$^{neo/neo}$ (■) and Foxn1$^{fl/fl}$::Foxn1-Cre (□) mice. Values indicate mean +SD. Pooled data of 3 independent experiments with 3 mice per group. Vβ frequencies from mice with less than 10 corresponding cells were excluded from the study. p values were determined using Mann-Whitney test. *p < 0.05, ** < 0.01, ***<0.001.

The collection of the Vβ repertoire analysed in Foxn1$^{fl/fl}$::Foxn1-Cre mice was comparable to the repertoire in wild type mice (Fig. 4.20). However if Foxn1 expression is reduced the T-cell repertoire showed minor changes. The variability in the T-cell receptor chain usage was expected as only few T-cells are exported into the lymphopenic environment where they undergo extensive homeostatic expansion, a phenomenon known to influence the composition of the TCR repertoire. In contrast the Vβ repertoire of nude mice was reported to be oligoclonal, and develop from only a few functional T-cells clones[283,284] further identifying a difference between the new Foxn1 mutant and the nude mice. However, the competence of TEC of Foxn1$^{neo/neo}$ and Foxn1$^{fl/fl}$::Foxn1-Cre mice to support thymopoiesis is (at least for some mice) significantly different because of their initial short expression of physiological Foxn1 levels.

4.7.2. Regulatory T-cells are present in the periphery of Foxn1$^{neo/neo}$ and Foxn1$^{fl/fl}$::Foxn1-Cre mice

Nude mice lack regulatory T-cells (Treg)[285]. In striking contrast to this finding, regulatory T-cells were detected at regular frequencies in adult Foxn1$^{neo/neo}$ and Foxn1$^{fl/fl}$::Foxn1-Cre mice (Fig. 4.21 A and B). Treg are characteristically either generated in the thymus or, alternatively, develop in the periphery via conversion from conventional effector T-cells. Thus, the Treg detected in Foxn1$^{neo/neo}$ and Foxn1$^{fl/fl}$::Foxn1-Cre mice could have been generated either in the thymus or in the periphery. Cell surface markers have been used to

distinguish between these two origins of Treg: Thymus-derived Treg express Helios[286] and higher surface concentrations of Neuropilin-1[287,288] (Nrp1). Using these phenotypic markers, I found that the majority of the Tregs detected in the periphery of Foxn1$^{neo/neo}$ and Foxn1$^{fl/fl}$::Foxn1-cre mice expressed Helios (Fig. 4.21 C). However recent reports questioned the use of the Helios cell marker as a way to distinguish between the origin of Tregs as Helios could be detected on both sets of T-regs[289] and, in addition on activated T-cells[290], rendering as an unreliable marker for the purpose to distinguish thymic from peripheral Tregs. In contrast, Nrp1 is exclusively expressed on thymic Tregs[287,288]. The extent of Nrp1 expression on Tregs isolated from Foxn1$^{neo/neo}$ and Foxn1$^{fl/fl}$::Foxn1-Cre was approximately 4-fold reduced when compared to wild type mice (Fig. 4.21 D), though a uniform staining pattern was observed. Taken together these data show that in the periphery of Foxn1$^{neo/neo}$ and Foxn1$^{fl/fl}$::Foxn1-Cre mice regulatory T-cells were detected, that were absent in nude mice. These results emphasise the difference in the CD4 compartment of mice without and with pathological Foxn1 expression and implies that Tregs in the latter mice are generated in the periphery. This conclusion is further supported by our finding that Aire protein was not detected in the thymic medulla of these mice because Treg are dependant on its expression[83]. The reason why CD4 T-cells from congenital nude mice are not able to convert into regulatory T-cells and why CD4 T-cells of Foxn1$^{neo/neo}$ and Foxn1$^{fl/fl}$::Foxn1-Cre mice do so remain unclear, but could be linked to impaired CD4 T-cell function in nude mice[204,291]. Hence, the normal frequency of Helios^{+} cells in Foxn1$^{neo/neo}$ and Foxn1$^{fl/fl}$::Foxn1-Cre mice could result from their activation status independent of a regulatory T-cell function.

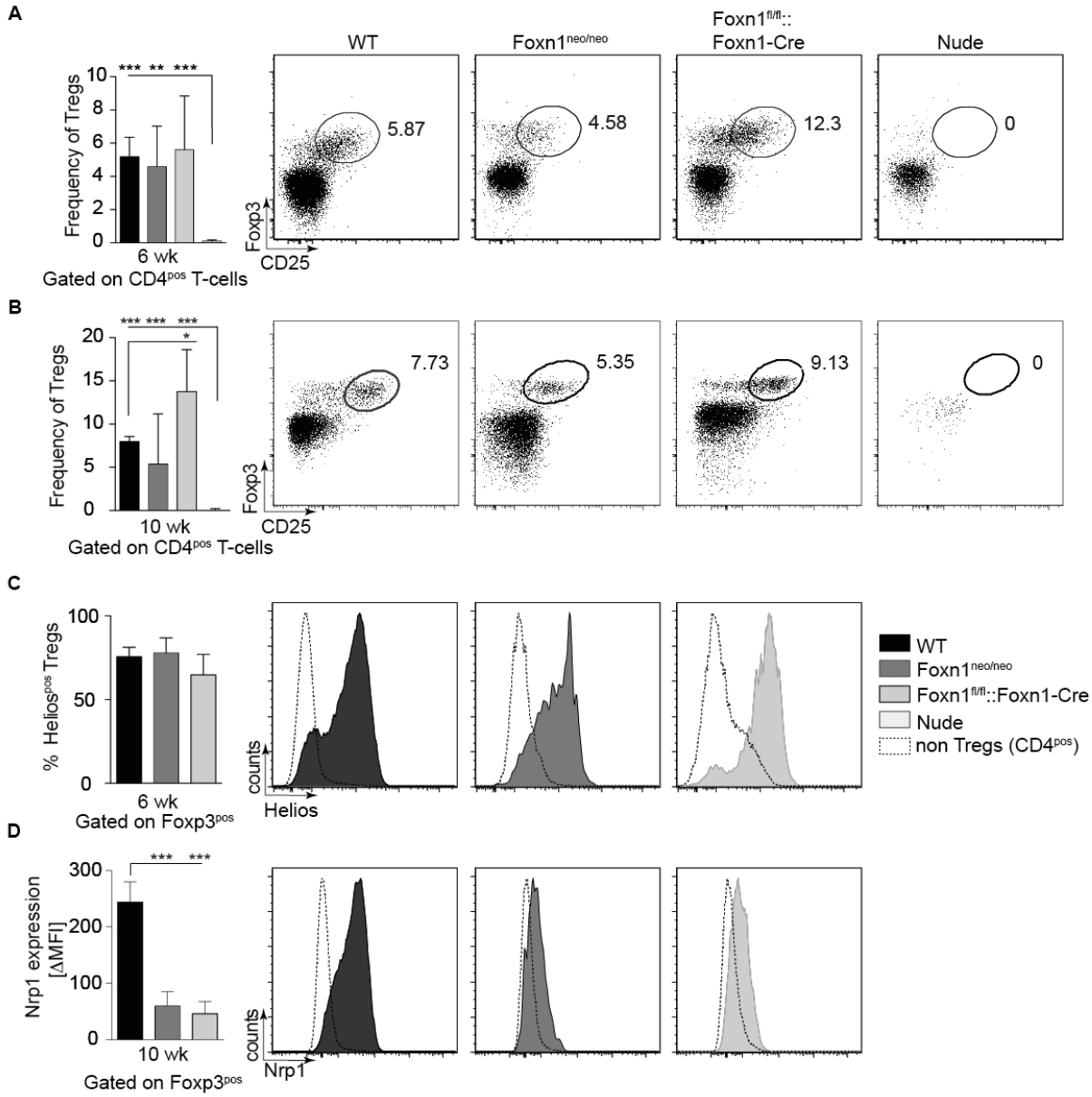

Figure 4.21: Regulatory T-cells are present in Foxn1$^{neo/neo}$ and Foxn1$^{fl/fl}$::Foxn1-Cre mice but lack in nude mice. Lymph nodes from wild type (WT; ■), Foxn1$^{neo/neo}$ (■), Foxn1$^{fl/fl}$::Foxn1-Cre (□) and nude (□) mice were analysed for the presence of Foxp3^{pos} CD25^{pos} regulatory T-cells. Representative FACS plots and frequency of regulatory T-cells among CD4 T-cells in mice 6 (A) and 10 weeks of age (B). (C) Expression of Helios in regulatory T-cells. (D) Expression of Neuropilin1 (Nrp1) among regulatory T-cells. ΔMean fluorescence intensity (MFI) of Nrp1 expression was defined as the MFI of Nrp1 expression in regulatory T-cells subtracted from the MFI of Nrp1 of CD4 T-cells. Values indicate mean +SD of three independent experiments with n ≥ 3 for each group analysed. p values were determined using Mann-Whitney test. *p < 0.05, ** < 0.01, *** < 0.005.

4.7.3. T-cell effector function in Foxn1$^{neo/neo}$ and Foxn1$^{fl/fl}$::Foxn1-Cre mice

Next, I assayed CD4 T-cell function in Foxn1$^{neo/neo}$ and Foxn1$^{fl/fl}$::Foxn1-Cre mice. For this purpose purified CD4 T-cells were stimulated using mitogenic concentrations of anti-CD3 antibodies and the cells proliferative response was measured using the dilution of CFSE label (details see Material and Methods section). T-cell proliferation (as revealed by the proliferation index) was significantly higher for cells isolated from Foxn1$^{neo/neo}$ (2.67 ± 1.02) and Foxn1$^{fl/fl}$::Foxn1-Cre (2.37 ± 0.75) mice when compared to T-cells from nude mice (1.18 + 0.01, Fig. 4.22 A), but remained significantly smaller when compared to wild type T-cells (Fig. 4.22 A). This reduced response may reflect their partial exhaustion due to homeostatic expansion. Consistent with their activation the population of CD4$^+$ T-cells from Foxn1$^{neo/neo}$ and Foxn1$^{fl/fl}$::Foxn1-Cre mice had subsequent to mitogenic stimulation an increased cell size (Fig. 4.22 B)[292]. The failure of CD4 T-cells from nude mice to proliferate in response to mitogenic stimulation has been linked to their reduced capacity to produce IL-2[291]. To extent this finding to CD4$^+$ T-cells from Foxn1$^{neo/neo}$ and Foxn1$^{fl/fl}$::Foxn1-Cre mice the supernatants of T-cell proliferation cultures were analysed on day 3 for the presence of IL-2. As expected, CD4 T-cells isolated from nude mice produced far less IL-2 when compared to CD4 T-cells isolated from Foxn1$^{neo/neo}$ or Foxn1$^{fl/fl}$::Foxn1-Cre mice which in turn expressed decreased concentrations of this cytokine in comparison to wild type controls (Fig. 4.22 C). Thus CD4 T-cells in Foxn1$^{neo/neo}$ and Foxn1$^{fl/fl}$::Foxn1-Cre mice demonstrate an intermediate functionality to TCR-mediated stimulation, which may reflect their exposure to extensive homeostatic expansion.

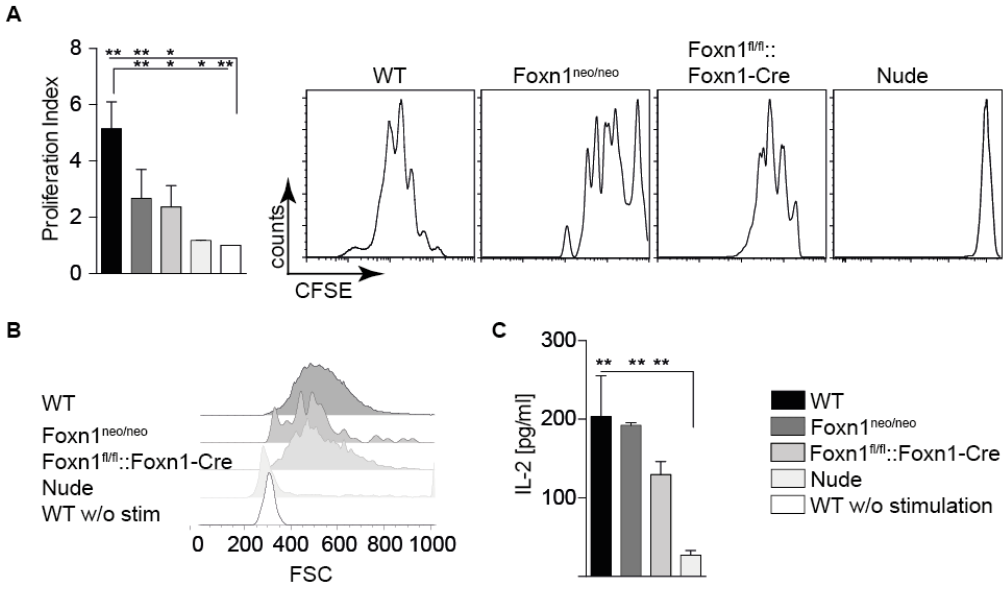

Figure 4.22: T-cells of Foxn1$^{neo/neo}$ and Foxn1$^{fl/fl}$::Foxn1-Cre mice proliferate *in vitro* in response to a mitogenic stimulus. Proliferation of CFSE labelled CD4 T cells isolated from wild type (WT; ■) Foxn1$^{neo/neo}$ (■), Foxn1$^{fl/fl}$::Foxn1-Cre (▭) and nude (▭) mice (experimental details are given in section 3.5). (A) Proliferation index of CD4 T-cells and representative CFSE profiles. Values indicate mean +SD: data was pooled from at least 3 independent experiments. (B) Cell size of CD4 cells as measured by forward scatter (FSC). (C) IL-2 concentration in the supernatant determined by ELISA (experimental details are given in section 3.8. Values indicates mean +SD from one representative experiment with n = 4. p values were determined using Mann-Whitney test. *p< 0.05, ** < 0.01, *** < 0.001.

4.7.4. Suppressive potential of regulatory T-cells

Treg function in Foxn1$^{neo/neo}$ and Foxn1$^{fl/fl}$::Foxn1-Cre mice was analysed using a standard *in vitro* suppression assay. For this purpose wild type CD4^{pos} T-effector cells were sorted, labelled with CFSE and cultured for 3 days in the presence or absence of purified CD4^{pos}CD25^{pos} regulatory T-cells used at a 1:1 ratio (the precise experimental details are given in section 3.5). T-cells with a CD4^{+}CD25^{+}phenotype isolated from nude mice were not able to suppress at all (Fig. 4.23 iv), whereas those isolated from Foxn1$^{fl/fl}$::Foxn1-Cre or from Foxn1$^{neo/neo}$ mice supressed the proliferation of wild type CD4 effector T-cells by 15 ± 8.4% and 25 ± 17.5% respectively (Fig. 4.23 ii and iii), which was still significantly smaller when compared to Treg from wild type mice (52.7% ± 16.1%, Fig. 4.23 i).

Though Tregs were identified and purified according to the expression of CD4^{+}CD25^{+} I cannot exclude that activated effector T-cells were included in the assay contributing to the reduced Treg suppression observed. This result together with an overall lower frequency of

Treg in Foxn1$^{neo/neo}$ and Foxn1$^{fl/fl}$::Foxn1-Cre should indeed result in a severely impaired Treg capacity in these mice. Consequently, these mice may be more susceptible to develop autoimmunity.

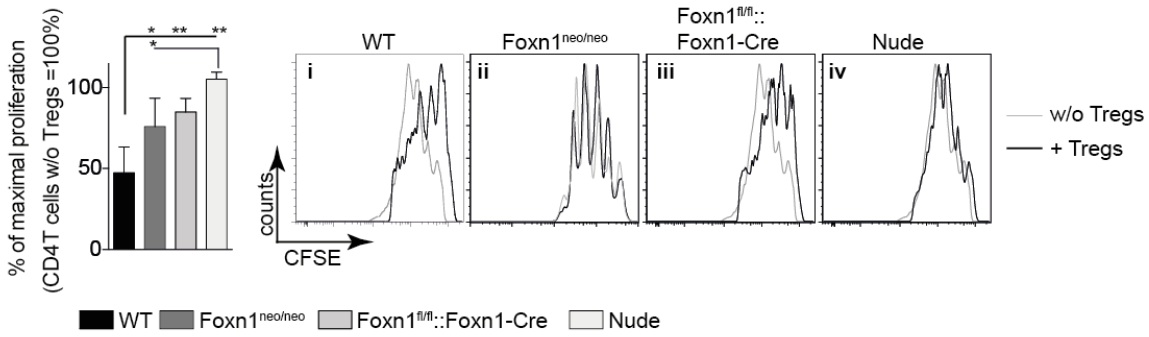

Figure 4.23: Regulatory T-cells from Foxn1$^{neo/neo}$ and Foxn1$^{fl/fl}$::Foxn1-Cre mice are less potent compared to those form wild type mice. Regulatory T-cells of wild type (WT; ■), Foxn1$^{neo/neo}$ (▬) Foxn1$^{fl/fl}$::Foxn1-Cre (▭) and nude mice (▭) were sorted according to their CD4 and CD25 expression and co-cultured with activated and CFSE labelled responder T-cells (in a 1:1 ratio), cell proliferation was measured at day 3 of culture. Values indicate mean +SD from at least 3 independent experiments. p values were determined using Mann-Whitney test. *p < 0.05, ** < 0.01, *** < 0.001.

4.8. Wasting disease induction by adoptive transfer of CD4$^+$ T-cells

One way to test the function of T-cells and their subpopulations *in vivo* is their adoptive transfer to T-cell deficient recipients. In the case of CD4 T-cells their adaptive transfer into Rag-deficient mice lacking all lymphocytes usually results in a severe wasting disease as these cells mount an immune reaction against the gut flora[293,294]. Hence, sorted CD4$^+$ T-cells from either wild type, Foxn1$^{neo/neo}$, Foxn1$^{fl/fl}$::Foxn1-Cre or nude mice were adoptively transferred into RAG2$^{-/-}$ mice and the occurrence of wasting disease was monitored by weight loss of 20 and more percent body weight.

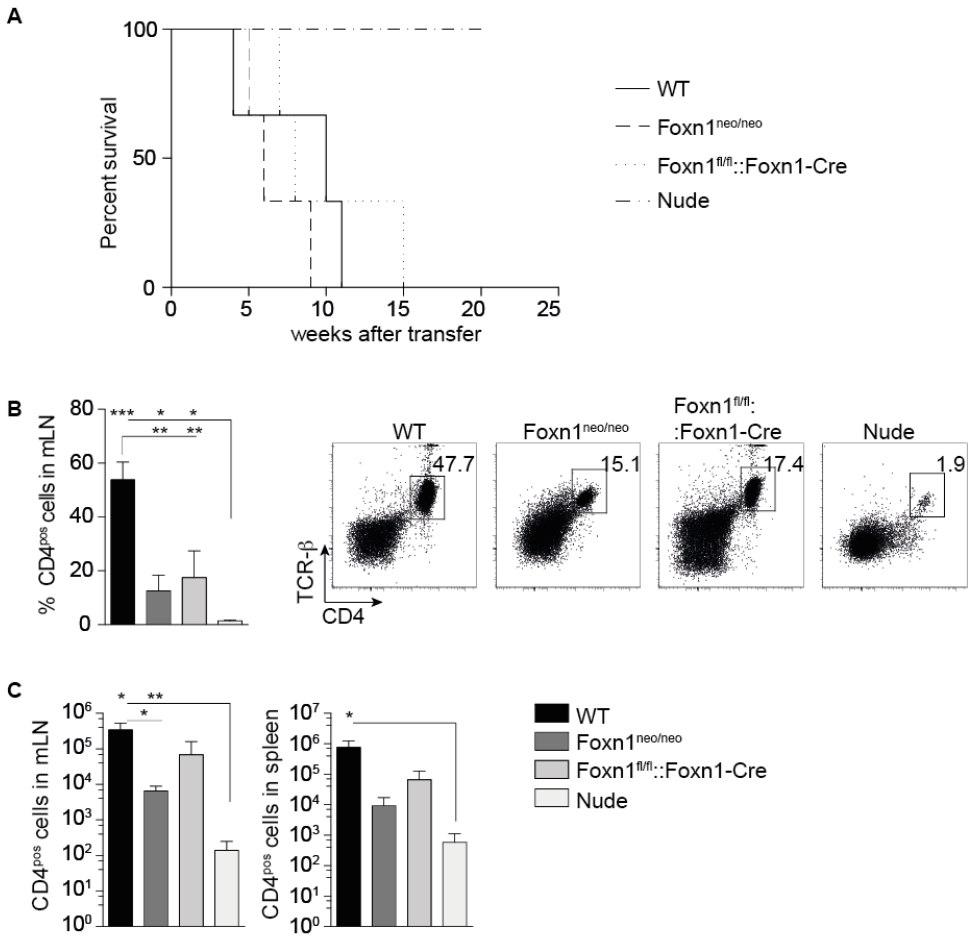

Figure 4.24: CD4 T-cells of Foxn1$^{neo/neo}$ and Foxn1$^{fl/fl}$::Foxn1-Cre mice induce wasting disease upon adoptive transfer to Rag2$^{-/-}$ mice. (A) Survival curves of Rag2$^{-/-}$ mice injected with 100'000 CD4 T-cells isolated from 6-10 week old wild type (WT; ——), Foxn1$^{neo/neo}$ (– –), Foxn1$^{fl/fl}$::Foxn1-Cre (….) and nude (–..) mice. Mice were scarified and analysed when they had lost 20 and more percent of their bodyweight at the time of T-cell transfer. (B) Frequency of donor CD4^{pos}/TCR-β^{pos} cells in mesenteric lymph nodes of adoptively transferred recipient Rag2$^{-/-}$ mice, and representative FACS blots. (C) Absolute numbers of recovered CD4 T-cells in mLN and spleen of Rag2$^{-/-}$ mice reconstituted with WT (■), Foxn1$^{neo/neo}$ (▩), Foxn1$^{fl/fl}$::Foxn1-Cre (▨) and nude (□) CD4 T-cells. p values were determined using Mann-Whitney test. *p < 0.05, ** < 0.01, *** < 0.001.

The adoptive transfer of CD4 T-cells from wild type, Foxn1$^{neo/neo}$ and Foxn1$^{fl/fl}$::Foxn1-Cre mice caused wasting disease with comparable kinetics (Fig. 4.24 A). Adoptive transfer of CD4 T-cells isolated from nude mice did not result in wasting disease, the CD4 T-cells did not mount an immune reaction against the gut flora (Fig. 4.24 A and B). Lymph nodes and spleen from the reconstituted RAG2-deficeint mice were next analysed for the presence of the transferred CD4^{+}/TCR-β^{+} cells. The highest frequency of these cells was recovered in recipients of CD4 T-cells from wild type mice (lymph nodes: 53.8% ± 6.6% and spleen:

6.36% ± 2.9%), followed by Foxn1$^{neo/neo}$ (lymph nodes: 12.5% ±5.9% and spleen: 0.08% ± 0.09%) and Foxn1$^{fl/fl}$::Foxn1-Cre animals (lymph nodes: 17.4% ± 9.9% and spleen: 1.379% ± 1%). Transferred CD4 T-cells from nude mice did accumulate only minimally (lymph nodes: 1.3% ± 0.4%, and spleen: 0.036% ± 0.035%, Fig. 24 B and C, and data not shown). Thus CD4 T-cells from Foxn1$^{neo/neo}$ and Foxn1$^{fl/fl}$::Foxn1-Cre mice could mount an immune response similar to that of wild type CD4 T-cells resulting in a wasting syndrome with comparable disease kinetics. Moreover these data underline the difference in functional competence between peripheral T-cell from nude and other mutant mice investigated here. There is a obvious possibility that T-cells in Foxn1$^{neo/neo}$ and Foxn1$^{fl/fl}$::Foxn1-Cre mice mount an immune response against the gut flora, since I showed that these cells are functional and both mutant mouse strains are lymphopenic, furthermore I demonstrated that the function of Tregs in Foxn1$^{neo/neo}$ and Foxn1$^{fl/fl}$::Foxn1-Cre mice is impaired *in vitro*, all factors that could promote wasting disease.

4.9. Reduced survival of Foxn1$^{neo/neo}$ and Foxn1$^{fl/fl}$::Foxn1-Cre mice

Foxn1$^{neo/neo}$ and Foxn1$^{fl/fl}$::Foxn1-Cre mice displayed a significantly higher risk for spontaneously developing wasting disease when compared to wild type and nude mice.

When followed up over 50 weeks, the mice had to be sacrificed for animal welfare reasons, when the lost more than 20% of their maximum weight, or they appeared passive, showed lack of grooming or developed a prolapse.

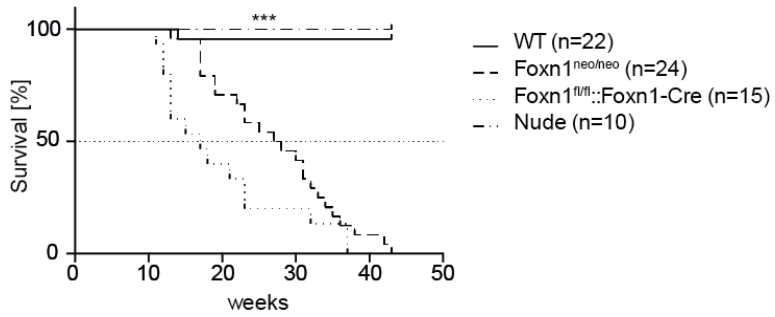

Figure 4.25: Reduced life expectancy of Foxn1$^{neo/neo}$ and Foxn1$^{fl/fl}$::Foxn1-Cre mice. Mice were monitored over a period of 50 weeks for weight loss and indicators of well being. Mice were euthanized when they lost more than 20% of their maximum bodyweight or when they appeared passive, showed lack of grooming or developed a prolapse. Monitored were 22 wild type (WT; ——), 25 Foxn1$^{neo/neo}$ (– –), 15 Foxn1$^{fl/fl}$::Foxn1-Cre (····) and 10 nude (– ··) mice. p values were determined using Mann-Whitney test. *p < 0.05, ** < 0.01, *** < 0.001.

Fifty percent of Foxn1$^{neo/neo}$ mice had to be sacrificed within 27 weeks, whereas the same percentage of Foxn1$^{fl/fl}$::Foxn1-Cre mice needed to be euthanized by 17 weeks after birth. In contrast all nude and all but one of the wild type mice were healthy and did not need to be put down during the first 50 weeks of their life under specific-pathogen free (SPF) conditions (Fig. 4.25). The precipitous weight loss observed in Foxn1$^{neo/neo}$ and Foxn1$^{fl/fl}$::Foxn1-Cre mice was sometimes accompanied by diarrhoea and approximately half of the Foxn1$^{fl/fl}$::Foxn1-Cre mice suffered from rectal prolapse, which was not observed in the other mice followed over time. Weight loss can be associated with gastrointestinal problems, therefore the colon of these mice were analysed.

4.10. Foxn1$^{neo/neo}$ and Foxn1$^{fl/fl}$::Foxn1-Cre mice develop colitis

To investigate the aetiology of the observed weight loss Foxn1$^{neo/neo}$ and Foxn1$^{fl/fl}$::Foxn1-Cre mice were analysed for the presence of intestinal inflammation, in particular colitis. Foxn1$^{neo/neo}$ and Foxn1$^{fl/fl}$::Foxn1-Cre mice demonstrated a thickened and shortened colon (Fig. 4.26 A) macro anatomical features compatible with colitis. On histological examination, colonic sections demonstrated many of the pathological features that are scored when assessing the histopathological hallmarks of colitis: epithelial cell hyperplasia, increase in leucocytes numbers, reduced mucin-secreting goblet cells and crypt abscesses (Fig. 4.26 B). These alterations were used to score and rate the colonic histopathological changes[295,296]. The colitis score in both wild type and nude mice was 0, whereas that in Foxn1$^{neo/neo}$ and Foxn1$^{fl/fl}$::Foxn1-Cre was 2.1 ± 1.3 and 2.8 ± 1.2, respectively (Fig. 4.26 C). The extent of pathology ranged in the affected mice from mild (score: 0.5) to severe (score: 4). This variance is explained by the limited T-cells available, which is different between each mouse, explaining the different extent of colitis and different age of disease onset.

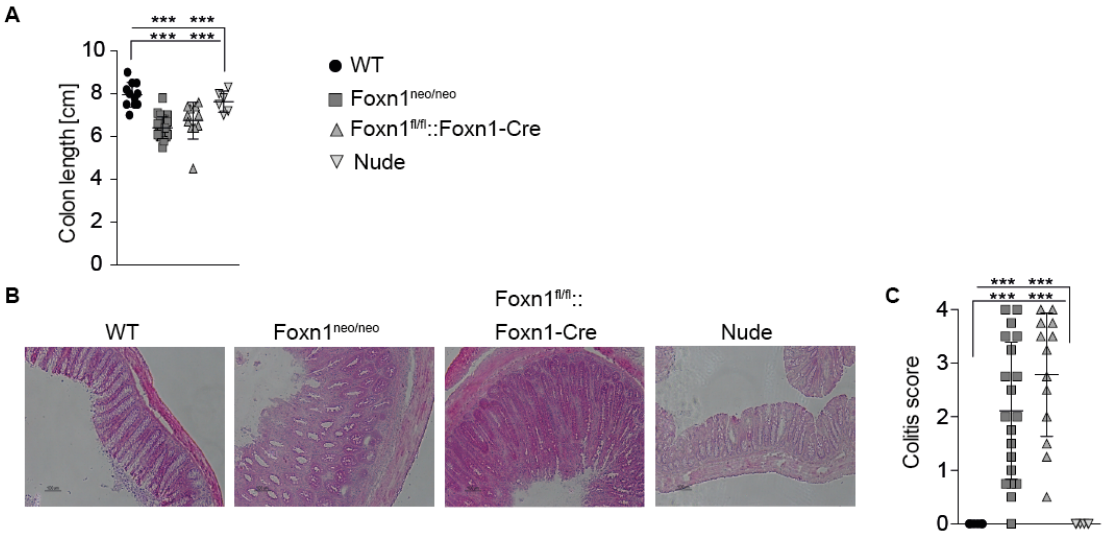

Figure 4.26: Foxn1$^{neo/neo}$ and Foxn1$^{fl/fl}$::Foxn1-Cre mice develop colitis. (A) Colon length of healthy wild type (WT, ●) and nude (▽) mice and colitic Foxn1$^{neo/neo}$ (■) and Foxn1$^{fl/fl}$::Foxn1-Cre (▲) mice. (B) Histological analysis of colons isolated from WT, Foxn1$^{neo/neo}$, Foxn1$^{fl/fl}$::Foxn1-Cre and nude mice. (C) Colitis score of healthy WT (●) and nude (▽) control mice and Foxn1$^{neo/neo}$ (■) and Foxn1$^{fl/fl}$::Foxn1-Cre (▲) mice. p values were determined using Mann-Whitney test. *p < 0.05, ** < 0.01, *** < 0.001. Analysed were 6 WT and nude mice, 20 Foxn1$^{neo/neo}$ and 13 Foxn1$^{fl/fl}$::Foxn1-Cre mice. The mice were analysed when they showed sign of colitis.

In summary the clinical signs of spontaneous wasting in mutant mice, with aberrant Foxn1 expression correlated with the macro anatomical and pathological changes of colitis. However these investigations did not reveal the mechanism how this is caused.

4.10.1. Colitis is induced by CD4 T-cells

The inflammatory infiltrations of the colon in Foxn1$^{neo/neo}$ and Foxn1$^{fl/fl}$::Foxn1-Cre mice was next investigated both at the level of the lamina propria and intraepithelial lymphocytes. In wild type and nude mice the majority of the TCR-β^{+} intraepithelial and lamina propria lymphocytes (IEL and LPL, respectively) were CD8 T-cells (Fig. 4. 27 A). CD4 T-cells could be predominantly detected in IEL and LPL of Foxn1$^{neo/neo}$ (78% ± 12.3% and 72.8% ± 15.9%, respectively) and Foxn1$^{fl/fl}$::Foxn1-Cre mice (77.8% ± 12.5% and 79% ± 14.7%). In contrast, these cells were less abundant in wild type (33.8% ± 17.7% and 36.1% ± 7.6%) and nude animals (10.4% ± 6.96 and 15% ± 19.5%, Fig. 4.27 B). Immunohistochemistry confirmed that the infiltrating leucocytes were CD4 T-cells (Fig. 4.27 C), and not B-cells. B220 allowed to further distinguish between isolated lymphoid follicles and infiltrating CD4 T-cells (data not

shown) in histology, as not all aggregates of CD4 T-cells are infiltrations. The absolute number of CD4 T-cells isolated from colon IEL and LPL of wild type, Foxn1$^{neo/neo}$ and Foxn1$^{fl/fl}$::Foxn1-Cre mice varied between individual mice somewhat their order of magnitude was similar and 200-fold more abundant than that observed in nude mice (Fig. 4.27 D). The increase in CD4 T-cells might be linked to their functionality to respond to antigens, whereas CD4 T-cells from nude mice do not respond and remain therefore low in numbers. In contrast colonic intraepithelial CD8 T-cells were reduced by five to ten fold in Foxn1$^{neo/neo}$, Foxn1$^{fl/fl}$::Foxn1-Cre and nude mice compared to wild type mice. The absolute number of lamina propria CD8 T-cells was four-fold lower in Foxn1$^{neo/neo}$ and Foxn1$^{fl/fl}$::Foxn1-Cre mice compared to wild type mice but still 20-fold more abundant when compared to nude mice. The mucosal CD8 T-cells in nude mice were generated solely in the periphery, whereas in Foxn1$^{neo/neo}$ and Foxn1$^{fl/fl}$::Foxn1-Cre the thymus rudiment also contributes to the T-cell pool. Thus Foxn1 withdrawal or reduced Foxn1 expression resulted in an infiltration of CD4 T-cells in the intraepithelial and lamina propria compartments. Despite a reduced thymic T-cell production in Foxn1$^{neo/neo}$ and Foxn1$^{fl/fl}$::Foxn1-Cre mice, the absolute of CD4 T-cells cellularity of the colon was comparable between wild type and these mutant strains of mice which strongly suggests that the few T-cells in the mutant mice had undergone massive antigen induced homeostatic expansion most likely in the colon.

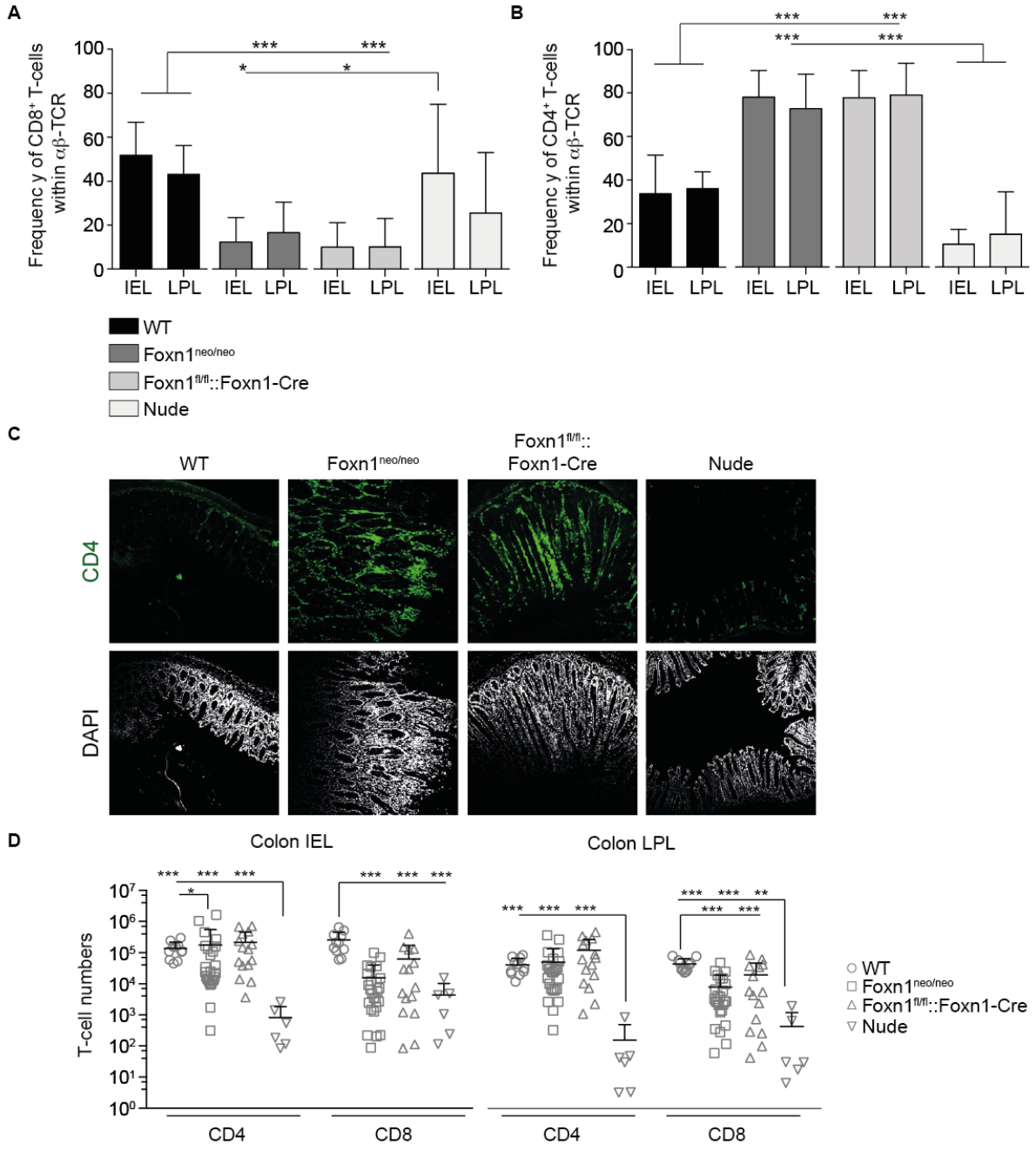

Figure 4.27: Colitis correlates with the presence of CD4 T-cells in colon IEL and LPL. Frequencies of colonic CD8 T-cells (A) and colonic CD4 T-cells (B) in healthy wild type (WT; ■) and nude (□) mice and colitic Foxn1$^{neo/neo}$ (■) and Foxn1$^{fl/fl}$::Foxn1-Cre (□) mice. (C) Confocal microscopy of colon tissue sections stained for CD4 (green) and DNA (grey). (D) Absolute CD4 and CD8 T-cells numbers in colon of healthy WT (○) and nude (▽) mice and colitic Foxn1$^{neo/neo}$ (□) and Foxn1$^{fl/fl}$::Foxn1-Cre (△) mice. n ≥ 6, the mice analysed were between 10 and 30 weeks old. p values were determined using Mann-Whitney test. *p < 0.05, ** < 0.01, *** < 0.001.

4.10.2. The CD4 IEL and LPL infiltrating in the colon have of a Th1 effector phenotype

Colitis can be induced by either Th1, Th2 or Th17 cells, though the most common effector subtype bear the Th1 type [259,297]. I therefore phenotyped the mucosal $CD4^+$ T-cells of affected mice for their cytokine secretion profile; IFN-γ for Th1, IL-10 for Th2 and IL-17 for Th17.

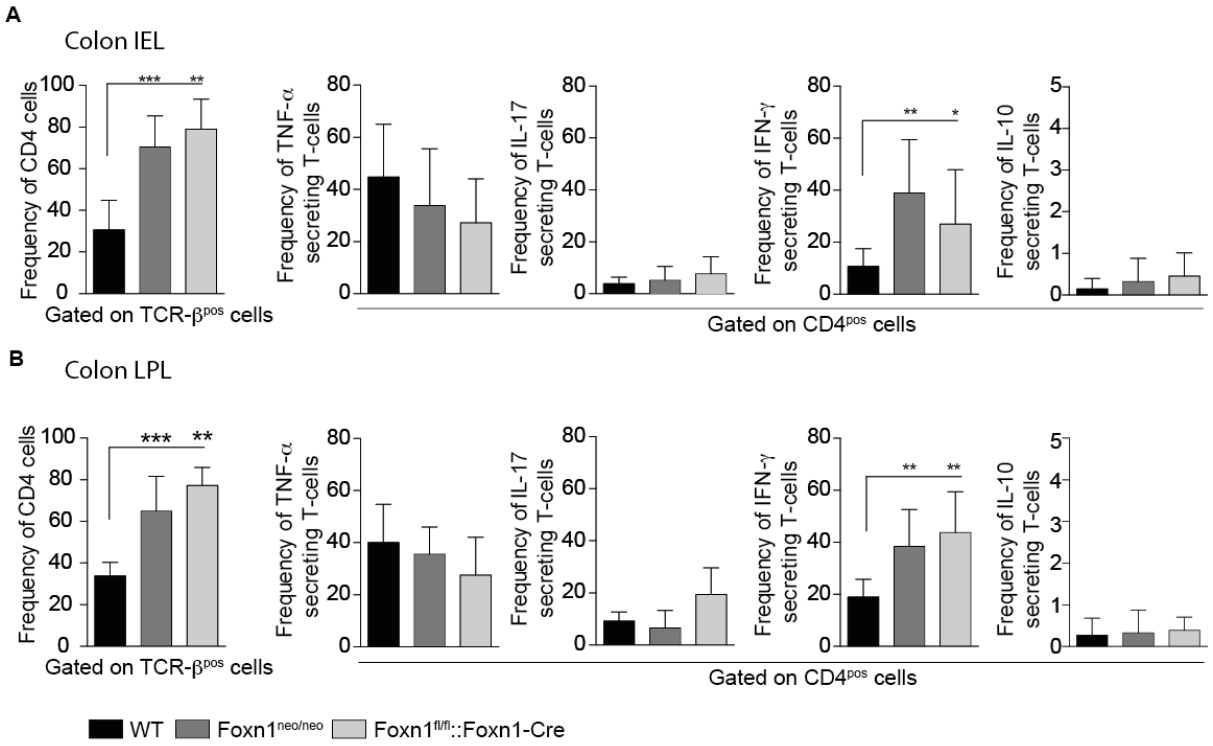

Figure 4.28: Colitis correlates with infiltrating CD4 T-cells with Th1 polarisation. Frequency and cytokine expression of CD4 T-cells isolated from colon IEL (A) and LPL (B) of healthy wild type (WT; ■) and sick Foxn1$^{neo/neo}$ (■) and Foxn1$^{fl/fl}$::Foxn1-Cre (▭) mice. The CD4 T-cells were analysed for production of TNF-α (i), IL-17 (ii), IFN-γ (iii), and IL-10 (iv). p values were determined using Mann-Whitney test. *p < 0.05, ** < 0.01, *** < 0.001.

CD4 T-cells producing IFN-γ cytokine were characteristic among colonic IEL and LPL of colitic Foxn1$^{neo/neo}$ (38.9% ± 20.5% and 38.4% ± 14.2% respectively) and Foxn1$^{fl/fl}$::Foxn1-Cre (27% ± 20.9% and 43.7% ± 15.7%) mice. In contrast the frequency of Th1 polarized CD4 IEL and LPL in the colon of wild type mice was significantly lower (Fig. 4.28) 10.8% ± 6.8% and 19% ± 6.8%, respectively. The production of IL-10, IL-17 and TNF-α however was unchanged between the different mouse strains analysed (Fig. 4.28 A and B). This suggests that the observed colitis is associated with Th1 polarized $CD4^+$ T-cells.

4.10.3. The draining mesenteric Lymph nodes were also affected by increase of CD4 T-cells

Mesenteric lymph nodes are affected in the context of the immunopathology causing colitis, associated with an immune activation in the gut associated lymphatic tissue (GALT). I therefore analysed the mesenteric and other lymph nodes of Foxn1$^{neo/neo}$ and Foxn1$^{fl/fl}$::Foxn1-Cre mice separately for the frequency of CD4 and CD8 T-cells and the cytokine secretion profile of the former cells. αβ TCR-positive lymphocytes were decreased in mesenteric lymph nodes of affected Foxn1$^{neo/neo}$ (6.8% ± 8.5%) and Foxn1$^{fl/fl}$::Foxn1-Cre mice (6.9% ± 4.9%) by up to 10-fold when compared to wild type mice but still significantly increased when compared to nude mice (1.5% ± 0.7%, Fig. 4.29 A). However the frequency of CD4^{+} T-cells in peripheral lymph nodes was comparable for colitic Foxn1$^{neo/neo}$ (55.2% ± 21.7%) and diseased Foxn1$^{fl/fl}$::Foxn1-Cre (45.3% ± 24.6%) compared to healthy wild type mice (57.0% ± 5.5%, Fig. 4.29 B). Hence, there was no generalized impact of colitis on other lymphoid tissues but the tributary ones. An elevated frequency of CD4 T-cells was detected in the mesenteric lymph nodes of Foxn1$^{neo/neo}$ (71.5% ± 12.7%) and Foxn1$^{fl/fl}$::Foxn1-Cre mice (66.7% ± 20.3%) with colitis when compared to healthy wild type mice (58.3% ± 5.2%, Fig. 4.29 B).

Colitis is the result of an imbalance of the gut homeostasis, which can be caused by an overreactivity of the immune system against the gut microbiota, which is helped by an absence of Treg. Indeed the adaptive transfer of Treg is known to prevent colitis[258]. I therefore tested whether a reduction in Treg cellularity in the Foxn1$^{neo/neo}$ and Foxn1$^{fl/fl}$::Foxn1-Cre mice may contribute or even account for the colitis observed. Treg were present at normal frequencies in mesenteric and peripheral lymph nodes of colitic Foxn1$^{neo/neo}$ and Foxn1$^{fl/fl}$::Foxn1-Cre mice (Fig. 4.29 C) but I had previously shown that these cells were functionally impaired *in vitro* (Fig. 4.23).

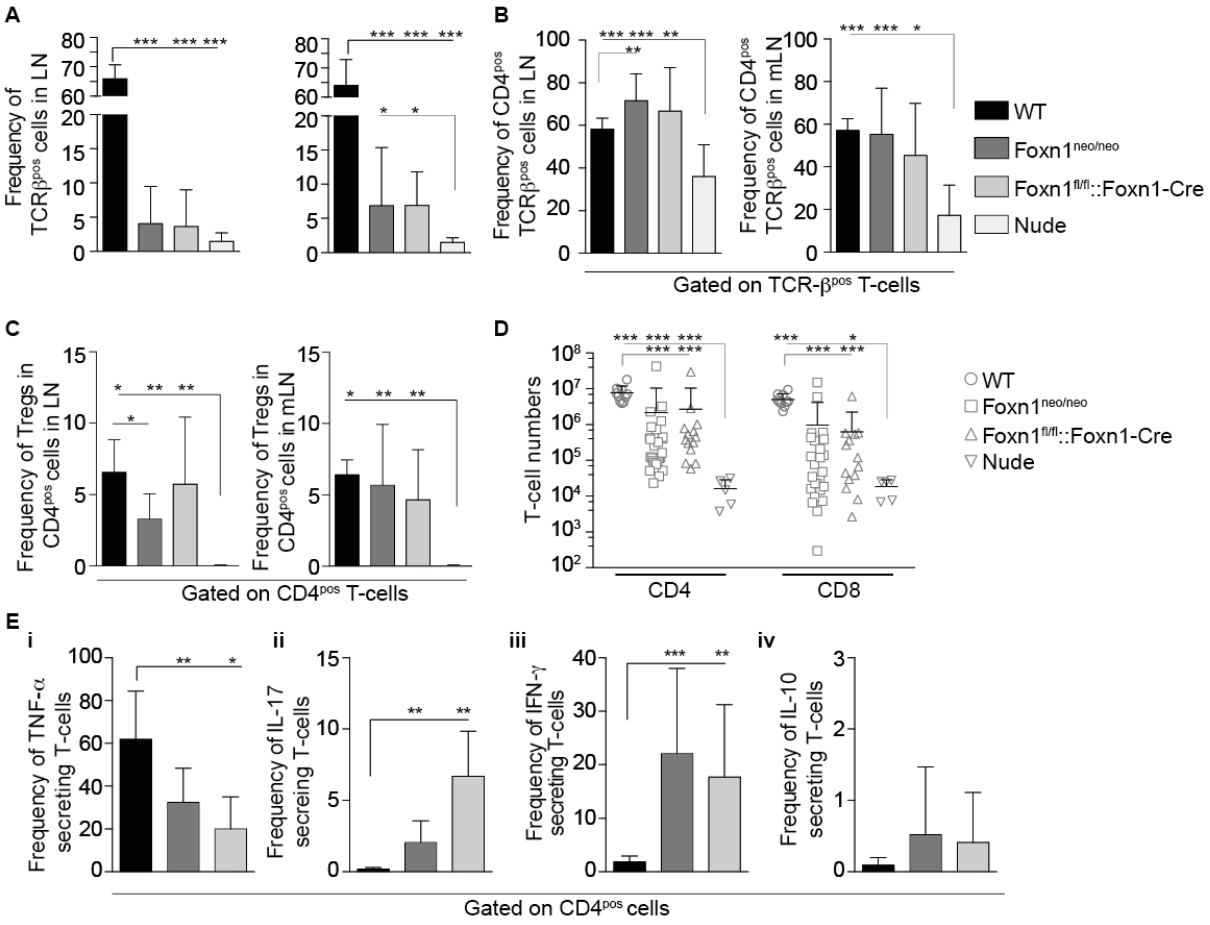

Figure 4.29: Increased frequency of CD4 T-cells in mesenteric lymph nodes of Foxn1$^{neo/neo}$ and Foxn1$^{fl/fl}$::Foxn1-Cre mice suffering from colitis. (A) Frequency of αβ-TCR$^+$ cells in peripheral and mesenteric lymph nodes of healthy wild type (WT; ■) and nude (□) mice and of colitic Foxn1$^{neo/neo}$ (■) and Foxn1$^{fl/fl}$::Foxn1-Cre (□) mice. (B) Frequency of CD4 T-cells in αβ-TCR$^+$ cells in peripheral and mesenteric lymph nodes of healthy WT and nude mice and colitic Foxn1$^{neo/neo}$ and Foxn1$^{fl/fl}$::Foxn1-Cre mice. (C) Frequency of regulatory T-cells among CD4 T-cells in the peripheral and mesenteric lymph nodes of healthy WT and nude mice and colitic Foxn1$^{neo/neo}$ and Foxn1$^{fl/fl}$::Foxn1-Cre mice. (D) Absolute number of CD4 and CD8 T-cells in mesenteric lymph nodes of healthy WT (○) and nude (▽) mice and colitic Foxn1$^{neo/neo}$ (□) and Foxn1$^{fl/fl}$::Foxn1-Cre mice (△). (E) Cytokine expression in CD4 T-cells isolated from mesenteric lymph nodes of healthy WT and colitic Foxn1$^{neo/neo}$ and Foxn1$^{fl/fl}$::Foxn1-Cre mice: (i) TNF-α, (ii) IL-17, (iii) IFN-γ and (iv) IL-10. At least 6 mice per experimental group and up to 30 weeks of age were analysed. p values were determined using Mann-Whitney test. *p < 0.05, ** < 0.01, *** < 0.001. Statistics were performed for all groups, indicated were only significances.

Both CD4 and CD8 T-cells were 2 to 8 fold reduced in the mesenteric lymph nodes of colitic Foxn1$^{neo/neo}$ and Foxn1$^{fl/fl}$::Foxn1-Cre mice compared to wild type mice, however compared to nude mice they were over 100 fold increased (Fig. 4.29 D). TNF-α producing CD4 T-cells in the mesenteric lymph nodes of Foxn1$^{neo/neo}$ and Foxn1$^{fl/fl}$::Foxn1-Cre mice were reduced by

50% compared to wild type mice (Fig. 4.29 E i). IL-17 and IFN-γ producing CD4 T-cells were increased more than ten fold in the mesenteric lymph nodes (Fig. 4.29 E ii, iii), the frequency of IL-10 producing CD4 T-cells was not altered (Fig. 4.29 E iv). These results showed that the mesenteric lymph nodes were affected by colitis with an increase in CD4 T-cells and the production of the pro-inflammatory cytokine IFN-γ. Therefore despite the presence of Tregs, extensive homeostatic proliferation of CD4 T-cell must have taken place leading to disease, indicating that the functionality of Tregs was impaired *in vivo*.

4.10.4. Foxn1$^{neo/neo}$ and Foxn1$^{fl/fl}$::Foxn1-Cre mice suffer from enteritis

I next investigated whether Foxn1$^{neo/neo}$ and Foxn1$^{fl/fl}$::Foxn1-Cre mice also suffered from enteritis. Small bowel tissue from wild type, Foxn1$^{neo/neo}$, Foxn1$^{fl/fl}$::Foxn1-Cre and nude mice was therefore microscopically investigated for changes in the mucosal integrity and signs of inflammation (Fig. 4.30 A). Half of the Foxn1$^{neo/neo}$ and two-third of the Foxn1$^{fl/fl}$::Foxn1-Cre mice displayed histopathological signs that scored as enteritis, though most of the animals showed only mild tissue injuries (enteritis score of 0.68 ± 0.8 for Foxn1$^{neo/neo}$ mice and 0.66 ± 1 for Foxn1$^{fl/fl}$::Foxn1-Cre mice (Fig. 4.30 B). To characterise the cellular elements of enteritis, small intestinal IEL and LPL were isolated and phenotyped. The frequency of CD4 T-IEL and LPL were significantly increased in Foxn1$^{neo/neo}$ (51.0% ± 27.6% and 60% ± 18%, respectively) and Foxn1$^{fl/fl}$::Foxn1-Cre (57.4% ± 26.1% and 61.8% ± 17.9%) mice compared to wild type (24.2% ± 6.9% and 34.1 ± 8.7%) and nude (22.2% ± 11.9% and 48.4% ± 28.3%) animals (Fig. 4.30 C). The absolute number of CD4 and CD8 IEL was however reduced in these mice (9- respectively 30-fold) with reference to wild type but was comparable to that of nude animals. The cellularity of the small intestinal LPL were comparable for wild type, Foxn1$^{neo/neo}$, Foxn1$^{fl/fl}$::Foxn1-Cre and nude mice (Fig. 4.30 D).

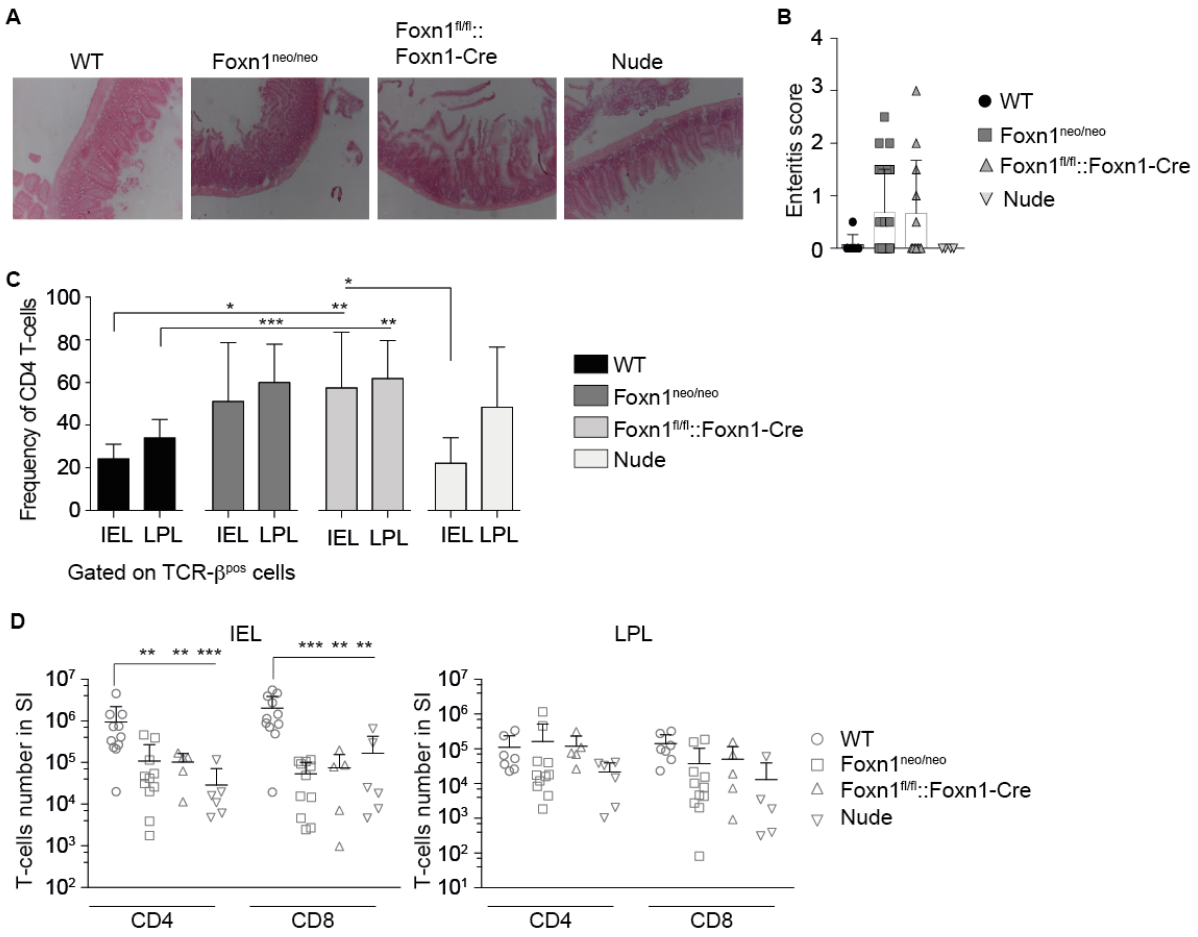

Figure 4.30: Small intestine of Foxn1$^{neo/neo}$ and Foxn1$^{fl/fl}$::Foxn1-Cre mice is not always and less affected. (A) Histology of small intestine from wild type (WT), Foxn1$^{neo/neo}$, Foxn1$^{fl/fl}$::Foxn1-Cre and nude mice. (B) Enteritis score of WT (●), Foxn1$^{neo/neo}$ (■), Foxn1$^{fl/fl}$::Foxn1-Cre (△) and nude mice (▽). (C) Frequencies of CD4 T-cells in small intestine IEL and LPL of healthy WT (■) and nude (▭) mice and sick Foxn1$^{neo/neo}$ (■) and Foxn1$^{fl/fl}$::Foxn1-Cre (▭)mice. (D) Absolute numbers of CD4 and CD8 T-cells isolated from small intestine IEL and LPL of healthy WT (○) and nude (▽) mice and sick Foxn1$^{neo/neo}$ (□) and Foxn1$^{fl/fl}$::Foxn1-Cre (△) mice. n ≥ 6, the mice were between 10 and 30 weeks old. p values were determined using Mann-Whitney test. *p < 0.05, ** < 0.01, *** < 0.005.

The prominence of the auto-inflammatory process rather in the colon than in the small intestine correlates with the difference in the local bacterial antigen load. This may also explain the higher frequency of CD4$^+$ T-cells in the lamina propria of the colon, which serves as the first line of defence in mucosal immunity.

4.10.5. Auto-antibodies in Foxn1$^{neo/neo}$ and Foxn1$^{fl/fl}$::Foxn1-Cre mice

Central T-cell tolerance induction critically depends on the correct composition, architectural organisation and function of the thymic stroma. Consequently, a lack in regular T-cell selection may also impact on the capacity to maintain B-cell tolerance to self-antigens as this requires the cooperation between the two lymphoid compartments[298,299]. To determine whether the altered T-cell antigen receptor repertoire of Foxn1$^{neo/neo}$ and Foxn1$^{fl/fl}$::Foxn1-Cre mice was permissive to break B-cell self-tolerance, sera from these mice were analysed for the presence of T-cell dependant anti-nuclear-antibodies (ANA). The detection of ANA is linked to different autoimmune diseases including systemic lupus erythematosus (SLE), Sjørgen's syndrome and mixed connective tissue diseases though they are not disease specific. The detection of these auto-antibodies is detailed in section 3.9. As shown in Figure 4.31 A and B, about half of all Foxn1$^{neo/neo}$ and Foxn1$^{fl/fl}$::Foxn1-Cre mice at ages above 10 weeks had ANA, whereas ANA were absent in wild type and nude controls. In contrast younger mutants and wild type or nude mice at any age had ANA, revealing again an age-related correlation with changes in T-cell numbers in Foxn1 mutants.

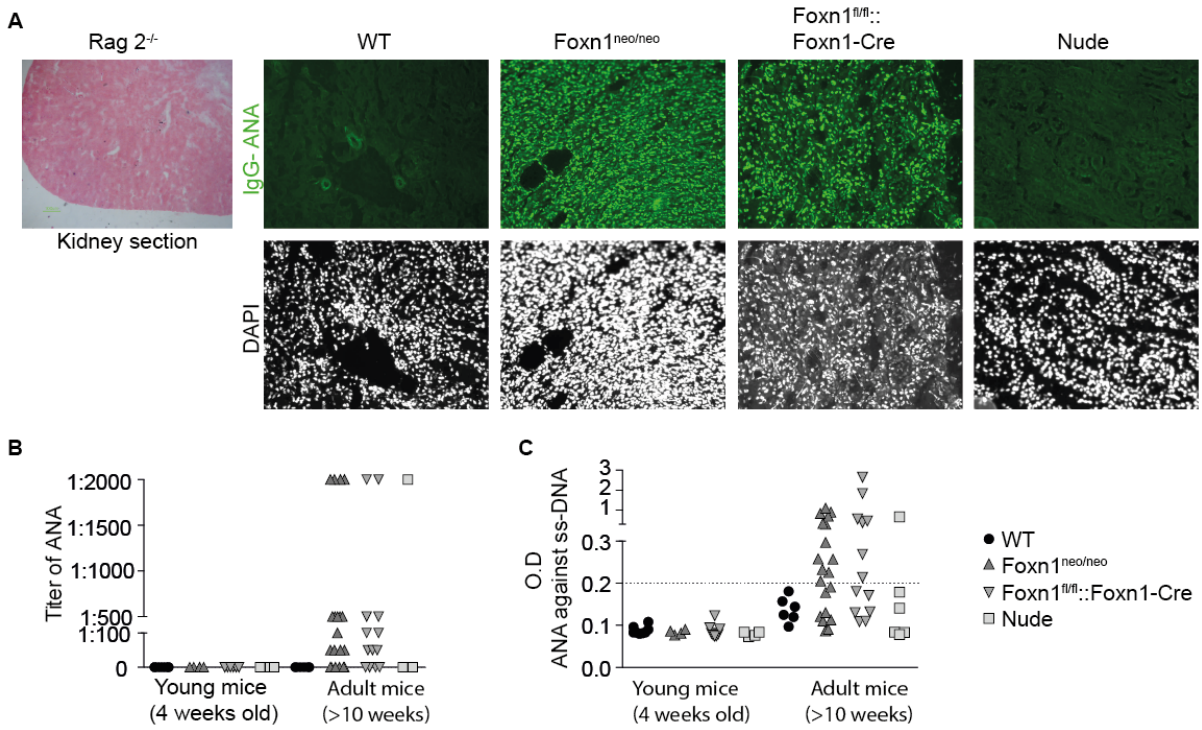

Figure 4.31: Presence of anti-nuclear-antibodies in Foxn1$^{neo/neo}$ and Foxn1$^{fl/fl}$::Foxn1-Cre mice. (A) Representative histological pictures of Rag2$^{-/-}$ kidney sections incubated with blood sera of the different mice analysed. (C) Titers of anti-nuclear-antibodies in the blood sera of young (4 week) and adult (10-30 week) wild type (WT; ●), Foxn1$^{neo/neo}$ (■), Foxn1$^{fl/fl}$::Foxn1-Cre (▲) and nu/nu (▽) mice. (C) Presence of anti-nuclear antibodies against ss-DNA determined by Elisa and indicated as O.D, values below 0.2 were considered as negative.

In aggregate, the loss of a regular thymic function in Foxn1$^{neo/neo}$ and Foxn1$^{fl/fl}$::Foxn1-Cre mice resulted in the generation of a peripheral T-cell compartment unable to maintain tolerance to self, including the suppression of anti-self responses (e.g. ANA, ss-DNA) by B-cells.

5. Discussion

The aim of this study was to elucidate the role of Foxn1 in thymus organogenesis and maintenance, in particular the timing of Foxn1 expression and gene dosage requirements. The study showed that both a short term full Foxn1 expression, and a continuous but reduced Foxn1 expression lead to dramatic changes in thymus development. The regular thymic architecture is changed, cortical and medullary areas are reduced to small islets and mesenchymal cells are replacing the thymic epithelial cells. Nevertheless a limited thymus function is preserved. T-cells emerge from the thymus rudiment and undergo extensive homeostatic or activation induced proliferation in the periphery, displaying a memory-like phenotype. In contrast to T-cells present in athymic nude mice, T-cells of $Foxn1^{neo/neo}$ and $Foxn1^{fl/fl}$::Foxn1-Cre mice proliferate upon mitogenic stimulation although the proliferation was reduced compared to wild type T-cells. Furthermore $Foxp3^{+}$ regulatory T-cells were present in $Foxn1^{neo/neo}$ and $Foxn1^{fl/fl}$::Foxn1-Cre mice, but not in nude mice. However Treg function was reduced compared to wild type mice. $Foxn1^{neo/neo}$ and $Foxn1^{fl/fl}$::Foxn1-Cre mice have a reduced life-span, develop colitis and anti-nuclear-antibodies with time. These results show how critical Foxn1 expression, both temporal and quantitative, is for thymus formation and function, and that modulations of Foxn1 expression can induce the generation of auto-reactive T-cells, that developed in an aberrant thymic microenvironment.

Thymic microenvironment

The differentiation into cortical (CK8) and medullary (CK5) areas was more progressed in $Foxn1^{neo/neo}$ and $Foxn1^{fl/fl}$::Foxn1-Cre mice compared to nude mice, where all TEC remain in a CK5CK8 double positive progenitor stage. However final maturation of TEC was impaired as shown by the absence of mature cTEC and mTEC indicated by the absence of β5t and Aire expression. Foxn1 is believed to regulate β5t expression[268] since β5t is absent in Foxn1 deficient mice, furthermore β5t expression was shown to be independent of thymocyte crosstalk as demonstrated by β5t expression in $Rag2^{-/-}$ mice[268]. In E12.5 $Foxn1^{fl/fl}$::Foxn1-Cre thymus Foxn1 protein is absent, and also β5t expression is absent. This result extends on the importance of Foxn1 as a regulator for β5t expression, as short-term expression at the onset of thymus organogenesis does not trigger β5t expression, demonstrating that stable and continuous high level of Foxn1 expression is required for β5t regulation. In new born

Foxn1$^{neo/neo}$ mice β5t expression is absent although Foxn1 protein was detected. This result is contrary to the literature[268], as it would suggest that β5t is not exclusively regulated by Foxn1 as its presence in Foxn1$^{neo/neo}$ mice did not induce stable β5t expression. Alternatively a Foxn1 gene dosage effect is responsible for the absence of β5t. This is supported by the finding that β5t expression is detected in only 25% of the embryos but not in post natal Foxn1$^{neo/neo}$ thymus. This suggests that the system is tightly regulated by a precise amount of Foxn1 and that β5t is strictly dependant on adequate Foxn1 expression. Furthermore it was shown that TEC development is sensitive to Foxn1 gene dosage[106]. Divergence of TEPC into the mTEC lineage does not require Foxn1 according to Nowell et al. however for development into cTEC lineage low amounts of Foxn1 are required. Already 15% of wild type Foxn1 transcripts allow progression into distinct cortical and medullary areas, Aire expressing mature mTEC, and T-cell development to occur. However the T-cell development displayed an increase in the CD4/CD8 double positive thymocytes and a reduction in single positive thymocytes. This is in contrast to Foxn1$^{neo/neo}$ mice, where Foxn1 transcripts were found to be reduced to 20% of wild type Foxn1 expression. These thymi did not show segregation into cortical and medullary areas, mature TEC were absent and thymocytes development was severely impaired. This discrepancy could be explained by the different targeting construct used. In Foxn1$^{neo/neo}$ mice exon 7&8 encoding in part for the DNA binding domain were targeted, whereas Nowell et al. targeted the intron 1b of the Foxn1 gene using a SV40 T antigen[106]. These results underline the importance of Foxn1 dosage on TEC development and function.

β5t is required for MHC Class I mediated positive selection of CD8 T-cells[97] and consequently, in the absence of β5t CD8 thymocytes are reduced. This reduction persisted also in the periphery. The reduction of CD8 T-cells in the peripheral T-cell pool of Foxn1$^{neo/neo}$ and Foxn1$^{fl/fl}$::Foxn1-Cre mice is probably not linked to the absence of β5t expression as T-cell development in general was severely impaired in Foxn1$^{neo/neo}$ and Foxn1$^{fl/fl}$::Foxn1-Cre thymus. However the quality of the CD8 repertoire including a lack of negative selection towards certain epitopes might be influenced by the absence of β5t.

Mature mTEC (MHC Class II^{high} Aire) were absent in Foxn1$^{fl/fl}$::Foxn1-Cre and Foxn1$^{neo/neo}$ thymus. This result is in line with previous reports[106] suggesting that Foxn1 regulates MHC Class II, thus explaining the absence of mature mTEC. A short term or reduced Foxn1 expression does not induce progression to mature mTEC expressing Aire, suggesting that T-

cells emerging from Foxn1$^{neo/neo}$ and Foxn1$^{fl/fl}$::Foxn1-Cre thymus were not properly negatively selected. RANKL produced by positively selected thymocytes plays a major role in the formation of the medulla and the presence of Aire^{+} TEC[113,269]. Mice deficient for RANKL displayed a reduction of mTEC numbers and size of the thymic medulla[269]. However thymocyte development in Foxn1$^{neo/neo}$ and Foxn1$^{fl/fl}$::Foxn1-Cre mice was drastically reduced explaining the absence of Aire^{+} TEC and the reduced medulla size. The thymus rudiment of Foxn1$^{neo/neo}$ and Foxn1$^{fl/fl}$::Foxn1-Cre had distinct cortical and medullary TEC, this is in contrast to nude thymus were mainly CK5 and CK8 double positive TEC precursors were detected. However the cortical and medullary TEC form rather small islets than large areas, explaining the absence of cortical and medullary areas in Haematoxylin and Erythrosine staining. CK5 and CK8 double positive TECs were also quite common in Foxn1$^{neo/neo}$ and Foxn1$^{fl/fl}$::Foxn1-Cre mice. Concomitant expression of CK5 and CK8 was observed in CD3ε transgenic mice, where thymocyte development is blocked at an early stage, due to an abrogated thymic crosstalk[94]. Since the thymus cellularity was not increasing with age in Foxn1$^{neo/neo}$ and Foxn1$^{fl/fl}$::Foxn1-Cre mice and the chemokines responsible for precursor attraction were severely reduced, the concomitant expression of CK5 and CK8 could represent absent or limited T-cell development. Nevertheless some TEC might interact with few thymocytes and develop thereby into distinct cTEC or mTEC. The increase in fibroblasts and restriction of cTEC and mTEC to small islets is also observed in thymus involution [300]. These results lead to the hypothesis that the thymus rudiment of Foxn1$^{neo/neo}$ and Foxn1$^{fl/fl}$::Foxn1-Cre mice is able to develop but thymic involution occurs prematurely, as the thymus rudiment resembles an aged thymus. Aging is also known to cause autoimmune features as observed in Foxn1$^{neo/neo}$ and Foxn1$^{fl/fl}$::Foxn1-Cre mice[166].

Foxn1 plays an essential role in thymus vascularisation[150] as it enables TEC to produce VEGF, which plays an essential role in the formation of blood vessel architecture in the thymus [42]. In nude mice, endothelial cells are detected outside of the thymus rudiment. Timed Foxn1 expression only at the onset of thymus organogenesis results in endothelial cells that were also detected inside the thymus rudiment, indicating that vascularisation takes place. Reduced Foxn1 expression does also allow thymus vascularisation to occur. The supply of hematopoietic precursors is low despite the presence of the vascularisation, indicating that the quality of the vessel might be changed e.g. the blood vessel are leaky resulting in a reduced entry of hematopoietic precursors. This finding is in line with other reports on thymus

vascularisation claiming a dosage effect of Foxn1 on thymus vascularisation and the presence of leaky vessels[301]. To analyse the quality of the vascular network angiography could be performed. Leaky vessels could thereby be identified and the density of the vessel network could be assessed[42]. The chemokines CCL25 and CCL21 are reduced in TEC of Foxn1$^{neo/neo}$ and Foxn1$^{fl/fl}$::Foxn1-Cre mice. CCL25 and CCL21 are required for the attraction of thymic lymphoid precursors, CCL25 was further reported to be regulated by Foxn1 expression[144]. Taken together the small thymus size reflects reduced precursor attraction early in thymus ontogenesis and a limited supply with blood-borne hematopoietic precursors as a consequence the crosstalk between thymocytes and TEC is abrogated resulting in a thymus devoid of mature TEC and TEC with concomitant expression of CK5 and CK8. Su et al.[152], however, showed that deletion of exon 3 of the Foxn1 gene result in an abrogated cross-talk despite the presence of thymocytes. This indicates that the presence of precursors would not rescue the phenotype, and that Foxn1 is required after the first initiation of the thymus.

Foxn1 in hair follicle development

At the time of Foxn1 withdrawal in Foxn1$^{fl/fl}$::Foxn1-Cre mice hair development is not initiated. Thus, Foxn1 is deleted in the hair follicle leading to alopecia similar to nude mice. Foxn1$^{neo/neo}$ mice, however had normal whiskers and coat at birth. After the first four weeks the fur got dull and scrubby and altogether less dense. This observation is in line with other transgenic mouse lines with reduced Foxn1 expression[106], where sporadic hair loss is observed after 6 weeks. This indicates that different amounts of Foxn1 are required for hair follicle development than for TEC development and maintenance. Moreover Foxn1$^{neo/neo}$ females were fertile and able to lactate their offspring whereas nude mice have underdeveloped mammary glands and are unable to effective lactate their offspring. Nude females were reported to have a reduction in the serum levels of estradiol, progesterone and thyroxine resulting in a reduced fertility[265]. In accordance with this report Foxn1$^{fl/fl}$::Foxn1-Cre females showed reduced fertility, as they were kept for 1 year in a mating and no offspring were born. However female mice with reduced Foxn1 expression were fertile. These observations underline the different requirements for Foxn1 in skin and thymus development. The N-terminus of *Foxn1* gene was reported to be only important for thymus formation but not for hair follicle development as deletion of exon 3 affects only the thymus but not the coat of the animals[152].

Impaired T-cell development

The altered microenvironment had a severe impact on T-cell development. Very low frequencies of CD4/CD8 double positive thymocytes were only detected in embryonic day 18.5, but not beyond. This result showed that the development was delayed and limited to a narrow time window or below our detected limit. The delayed development is in accordance with other reports[152]. Mice lacking the N-terminus of Foxn1 protein display also a delayed and impaired T-cell development[152], characterised by a block in DNI to DNII transition similar to Foxn1$^{neo/neo}$ and Foxn1$^{fl/fl}$::Foxn1-Cre mice. Moreover the DNI precursors develop directly to DNIV without passing through DNII and DNIII stages. In contrast to Foxn1$^{neo/neo}$ and Foxn1$^{fl/fl}$::Foxn1-Cre mice these mice had a substantial population of CD4/CD8 double positive thymocytes. This does not exclude, however, that the development of CD4/CD8 double positive thymocytes was completely abolished in Foxn1$^{neo/neo}$ and Foxn1$^{fl/fl}$::Foxn1-Cre mice as it might be reduced to an extent below our detection limit. Alternatively T-cell development might follow other rules and develop without passing through a CD4/CD8 double positive stage[302]. These cells might acquire CD4 or CD8 expression later in the periphery upon contact with MHC Class II or MHC Class I, respectively. Furthermore for the generation of CD8αα intraepithelial lymphocytes a pathway that consists of a first thymic phase followed by an extrathymic maturation was described[235]. CD4$^-$CD8$^-$CD3$^-$CD44$^+$CD25^{int} precursors were shown to be able to leave the thymus and mature in the periphery.

Foxn1 is also expressed in the bone marrow of wild type mice. Both reduction and overexpression of Foxn1 have an influence on the bone marrow as demonstrated in a recent report. It was suggested that the role of Foxn1 in the bone marrow niche is to skew the multipotent progenitors towards T-cell lineage progenitors[282]. During aging Foxn1 expression in the bone marrow is reduced and as a consequence the multipotent progenitors are reduced. Therefore it could be that not only reduced expression of chemokines involved in attraction of hematopoietic precursors and impaired vascularisation contribute to the small thymus rudiment but also a reduction in precursors due to Foxn1 ablation in the bone marrow. However in Foxn1$^{neo/neo}$ and Foxn1$^{fl/fl}$::Foxn1-Cre mice the LSK population was increased compared to wild type mice, arguing against an influence on the capacity of the bone marrow niches for maintaining LSK.

Peripheral T-cells

The peripheral T-cell pool of Foxn1$^{neo/neo}$ and Foxn1$^{fl/fl}$::Foxn1-Cre mice was quantitatively and qualitatively different from nude mice. T-cells in nude mice are generated in the periphery, mainly in the mesenteric lymph nodes[197]. Peripheral T-cell generation has some special features. T-cells generated in the periphery are mainly CD8 T-cells[194], whereas in Foxn1$^{neo/neo}$ and Foxn1$^{fl/fl}$::Foxn1-Cre mice predominantly CD4 T-cells were detected, which favours a thymic origin of these T-cells. This thymic origin is also supported by the finding that extrathmyic T-cells do not respond to mitogenic stimuli and fail to provide B-cell help[204,291]. Both features however were detected in CD4 T-cells isolated from Foxn1$^{neo/neo}$ and Foxn1$^{fl/fl}$::Foxn1-Cre mice. CD4 T-cells isolated from Foxn1$^{neo/neo}$ and Foxn1$^{fl/fl}$::Foxn1-Cre mice were able to respond to mitogenic stimuli as indicated by proliferation, increase of size and Il-2 production. Furthermore they were able to induce colitis upon adaptive transfer into Rag2$^{-/-}$ mice. In addition CD4 T-cells of Foxn1$^{neo/neo}$ and Foxn1$^{fl/fl}$::Foxn1-Cre mice provided B-cell help, as shown by the presence of anti-nuclear-antibodies. Moreover regulatory T-cells were detected in Foxn1$^{neo/neo}$ and Foxn1$^{fl/fl}$::Foxn1-Cre mice but absent in nude mice. Taken together all these observations suggest that the CD4 T-cells are quantitatively and qualitatively different from extrathymically derived CD4 T-cells of nude mice. CD4 T-cells in Foxn1$^{neo/neo}$ and Foxn1$^{fl/fl}$::Foxn1-Cre mice accumulate with age and are significantly increased compared to nude mice after 10 weeks postnatal. As only few T-cells emerge from the thymus rudiment, the CD4 T-cells probably underwent homeostatic expansion in the periphery, acquiring an activated/memory-like phenotype that is also common in extrathymic derived T-cells[187,303]. The presence of colitis suggest that antigenic activation contributes to this phenotype. Similar observations were made with T-cells isolated from Foxn1$^{\Delta/\Delta}$ mutant mice lacking the N-terminus of the Foxn1 gene. The T-cells displayed an atypical memory phenotype combined with low homeostatic potential and impaired regulatory T-cell function[154]. These T-cells were of thymic origin, however they developed from a kit negative progenitor and developed without passing through DNII and DNIII stages[152,153]. Nevertheless these mice were not reported do develop colitis.

However it can not be excluded that a cryptic extrathymic T-cell development pathway is induced by the short term or reduced Foxn1 expression. To test the hypothesis that the autoimmune feature causing T-cells emerged the thymus rudiment and were not generated in the periphery, thymus rudiments isolated from Foxn1$^{neo/neo}$ and Foxn1$^{fl/fl}$::Foxn1-Cre mice at

embryonic day 12.5 are placed under the kidney capsule of nude mice. First preliminary data showed that transplantation of E12.5 Foxn1$^{neo/neo}$ thymi under the kidney capsule of nude mice result in an altered CD4:CD8 ratio. Furthermore by three months after grafting the transplanted mouse suffered from colitis. The colon showed epithelial cell hyperplasia and leucocytes infiltrations. As observed in Foxn1$^{neo/neo}$ mice the infiltrating cells were CD4 T-cells. These preliminary results showed that the thymus rudiment transplanted at E12.5 is able to support T-cell development and that the emerging T-cells can cause disease. To exclude the possibility that Foxn1 ablation has an unexpected influence on the lymphoid precursors in the bone marrow, bone marrow chimeras should be analysed. It could be that Foxn1 ablation causes changes in the bone marrow and that therefore the T-cells causing colitis do not necessarily result from a defective selection in the thymus but are rather a result of altered hematopoietic precursors that might develop in the periphery to T-cells causing harm, despite all the evidence arguing for thymic T-cell development.

In addition regulatory T-cells were present in the periphery of Foxn1$^{neo/neo}$ and Foxn1$^{fl/fl}$::Foxn1-Cre mice but absent in nude mice. Although Helios was present on Tregs, it can not be concluded that these cells were thymus derived, as recent studies showed, that Helios can also be detected on induced Tregs and represent the activation status[289]. Neuropilin-1 was used as a second marker to distinguish thymic and extrathymic derived Tregs. Foxn1$^{neo/neo}$ and Foxn1$^{fl/fl}$::Foxn1-Cre Tregs expressed higher amounts of Nrp1 compared to non Tregs, but the expression is reduced compared to wild type Tregs. Thus Tregs display some, but not all, characteristics of thymic origin. Furthermore the absence of Aire expression and aberrant selection might also impair Treg development in the thymus[88,304]. Whether the periphery of nude mice does not support conversion of CD4 T-cells to Tregs or whether the CD4 T-cells are not able to convert into Tregs is currently not known. Conversion into Tregs requires the presence of TGF-β[305] and IL-2. Nude CD4 T-cells fail to produce IL-2 at substantial amounts[291], which might prevent the conversion of CD4 T-cells into Tregs. CD4 T-cells isolated from Foxn1$^{neo/neo}$ and Foxn1$^{fl/fl}$::Foxn1-Cre mice produce IL-2 and regulatory T-cells are detected in the periphery. However the potential of these regulatory T-cells is severely impaired *in vitro*. This is in contrast to other lymphopenic mouse models where Tregs were more potent than wild type Tregs[306], one explanation could be that these Tregs emerged from conversion of conventional CD4 T-cells. These

conventional T-cells might be exhausted from the homeostatic expansion, resulting in a reduced function. Thus, reduced Foxn1 expression indirectly influences Treg quality.

Reduced life expectancy

Foxn1$^{neo/neo}$ and Foxn1$^{fl/fl}$::Foxn1-Cre mice have a reduced life-span compared to wild type and congenital nude mice. These mice have a sudden weight loss accompanied sometimes by diarrhoea. Closer examination of the colon revealed the presence of colitis caused by Th1 polarised CD4 T-cells. In congenital nude mice, colitis was not observed in young or old mice. Thus indicate that the CD4 T-cells causing colitis in Foxn1$^{neo/neo}$ and Foxn1$^{fl/fl}$::Foxn1-Cre mice emerged from the thymus and were either not properly selected or underwent antigen driven homeostatic expansion, since T-cells detected in nude mice did not induce disease, which might be linked to the limited response to mitogenic stimuli observed. Aberrant thymic selection was shown to cause colitis[307], but colitis can also be induced by homeostatic expansion[308,309].

Adoptive transfer of naïve CD4 T-cells into nude mice does not result in colitis despite lymphopenia. The presence of host intraepithelial CD8 T-cells is protective. However transferring activated CD4 T-cells overcomes this protective effect[222]. In wild type mice the IEL are shown to be thymus derived and increased in numbers compared to nude mice[233,234]. The increase in IEL detected in Foxn1$^{neo/neo}$ and Foxn1$^{fl/fl}$::Foxn1-Cre mice compared to nude mice is indicating that the IEL are of thymic origin and could therefore be impaired in their function due to impaired selection. To test the functionality of CD8 IEL of Foxn1$^{neo/neo}$ and Foxn1$^{fl/fl}$::Foxn1-Cre mice, CD8 IEL could be transferred to a RAG2$^{-/-}$ recipient mouse one week prior to reconstitution with wild type CD4 T-cells. The presence of functional CD8 IEL should result in a mitigated colitis. Furthermore Tregs play also a crucial role in maintaining the mucosal immune homeostasis[258], therefore the colitis observed in Foxn1$^{neo/neo}$ and Foxn1$^{fl/fl}$::Foxn1-Cre mice might also be related to the dysfunction of Tregs. To test the hypothesis that reduced Treg function leads to colitis in Foxn1$^{neo/neo}$ and Foxn1$^{fl/fl}$::Foxn1-Cre mice these mice were reconstituted with wild type Tregs. Preliminary data showed that the onset of disease is delayed by reconstitution with wild type Tregs however the mice can not be rescued. Alternatively it might also be that the effector CD4 T-cells isolated from Foxn1$^{neo/neo}$ and Foxn1$^{fl/fl}$::Foxn1-Cre mice are more resistant to suppression as observed in Gαi2$^{-/-}$ mice[310]. However in contrast to Gαi2$^{-/-}$ CD4 T-cells, the CD4 T-cells of Foxn1$^{neo/neo}$

and Foxn1$^{fl/fl}$::Foxn1-Cre mice have less effector function *in vitro* .To exclude the possibility that these CD4 T-cells are more resistant to suppression, experiments with wild type Tregs and effector T-cells isolated from Foxn1$^{neo/neo}$ and Foxn1$^{fl/fl}$::Foxn1-Cre mice will be made.
There are also reports showing that auto-immunity and aging are closely linked and that not properly selected extrathymic T-cells can cause autoimmunity with age[311]. Moreover there is a link between auto-reactive extrathymic T-cells and elimination of abnormal self cells generated during aging. The onset of autoimmune disease is often linked with thymic involution and activation of the extrathymic pathway for T-cell generation. During thymic involution, TECs are reduced and cortical and medullary areas vanish and are replaced by mesenchymal cells[176]. Despite these changes in the thymic architecture the thymus preserves a low thymic output. The replacement of TEC with mesenchymal cells was also observed in Foxn1$^{neo/neo}$ and Foxn1$^{fl/fl}$::Foxn1-Cre thymus, reminiscent of aged thymus. This finding is in line with other reports showing that the deletion of Foxn1 in the postnatal thymus result in a premature thymic involution[156,157]. Furthermore it was suggested that thymic involution is initiated by the bone marrow with a decline of the multipotent hematopoietic precursors[312]. Recent studies identified Foxn1 expression in the bone marrow and linked it further to thymic involution[282]. Therefore the absence or reduction of Foxn1 seems to induce thymic involution from an early time point in thymus development. In old mice anti-nuclear-antibodies are detected without causing harm to the patients[311]. 50% of all Foxn1$^{neo/neo}$ and Foxn1$^{fl/fl}$::Foxn1-Cre mice displayed anti-nuclear-antibodies, whereas they were not detected in aged matched controls, indicating that Foxn1$^{neo/neo}$ and Foxn1$^{fl/fl}$::Foxn1-Cre mice resemble old mice concerning the thymus architecture and the presence of anti-nuclear antibodies.

Collectively these data showed that Foxn1 expression is not only critical at the onset of thymus organogenesis but also for thymus maintenance. Furthermore these data showed that Foxn1 target genes are tightly regulated by Foxn1 expression, as demonstrated by the absence of β5t despite reduced Foxn1 expression. Reduced Foxn1 expression does not suffice for thymus development. However reduced Foxn1 expression allows initial divergence of cTEC and mTEC linages, although they do not fully mature. This partial rescue was also shown be Nowell et al., however this study underlines the importance of Foxn1 not only in thymus organogenesis but also in thymus maintenance. These experiments demonstrate to our knowledge for the first time that mice with insufficient Foxn1 expression develop a T-cell

repertoire that is able to cause autoimmune features as shown by the development of colitis and anti-nuclear antibodies. This indicates that Foxn1 expression below a certain threshold, still allows few T-cells to emerge from the rudiment, although these T-cells were not properly selected. Whereas in the complete absence of Foxn1 no T-cells emerge the rudiment and above the threshold regular T-cell development occurs and the emerging T-cells were properly selected and do not cause autoimmunity. In all Foxn1 targeted mouse models described so far no autoimmunity was reported. Furthermore these data suggest that the thymus of $Foxn1^{neo/neo}$ and $Foxn1^{fl/fl}$::Foxn1-Cre mice supports some aspects of T-cell development despite the withdrawal or reduction of Foxn1 expression, however this function might be limited to a short time window during early thymus organogenesis. A first wave of T-cells emerges the thymus, however due to a lack of an organised thymus architecture and mature TEC these T-cells are improperly selected, resulting in a T-cell repertoire that reveals its auto-reactivity over time.

However many aspects of Foxn1 function and requirements for thymus organogenesis remain still elusive, in particular it's role in cTEC/mTEC development after thymus organogenesis and its role in maintaining the bone marrow niche for T cell progenitors.

6. Conclusion

This study showed, that an adequate and stable Foxn1 expression is required for thymus formation and function, as a reduced or short-term expression of Foxn1 at the induction of thymus development is not sufficient for thymus formation. Cortical and medullary TECs are detected, however they do not fully mature, and TEC that concomitantly express CK5 and CK8 are present, indicating severely reduced T-cell development. Nevertheless a reduced thymic output is still preserved. The peripheral T-cell pool of Foxn1 targeted mice contains CD4 T-cells that are functional and cause autoimmune pathologies over time. Thus adequate Foxn1 expression is required not only during organogenesis but also in the adult thymus. Therefore inadequate Foxn1 expression result in a T-cell repertoire that reveals its autoreactivity over time.

7. References

1. Miller, J. F. a P. The discovery of thymus function and of thymus-derived lymphocytes. *Immunol. Rev.* **185,** 7–14 (2002).

2. Miller, J. F. Immunological function of the thymus. *Lancet* **2,** 748–9 (1961).

3. Miller, J. F. & Mitchell, G. F. Cell to cell interaction in the immune response. I. Hemolysin-forming cells in neonatally thymectomized mice reconstituted with thymus or thoracic duct lymphocytes. *J. Exp. Med.* **128,** 801–20 (1968).

4. Mitchell, G. F. & Miller, J. F. Cell to cell interaction in the immune response. II. The source of hemolysin-forming cells in irradiated mice given bone marrow and thymus or thoracic duct lymphocytes. *J. Exp. Med.* **128,** 821–37 (1968).

5. Van Ewijk, W. *et al.* Thymic microenvironments, 3-D versus 2-D? *Semin. Immunol.* **11,** 57–64 (1999).

6. Anderson, G. & Jenkinson, E. J. Lymphostromal interactions in thymic development and function. *Nat. Rev. Immunol.* **1,** 31–40 (2001).

7. Gray, D. H. D. *et al.* Developmental kinetics, turnover, and stimulatory capacity of thymic epithelial cells. *Blood* **108,** 3777–85 (2006).

8. Manley, N. R. Thymus organogenesis and molecular mechanisms of thymic epithelial cell differentiation. *Semin. Immunol.* **12,** 421–428 (2000).

9. Cordier, a C. & Haumont, S. M. Development of thymus, parathyroids, and ultimobranchial bodies in NMRI and nude mice. *Am. J. Anat.* **157,** 227–63 (1980).

10. Cordier, a C. & Heremans, J. F. Nude mouse embryo: ectodermal nature of the primordial thymic defect. *Scand. J. Immunol.* **4,** 193–6 (1975).

11. Le Douarin, N. M. & Jotereau, F. V. Tracing of cells of the avian thymus through embryonic life in interspecific chimeras. *J. Exp. Med.* **142,** 17–40 (1975).

12. Gordon, J. & Manley, N. R. Mechanisms of thymus organogenesis and morphogenesis. *Development* **138,** 3865–78 (2011).

13. Gordon, J. *et al.* Functional evidence for a single endodermal origin for the thymic epithelium. *Nat. Immunol.* **5,** 546–53 (2004).

14. Sun, X. *et al.* Directed differentiation of human embryonic stem cells into thymic epithelial progenitor-like cells reconstitutes the thymic microenvironment in vivo. *Cell Stem Cell* **13,** 230–6 (2013).

15. Parent, A. V *et al.* Generation of functional thymic epithelium from human embryonic stem cells that supports host T cell development. *Cell Stem Cell* **13,** 219–29 (2013).

16. Hetzer-Egger, C. *et al.* Thymopoiesis requires Pax9 function in thymic epithelial cells. *Eur. J. Immunol.* **32,** 1175–1181 (2002).

17. Frank, D. U. *et al.* An Fgf8 mouse mutant phenocopies human 22q11 deletion syndrome. *Development* **129,** 4591–4603 (2002).

18. Wallin, J. *et al.* Pax1 is expressed during development of the thymus epithelium and is required for normal T-cell maturation. *Development* **122,** 23–30 (1996).

19. Xu, P.-X. *et al.* Eya1 is required for the morphogenesis of mammalian thymus, parathyroid and thyroid. *Development* **129,** 3033–44 (2002).

20. Zou, D. *et al.* Patterning of the third pharyngeal pouch into thymus/parathyroid by Six and Eya1. *Dev. Biol.* **293,** 499–512 (2006).

21. Manley, N. R. & Capecchi, M. R. The role of Hoxa-3 in mouse thymus and thyroid development. *Development* **121,** 1989–2003 (1995).

22. Gordon, J., Bennett, a R., Blackburn, C. C. & Manley, N. R. Gcm2 and Foxn1 mark early parathyroid- and thymus-specific domains in the developing third pharyngeal pouch. *Mech. Dev.* **103,** 141–3 (2001).

23. Liu, Z., Yu, S. & Manley, N. R. Gcm2 is required for the differentiation and survival of parathyroid precursor cells in the parathyroid/thymus primordia. *Dev. Biol.* **305,** 333–346 (2007).

24. Nehls, M., Pfeifer, D., Schorpp, M., Hedrich, H. & Boehm, T. New member of the winged-helix protein family disrupted in mouse and rat nude mutations. *Nature* **372,** 103–107 (1994).

25. Nehls, M. *et al.* Two genetically separable steps in the differentiation of thymic epithelium. *Science* **272,** 886–9 (1996).

26. Itoi, M., Kawamoto, H., Katsura, Y. & Amagai, T. Two distinct steps of immigration of hematopoietic progenitors into the early thymus anlage. *Int. Immunol.* **13,** 1203–11 (2001).

27. Boehm, T., Bleul, C. C. & Schorpp, M. Genetic dissection of thymus development in mouse and zebrafish. *Immunol. Rev.* **195,** 15–27 (2003).

28. Vroegindeweij, E. *et al.* Thymic cysts originate from Foxn1 positive thymic medullary epithelium. *Mol. Immunol.* **47,** 1106–13 (2010).

29. Blackburn, C. C. & Manley, N. R. Developing a new paradigm for thymus organogenesis. *Nat. Rev. Immunol.* **4,** 278–89 (2004).

30. Chen, L. *et al.* Mouse and zebrafish Hoxa3 orthologues have nonequivalent in vivo protein function. *Proc. Natl. Acad. Sci. U. S. A.* **107,** 10555–60 (2010).

31. Griffith, A. V *et al.* Increased thymus- and decreased parathyroid-fated organ domains in Splotch mutant embryos. *Dev. Biol.* **327,** 216–27 (2009).

32. Gordon, J., Patel, S. R., Mishina, Y. & Manley, N. R. Evidence for an early role for BMP4 signaling in thymus and parathyroid morphogenesis. *Dev. Biol.* **339,** 141–54 (2010).

33. Takahashi, Y. & Sato, Y. Somitogenesis as a model to study the formation of morphological boundaries and cell epithelialization. *Dev. Growth Differ.* **50 Suppl 1,** S149–55 (2008).

34. Foster, K. E. *et al.* EphB-ephrin-B2 interactions are required for thymus migration during organogenesis. *Proc. Natl. Acad. Sci. U. S. A.* **107,** 13414–9 (2010).

35. Alt, B. *et al.* Arteries define the position of the thyroid gland during its developmental relocalisation. *Development* **133,** 3797–3804 (2006).

36. Jenkinson, W. E., Jenkinson, E. J. & Anderson, G. Differential requirement for mesenchyme in the proliferation and maturation of thymic epithelial progenitors. *J. Exp. Med.* **198,** 325–332 (2003).

37. Bockman, D. E. & Kirby, M. L. Dependence of thymus development on derivatives of the neural crest. *Science* **223,** 498–500 (1984).

38. Suniara, R. K., Jenkinson, E. J. & Owen, J. J. An essential role for thymic mesenchyme in early T cell development. *J. Exp. Med.* **191,** 1051–1056 (2000).

39. Revest, J. M., Suniara, R. K., Kerr, K., Owen, J. J. & Dickson, C. Development of the thymus requires signaling through the fibroblast growth factor receptor R2-IIIb. *J. Immunol.* **167,** 1954–61 (2001).

40. Dooley, J., Erickson, M., Larochelle, W. J., Gillard, G. O. & Farr, A. G. FGFR2IIIb signaling regulates thymic epithelial differentiation. *Dev. Dyn.* **236,** 3459–3471 (2007).

41. Jenkinson, W. E., Rossi, S. W., Parnell, S. M., Jenkinson, E. J. & Anderson, G. PDGFRalpha-expressing mesenchyme regulates thymus growth and the availability of intrathymic niches. *Blood* **109,** 954–60 (2007).

42. Müller, S. M. *et al.* Gene targeting of VEGF-A in thymus epithelium disrupts thymus blood vessel architecture. *Proc. Natl. Acad. Sci. U. S. A.* **102,** 10587–10592 (2005).

43. Müller, S. M. *et al.* Neural crest origin of perivascular mesenchyme in the adult thymus. *J. Immunol.* **180,** 5344–5351 (2008).

44. Yamazaki, H. *et al.* Presence and distribution of neural crest-derived cells in the murine developing thymus and their potential for differentiation. *Int. Immunol.* **17,** 549–558 (2005).

45. Jiang, X., Rowitch, D. H., Soriano, P., McMahon, A. P. & Sucov, H. M. Fate of the mammalian cardiac neural crest. *Development* **127,** 1607–1616 (2000).

46. Foster, K. *et al.* Contribution of neural crest-derived cells in the embryonic and adult thymus. *J. Immunol.* **180,** 3183–9 (2008).

47. Sitnik, K. M. *et al.* Mesenchymal cells regulate retinoic acid receptor-dependent cortical thymic epithelial cell homeostasis. *J. Immunol.* **188,** 4801–9 (2012).

48. Owen, J. J. & Ritter, M. A. Tissue interaction in the development of thymus lymphocytes. *J. Exp. Med.* **129,** 431–442 (1969).

49. Liu, C. *et al.* The role of CCL21 in recruitment of T-precursor cells to fetal thymi. *Blood* **105,** 31–9 (2005).

50. Le Douarin, N. A biological cell labeling technique and its use in expermental embryology. *Dev. Biol.* **30,** 217–22 (1973).

51. Jotereau, F., Heuze, F., Salomon-Vie, V. & Gascan, H. Cell kinetics in the fetal mouse thymus: precursor cell input, proliferation, and emigration. *J. Immunol.* **138,** 1026–1030 (1987).

52. Douagi, I., André, I., Ferraz, J. C. & Cumano, A. Characterization of T cell precursor activity in the murine fetal thymus: evidence for an input of T cell precursors between days 12 and 14 of gestation. *Eur. J. Immunol.* **30,** 2201–10 (2000).

53. Klug, D. B., Carter, C., Gimenez-Conti, I. B. & Richie, E. R. Cutting edge: thymocyte-independent and thymocyte-dependent phases of epithelial patterning in the fetal thymus. *J. Immunol.* **169,** 2842–5 (2002).

54. Ritter, M. A. & Boyd, R. L. Development in the thymus: it takes two to tango. *Immunol. Today* **14,** 462–469 (1993).

55. Nitta, T., Ohigashi, I., Nakagawa, Y. & Takahama, Y. Cytokine crosstalk for thymic medulla formation. *Curr. Opin. Immunol.* **23,** 190–197 (2011).

56. Holländer, G. A. *et al.* Developmental control point in induction of thymic cortex regulated by a subpopulation of prothymocytes. *Nature* **373,** 350–3 (1995).

57. Van Ewijk, W., Holländer, G., Terhorst, C. & Wang, B. Stepwise development of thymic microenvironments in vivo is regulated by thymocyte subsets. *Development* **127,** 1583–91 (2000).

58. Palmer, D. B., Viney, J. L., Ritter, M. A., Hayday, A. C. & Owen, M. J. Expression of The αβ T-Cell Receptor Is Necessary for The Generation of The Thymic Medulla. *Dev. Immunol.* **3,** 175–179 (1993).

59. Surh, C. D., Ernst, B. & Sprent, J. Growth of epithelial cells in the thymic medulla is under the control of mature T cells. *J. Exp. Med.* **176,** 611–6 (1992).

60. Naspetti, M. *et al.* Thymocytes and RelB-dependent medullary epithelial cells provide growth-promoting and organization signals, respectively, to thymic medullary stromal cells. *Eur. J. Immunol.* **27,** 1392–1397 (1997).

61. Kadish, J. L. & Basch, R. S. Hematopoietic thymocyte precursors. I. Assay and kinetics of the appearance of progeny. *J. Exp. Med.* **143,** 1082–1099 (1976).

62. Lepault, F. & Weissman, I. L. An in vivo assay for thymus-homing bone marrow cells. *Nature* **293,** 151–4 (1981).

63. Peaudecerf, L. *et al.* Thymocytes may persist and differentiate without any input from bone marrow progenitors. *J. Exp. Med.* **209,** 1401–8 (2012).

64. Martins, V. C. *et al.* Thymus-autonomous T cell development in the absence of progenitor import. *J. Exp. Med.* **209,** 1409–17 (2012).

65. Lind, E. F., Prockop, S. E., Porritt, H. E. & Petrie, H. T. Mapping precursor movement through the postnatal thymus reveals specific microenvironments supporting defined stages of early lymphoid development. *J. Exp. Med.* **194,** 127–134 (2001).

66. Uehara, S., Grinberg, A., Farber, J. M. & Love, P. E. A role for CCR9 in T lymphocyte development and migration. *J. Immunol.* **168,** 2811–9 (2002).

67. Foss, D. L., Donskoy, E. & Goldschneider, I. The importation of hematogenous precursors by the thymus is a gated phenomenon in normal adult mice. *J. Exp. Med.* **193,** 365–74 (2001).

68. Bell, J. J. & Bhandoola, A. The earliest thymic progenitors for T cells possess myeloid lineage potential. *Nature* **452,** 764–767 (2008).

69. Feyerabend, T. B. *et al.* Deletion of Notch1 converts pro-T cells to dendritic cells and promotes thymic B cells by cell-extrinsic and cell-intrinsic mechanisms. *Immunity* **30,** 67–79 (2009).

70. Wada, H. *et al.* Adult T-cell progenitors retain myeloid potential. *Nature* **452,** 768–72 (2008).

71. Porritt, H. E., Gordon, K. & Petrie, H. T. Kinetics of steady-state differentiation and mapping of intrathymic-signaling environments by stem cell transplantation in nonirradiated mice. *J. Exp. Med.* **198,** 957–62 (2003).

72. Koch, U. *et al.* Delta-like 4 is the essential, nonredundant ligand for Notch1 during thymic T cell lineage commitment. *J. Exp. Med.* **205,** 2515–2523 (2008).

73. Petrie, H. T. & Zúñiga-Pflücker, J. C. Zoned out: functional mapping of stromal signaling microenvironments in the thymus. *Annu. Rev. Immunol.* **25,** 649–679 (2007).

74. Von Boehmer, H. Unique features of the pre-T-cell receptor alpha-chain: not just a surrogate. *Nat. Rev. Immunol.* **5,** 571–7 (2005).

75. Lucas, B. & Germain, R. N. Unexpectedly complex regulation of CD4/CD8 coreceptor expression supports a revised model for CD4+CD8+ thymocyte differentiation. *Immunity* **5,** 461–77 (1996).

76. Sant'Angelo, D. B. *et al.* A molecular map of T cell development. *Immunity* **9,** 179–86 (1998).

77. Von Boehmer, H. Positive selection of lymphocytes. *Cell* **76,** 219–28 (1994).

78. Palmer, E. Negative selection--clearing out the bad apples from the T-cell repertoire. *Nat. Rev. Immunol.* **3,** 383–391 (2003).

79. Barthlott, T., Kohler, H. & Eichmann, K. Asynchronous coreceptor downregulation after positive thymic selection: prolonged maintenance of the double positive state in CD8 lineage differentiation due to sustained biosynthesis of the CD4 coreceptor. *J. Exp. Med.* **185,** 357–62 (1997).

80. Klein, L., Hinterberger, M., Wirnsberger, G. & Kyewski, B. Antigen presentation in the thymus for positive selection and central tolerance induction. *Nat. Rev. Immunol.* **9,** 833–844 (2009).

81. Kyewski, B. & Klein, L. A central role for central tolerance. *Annu Rev Immunol* **24,** 571–606 (2006).

82. Derbinski, J., Schulte, A., Kyewski, B. & Klein, L. Promiscuous gene expression in medullary thymic epithelial cells mirrors the peripheral self. *Nat. Immunol.* **2,** 1032–1039 (2001).

83. Aschenbrenner, K. *et al.* Selection of Foxp3+ regulatory T cells specific for self antigen expressed and presented by Aire+ medullary thymic epithelial cells. *Nat. Immunol.* **8,** 351–358 (2007).

84. Picca, C. C. *et al.* Thymocyte deletion can bias Treg formation toward low-abundance self-peptide. *Eur. J. Immunol.* **39,** 3301–6 (2009).

85. Ouyang, W., Beckett, O., Ma, Q. & Li, M. O. Transforming growth factor-beta signaling curbs thymic negative selection promoting regulatory T cell development. *Immunity* **32,** 642–53 (2010).

86. Burchill, M. A., Yang, J., Vang, K. B. & Farrar, M. A. Interleukin-2 receptor signaling in regulatory T cell development and homeostasis. *Immunol. Lett.* **114,** 1–8 (2007).

87. Moran, A. E. & Hogquist, K. a. T-cell receptor affinity in thymic development. *Immunology* **135,** 261–7 (2012).

88. Coquet, J. M. *et al.* Epithelial and dendritic cells in the thymic medulla promote CD4+Foxp3+ regulatory T cell development via the CD27-CD70 pathway. *J. Exp. Med.* **210,** 715–28 (2013).

89. Germain, R. N. T-cell development and the CD4-CD8 lineage decision. *Nat. Rev. Immunol.* **2,** 309–22 (2002).

90. Matloubian, M. *et al.* Lymphocyte egress from thymus and peripheral lymphoid organs is dependent on S1P receptor 1. *Nature* **427,** 355–60 (2004).

91. Gray, D. H. D., Chidgey, A. P. & Boyd, R. L. Analysis of thymic stromal cell populations using flow cytometry. *J. Immunol. Methods* **260,** 15–28 (2002).

92. Rouse, R. V., Bolin, L. M., Bender, J. R. & Kyewski, B. a. Monoclonal antibodies reactive with subsets of mouse and human thymic epithelial cells. *J. Histochem. Cytochem.* **36,** 1511–1517 (1988).

93. Rode, I. & Boehm, T. Regenerative capacity of adult cortical thymic epithelial cells. *Proc. Natl. Acad. Sci. U. S. A.* **109,** 3463–8 (2012).

94. Klug, D. B. *et al.* Interdependence of cortical thymic epithelial cell differentiation and T-lineage commitment. *Proc. Natl. Acad. Sci. U. S. A.* **95,** 11822–7 (1998).

95. Baik, S., Jenkinson, E. J., Lane, P. J. L., Anderson, G. & Jenkinson, W. E. Generation of both cortical and Aire(+) medullary thymic epithelial compartments from CD205(+) progenitors. *Eur. J. Immunol.* **43,** 589–94 (2013).

96. Nakagawa, T. *et al.* Cathepsin L: critical role in Ii degradation and CD4 T cell selection in the thymus. *Science* **280,** 450–453 (1998).

97. Murata, S. *et al.* Regulation of CD8+ T cell development by thymus-specific proteasomes. *Science* **316,** 1349–53 (2007).

98. Jiang, W. *et al.* The receptor DEC-205 expressed by dendritic cells and thymic epithelial cells is involved in antigen processing. *Nature* **375,** 151–5 (1995).

99. Shrimpton, R. E. *et al.* CD205 (DEC-205): a recognition receptor for apoptotic and necrotic self. *Mol. Immunol.* **46,** 1229–39 (2009).

100. Jenkinson, W. E., Nakamura, K., White, A. J., Jenkinson, E. J. & Anderson, G. Normal T cell selection occurs in CD205-deficient thymic microenvironments. *PLoS One* **7,** e53416 (2012).

101. Honey, K. *et al.* Thymocyte expression of cathepsin L is essential for NKT cell development. *Nat. Immunol.* **3,** 1069–1074 (2002).

102. Lombardi, G. *et al.* Cathepsin-L influences the expression of extracellular matrix in lymphoid organs and plays a role in the regulation of thymic output and of peripheral T cell number. *J. Immunol.* **174,** 7022–32 (2005).

103. Jenkinson, E. J., Van Ewijk, W. & Owen, J. J. Major histocompatibility complex antigen expression on the epithelium of the developing thymus in normal and nude mice. *J. Exp. Med.* **153,** 280–292 (1981).

104. Depreter, M. G. L. *et al.* Identification of Plet-1 as a specific marker of early thymic epithelial progenitor cells. *Proc. Natl. Acad. Sci. U. S. A.* **105,** 961–6 (2008).

105. Ohigashi, I. *et al.* Aire-expressing thymic medullary epithelial cells originate from β5t-expressing progenitor cells. *Proc. Natl. Acad. Sci. U. S. A.* **110,** 9885–90 (2013).

106. Nowell, C. S. *et al.* Foxn1 regulates lineage progression in cortical and medullary thymic epithelial cells but is dispensable for medullary sublineage divergence. *PLoS Genet.* **7,** e1002348 (2011).

107. Blackburn, C. C. *et al.* The nu gene acts cell-autonomously and is required for differentiation of thymic epithelial progenitors. *Proc. Natl. Acad. Sci. U. S. A.* **93,** 5742–5746 (1996).

108. Derbinski, J. *et al.* Promiscuous gene expression in thymic epithelial cells is regulated at multiple levels. *J. Exp. Med.* **202,** 33–45 (2005).

109. Seach, N. *et al.* The lymphotoxin pathway regulates Aire-independent expression of ectopic genes and chemokines in thymic stromal cells. *J. Immunol.* **180,** 5384–5392 (2008).

110. Liston, A., Lesage, S., Wilson, J., Peltonen, L. & Goodnow, C. C. Aire regulates negative selection of organ-specific T cells. *Nat. Immunol.* **4,** 350–354 (2003).

111. Anderson, M. S. *et al.* Projection of an immunological self shadow within the thymus by the aire protein. *Science* **298,** 1395–401 (2002).

112. DeVoss, J. *et al.* Spontaneous autoimmunity prevented by thymic expression of a single self-antigen. *J. Exp. Med.* **203,** 2727–2735 (2006).

113. Rossi, S. W. *et al.* RANK signals from CD4(+)3(-) inducer cells regulate development of Aire-expressing epithelial cells in the thymic medulla. *J. Exp. Med.* **204,** 1267–72 (2007).

114. Nishikawa, Y. *et al.* Biphasic Aire expression in early embryos and in medullary thymic epithelial cells before end-stage terminal differentiation. *J. Exp. Med.* **207,** 963–971 (2010).

115. Wang, X. *et al.* Post-Aire maturation of thymic medullary epithelial cells involves selective expression of keratinocyte-specific autoantigens. *Front. Immunol.* **3,** 19 (2012).

116. Metzger, T. C. *et al.* Lineage tracing and cell ablation identify a post-aire-expressing thymic epithelial cell population. *Cell Rep.* **5,** 166–79 (2013).

117. Rossi, S. W., Jenkinson, W. E., Anderson, G. & Jenkinson, E. J. Clonal analysis reveals a common progenitor for thymic cortical and medullary epithelium. *Nature* **441,** 988–991 (2006).

118. Bleul, C. C. *et al.* Formation of a functional thymus initiated by a postnatal epithelial progenitor cell. *Nature* **441,** 992–996 (2006).

119. Röpke, C., Van Soest, P., Platenburg, P. P. & Van Ewijk, W. A common stem cell for murine cortical and medullary thymic epithelial cells? *Dev. Immunol.* **4,** 149–56 (1995).

120. Shakib, S. *et al.* Checkpoints in the development of thymic cortical epithelial cells. *J. Immunol.* **182,** 130–7 (2009).

121. Rodewald, H. R., Paul, S., Haller, C., Bluethmann, H. & Blum, C. Thymus medulla consisting of epithelial islets each derived from a single progenitor. *Nature* **414,** 763–8 (2001).

122. Alves, N. L. *et al.* Serial progression of cortical and medullary thymic epithelial microenvironments. *Eur. J. Immunol.* **44,** 16–22 (2014).

123. Kaestner, K. H., Knochel, W. & Martinez, D. E. Unified nomenclature for the winged helix/forkhead transcription factors. *Genes Dev.* **14,** 142–6 (2000).

124. Kaufmann, E. & Knöchel, W. Five years on the wings of fork head. *Mech. Dev.* **57,** 3–20 (1996).

125. Schorpp, M., Hofmann, M., Dear, T. N. & Boehm, T. Characterization of mouse and human nude genes. *Immunogenetics* **46,** 509–515 (1997).

126. Nehls, M. *et al.* Yeast Artificial Chromosome Contig on Mouse Chromosome-11 Encompassing the Nu-Locus. *Eur. J. Immunol.* **24,** 1721–1723 (1994).

127. Frank, J. *et al.* Exposing the human nude phenotype. *Nature* **398,** 473–4 (1999).

128. Schlake, T. The nude gene and the skin. *Exp. Dermatol.* **10,** 293–304 (2001).

129. Militzer, K. & Schwalenstöcker, H. Postnatal and postpartal morphology of the mammary gland in nude mice. *J. Exp. Anim. Sci.* **38,** 1–12 (1996).

130. Pantelouris, E. M. Absence of thymus in a mouse mutant. *Nature* **217,** 370–1 (1968).

131. Pantelouris, E. M. & Hair, J. Thymus dysgenesis in nude (nu nu) mice. *J. Embryol. Exp. Morphol.* **24,** 615–23 (1970).

132. Flanagan, S. P. "Nude", a new hairless gene with pleiotropic effects in the mouse. *Genet. Res.* **8,** 295–309 (1966).

133. Belizário, J. Immunodeficient mouse models: an overview. *Open Immunol. J.* **2,** 79–85 (2009).

134. Shultz, L. D. & Sidman, C. L. Genetically determined murine models of immunodeficiency. *Annu. Rev. Immunol.* **5,** 367–403 (1987).

135. Balciunaite, G. *et al.* Wnt glycoproteins regulate the expression of FoxN1, the gene defective in nude mice. *Nat. Immunol.* **3,** 1102–1108 (2002).

136. Zuklys, S. *et al.* Stabilized beta-catenin in thymic epithelial cells blocks thymus development and function. *J. Immunol.* **182,** 2997–3007 (2009).

137. Itoi, M., Tsukamoto, N. & Amagai, T. Expression of Dll4 and CCL25 in Foxn1-negative epithelial cells in the post-natal thymus. *Int. Immunol.* **19,** 127–32 (2007).

138. Osada, M. *et al.* The Wnt Signaling Antagonist Kremen1 is Required for Development of Thymic Architecture. *Clin. Dev. Immunol.* **13,** 299–319 (2006).

139. Patel, S. R., Gordon, J., Mahbub, F., Blackburn, C. C. & Manley, N. R. Bmp4 and Noggin expression during early thymus and parathyroid organogenesis. *Gene Expr. Patterns* **6,** 794–799 (2006).

140. Tsai, P. T., Lee, R. a & Wu, H. BMP4 acts upstream of FGF in modulating thymic stroma and regulating thymopoiesis. *Blood* **102,** 3947–53 (2003).

141. Moore-Scott, B. A. & Manley, N. R. Differential expression of Sonic hedgehog along the anterior-posterior axis regulates patterning of pharyngeal pouch endoderm and pharyngeal endoderm-derived organs. *Dev. Biol.* **278,** 323–335 (2005).

142. Frank, D. U. *et al.* An Fgf8 mouse mutant phenocopies human 22q11 deletion syndrome. *Development* **129,** 4591–603 (2002).

143. Tsukamoto, N., Itoi, M., Nishikawa, M. & Amagai, T. Lack of Delta like 1 and 4 expressions in nude thymus anlages. *Cell. Immunol.* **234,** 77–80 (2005).

144. Bleul, C. C. & Boehm, T. Chemokines define distinct microenvironments in the developing thymus. *Eur. J. Immunol.* **30,** 3371–3379 (2000).

145. Bleul, C. C. & Boehm, T. Laser capture microdissection-based expression profiling identifies PD1-ligand as a target of the nude locus gene product. *Eur. J. Immunol.* **31,** 2497–503 (2001).

146. Nishimura, H. *et al.* Developmentally regulated expression of the PD-1 protein on the surface of double-negative (CD4-CD8-) thymocytes. *Int. Immunol.* **8,** 773–780 (1996).

147. Nishimura, H., Nose, M., Hiai, H., Minato, N. & Honjo, T. Development of lupus-like autoimmune diseases by disruption of the PD-1 gene encoding an ITIM motif-carrying immunoreceptor. *Immunity* **11,** 141–151 (1999).

148. Calderón, L. & Boehm, T. Three chemokine receptors cooperatively regulate homing of hematopoietic progenitors to the embryonic mouse thymus. *Proc. Natl. Acad. Sci. U. S. A.* **108,** 7517–7522 (2011).

149. Rodewald, H. R., Kretzschmar, K., Swat, W. & Takeda, S. Intrathymically expressed c-kit ligand (stem cell factor) is a major factor driving expansion of very immature thymocytes in vivo. *Immunity* **3,** 313–9 (1995).

150. Mori, K., Itoi, M., Tsukamoto, N. & Amagai, T. Foxn1 is essential for vascularization of the murine thymus anlage. *Cell. Immunol.* **260,** 66–9 (2010).

151. Guo, J. *et al.* Morphogenesis and maintenance of the 3D thymic medulla and prevention of nude skin phenotype require FoxN1 in pre- and post-natal K14 epithelium. *J. Mol. Med. (Berl).* **89,** 263–277 (2011).

152. Su, D., Navarre, S., Oh, W., Condie, B. G. & Manley, N. R. A domain of Foxn1 required for crosstalk-dependent thymic epithelial cell differentiation. *Nat. Immunol.* **4,** 1128–35 (2003).

153. Xiao, S., Su, D. & Manley, N. R. T cell development from kit-negative progenitors in the Foxn1Delta/Delta mutant thymus. *J. Immunol.* **180,** 914–21 (2008).

154. Xiao, S., Su, D. & Manley, N. R. Atypical memory phenotype T cells with low homeostatic potential and impaired TCR signaling and regulatory T cell function in Foxn1Delta/Delta mutant mice. *J. Immunol.* **179,** 8153–63 (2007).

155. Porritt, H. E. *et al.* Heterogeneity among DN1 prothymocytes reveals multiple progenitors with different capacities to generate T cell and non-T cell lineages. *Immunity* **20,** 735–45 (2004).

156. Chen, L., Xiao, S. & Manley, N. R. Foxn1 is required to maintain the postnatal thymic microenvironment in a dosage-sensitive manner. *Blood* **113,** 567–74 (2009).

157. Cheng, L. *et al.* Postnatal tissue-specific disruption of transcription factor FoxN1 triggers acute thymic atrophy. *J. Biol. Chem.* **285,** 5836–5847 (2010).

158. Pignata, C. *et al. Congenital Alopecia and nail dystrophy associated with severe functional T-cell immunodeficiency in two sibs. Am. J. Med. Genet.* **65,** 167–170 (1996).

159. Pignata, C. Human equivalent of the mouse Nude/SCID phenotype: long-term evaluation of immunologic reconstitution after bone marrow transplantation. *Blood* **97,** 880–885 (2001).

160. Markert, M. L. *et al.* First use of thymus transplantation therapy for FOXN1 deficiency (nude/SCID): a report of 2 cases. *Blood* **117,** 688–96 (2011).

161. Albuquerque, A. S. *et al.* Human FOXN1-deficiency is associated with αβ double-negative and FoxP3+ T-cell expansions that are distinctly modulated upon thymic transplantation. *PLoS One* **7,** e37042 (2012).

162. Shanley, D. P., Aw, D., Manley, N. R. & Palmer, D. B. An evolutionary perspective on the mechanisms of immunosenescence. *Trends Immunol.* **30,** 374–381 (2009).

163. Taub, D. D. & Longo, D. L. Insights into thymic aging and regeneration. *Immunol. Rev.* **205,** 72–93 (2005).

164. Aw, D., Taylor-Brown, F., Cooper, K. & Palmer, D. B. Phenotypical and morphological changes in the thymic microenvironment from ageing mice. *Biogerontology* **10,** 311–322 (2009).

165. Gruver, A. L., Hudson, L. L. & Sempowski, G. D. Immunosenescence of ageing. *J. Pathol.* **211,** 144–56 (2007).

166. Griffith, A. V, Fallahi, M., Venables, T. & Petrie, H. T. Persistent degenerative changes in thymic organ function revealed by an inducible model of organ regrowth. *Aging Cell* **11,** 169–77 (2012).

167. Takeoka, Y. *et al.* The murine thymic microenvironment: changes with age. *Int. Arch. Allergy Immunol.* **111,** 5–12 (1996).

168. Akbar, A. N. & Fletcher, J. M. Memory T cell homeostasis and senescence during aging. *Curr. Opin. Immunol.* **17,** 480–5 (2005).

169. Ortman, C. L., Dittmar, K. A., Witte, P. L. & Le, P. T. Molecular characterization of the mouse involuted thymus: aberrations in expression of transcription regulators in thymocyte and epithelial compartments. *Int. Immunol.* **14,** 813–822 (2002).

170. Gui, J., Mustachio, L. M., Su, D. & Craig, R. W. Thymus Size and Age-related Thymic Involution: Early Programming, Sexual Dimorphism, Progenitors and Stroma. *Aging Dis.* **3,** 280–90 (2012).

171. Sun, L. *et al.* Declining expression of a single epithelial cell-autonomous gene accelerates age-related thymic involution. *Aging Cell* **9,** 347–57 (2010).

172. Zook, E. C. *et al.* Overexpression of Foxn1 attenuates age-associated thymic involution and prevents the expansion of peripheral CD4 memory T cells. *Blood* **118,** 5723–5731 (2011).

173. Nikolich-Zugich, J. & Rudd, B. D. Immune memory and aging: an infinite or finite resource? *Curr. Opin. Immunol.* **22,** 535–40 (2010).

174. Nikolich-Zugich, J. Ageing and life-long maintenance of T-cell subsets in the face of latent persistent infections. *Nat. Rev. Immunol.* **8,** 512–22 (2008).

175. Dixit, V. D. Thymic fatness and approaches to enhance thymopoietic fitness in aging. *Curr. Opin. Immunol.* **22,** 521–8 (2010).

176. Youm, Y.-H. *et al.* Deficient ghrelin receptor-mediated signaling compromises thymic stromal cell microenvironment by accelerating thymic adiposity. *J. Biol. Chem.* **284,** 7068–7077 (2009).

177. Strutz, F. *et al.* Identification and characterization of a fibroblast marker: FSP1. *J. Cell Biol.* **130,** 393–405 (1995).

178. Yang, H. *et al.* Obesity accelerates thymic aging. *Blood* **114,** 3803–12 (2009).

179. Yang, H., Youm, Y.-H. & Dixit, V. D. Inhibition of thymic adipogenesis by caloric restriction is coupled with reduction in age-related thymic involution. *J. Immunol.* **183,** 3040–52 (2009).

180. Min, D. *et al.* Sustained thymopoiesis and improvement in functional immunity induced by exogenous KGF administration in murine models of aging. *Blood* **109,** 2529–37 (2007).

181. Gui, J. *et al.* The aged thymus shows normal recruitment of lymphohematopoietic progenitors but has defects in thymic epithelial cells. *Int. Immunol.* **19,** 1201–11 (2007).

182. Boyman, O., Létourneau, S., Krieg, C. & Sprent, J. Homeostatic proliferation and survival of naïve and memory T cells. *Eur. J. Immunol.* **39,** 2088–94 (2009).

183. Boyman, O., Purton, J. F., Surh, C. D. & Sprent, J. Cytokines and T-cell homeostasis. *Curr. Opin. Immunol.* **19,** 320–326 (2007).

184. Sprent, J. & Surh, C. D. T cell memory. *Annu. Rev. Immunol.* **20,** 551–79 (2002).

185. Tough, D. F. Turnover of naive- and memory-phenotype T cells. *J. Exp. Med.* **179,** 1127–1135 (1994).

186. Tan, J. T. *et al.* IL-7 is critical for homeostatic proliferation and survival of naive T cells. *Proc. Natl. Acad. Sci. U. S. A.* **98,** 8732–7 (2001).

187. Cho, B. K., Rao, V. P., Ge, Q., Eisen, H. N. & Chen, J. Homeostasis-stimulated proliferation drives naive T cells to differentiate directly into memory T cells. *J. Exp. Med.* **192,** 549–556 (2000).

188. Kieper, W. C., Prlic, M., Schmidt, C. S., Mescher, M. F. & Jameson, S. C. Il-12 enhances CD8 T cell homeostatic expansion. *J. Immunol.* **166,** 5515–21 (2001).

189. Surh, C. D. & Sprent, J. Homeostasis of naive and memory T cells. *Immunity* **29,** 848–62 (2008).

190. Min, B., Yamane, H., Hu-Li, J. & Paul, W. E. Spontaneous and homeostatic proliferation of CD4 T cells are regulated by different mechanisms. *J. Immunol.* **174,** 6039–44 (2005).

191. Prlic, M. & Jameson, S. C. Homeostatic expansion versus antigen-driven proliferation: common ends by different means? *Microbes Infect.* **4,** 531–7 (2002).

192. Kieper, W. C. *et al.* Recent immune status determines the source of antigens that drive homeostatic T cell expansion. *J. Immunol.* **174,** 3158–63 (2005).

193. MacDonald, H. R. *et al.* Age-associated increase in expression of the T cell surface markers Thy-1, Lyt-1, and Lyt-2 in congenitally athymic (nu/nu) mice: analysis by flow microfluorometry. *J. Immunol.* **126,** 865–70 (1981).

194. MacDonald, H. R., Blanc, C., Lees, R. K. & Sordat, B. Abnormal distribution of T cell subsets in athymic mice. *J. Immunol.* **136,** 4337–9 (1986).

195. Suzuki, K. *et al.* Gut cryptopatches: direct evidence of extrathymic anatomical sites for intestinal T lymphopoiesis. *Immunity* **13,** 691–702 (2000).

196. Oida, T. *et al.* Role of gut cryptopatches in early extrathymic maturation of intestinal intraepithelial T cells. *J. Immunol.* **164,** 3616–26 (2000).

197. Guy-Grand, D. *et al.* Extrathymic T Cell Lymphopoiesis: Ontogeny and Contribution to Gut Intraepithelial Lymphocytes in Athymic and Euthymic Mice. *J. Exp. Med.* **197,** 333–341 (2003).

198. Holland, A. M. *et al.* Extrathymic development of murine T cells after bone marrow transplantation. *J. Clin. Invest.* **122,** 4716–26 (2012).

199. Clegg, C. H., Rulffes, J. T., Wallace, P. M. & Haugen, H. S. Regulation of an extrathymic T-cell development pathway by oncostatin M. *Nature* **384,** 261–3 (1996).

200. Terra, R., Labrecque, N. & Perreault, C. Thymic and extrathymic T cell development pathways follow different rules. *J. Immunol.* **169,** 684–92 (2002).

201. Blais, M.-E., Louis, I. & Perreault, C. T-cell development: an extrathymic perspective. *Immunol. Rev.* **209,** 103–14 (2006).

202. Gardner, J. M. *et al.* Deletional tolerance mediated by extrathymic Aire-expressing cells. *Science* **321,** 843–7 (2008).

203. Boileau, C., Houde, M., Dulude, G., Clegg, C. H. & Perreault, C. Regulation of extrathymic T cell development and turnover by oncostatin M. *J. Immunol.* **164,** 5713–20 (2000).

204. Blais, M.-E. *et al.* Do thymically and strictly extrathymically developing T cells generate similar immune responses? *Blood* **103,** 3102–10 (2004).

205. Artis, D. Epithelial-cell recognition of commensal bacteria and maintenance of immune homeostasis in the gut. *Nat. Rev. Immunol.* **8,** 411–420 (2008).

206. Xiao, H. *et al.* The Toll-interleukin-1 receptor member SIGIRR regulates colonic epithelial homeostasis, inflammation, and tumorigenesis. *Immunity* **26,** 461–75 (2007).

207. Wald, D. *et al.* SIGIRR, a negative regulator of Toll-like receptor-interleukin 1 receptor signaling. *Nat. Immunol.* **4,** 920–7 (2003).

208. Garlanda, C. *et al.* Intestinal inflammation in mice deficient in Tir8, an inhibitory member of the IL-1 receptor family. *Proc. Natl. Acad. Sci. U. S. A.* **101,** 3522–6 (2004).

209. Schilling, J. D., Martin, S. M., Hung, C. S., Lorenz, R. G. & Hultgren, S. J. Toll-like receptor 4 on stromal and hematopoietic cells mediates innate resistance to uropathogenic Escherichia coli. *Proc. Natl. Acad. Sci. U. S. A.* **100,** 4203–8 (2003).

210. Lebeis, S. L., Bommarius, B., Parkos, C. a, Sherman, M. a & Kalman, D. TLR signaling mediated by MyD88 is required for a protective innate immune response by neutrophils to Citrobacter rodentium. *J. Immunol.* **179,** 566–77 (2007).

211. Johansson, M. E. V, Sjövall, H. & Hansson, G. C. The gastrointestinal mucus system in health and disease. *Nat. Rev. Gastroenterol. Hepatol.* **10,** 352–61 (2013).

212. McAuley, J. L. *et al.* MUC1 cell surface mucin is a critical element of the mucosal barrier to infection. *J. Clin. Invest.* **117,** 2313–24 (2007).

213. Cash, H. L., Whitham, C. V, Behrendt, C. L. & Hooper, L. V. Symbiotic bacteria direct expression of an intestinal bactericidal lectin. *Science* **313,** 1126–30 (2006).

214. Jung, C., Hugot, J.-P. & Barreau, F. Peyer's Patches: The Immune Sensors of the Intestine. *Int. J. Inflam.* **2010,** 823710 (2010).

215. Eberl, G. & Lochner, M. The development of intestinal lymphoid tissues at the interface of self and microbiota. *Mucosal Immunol.* **2,** 478–85 (2009).

216. Shale, M., Schiering, C. & Powrie, F. CD4(+) T-cell subsets in intestinal inflammation. *Immunol. Rev.* **252,** 164–82 (2013).

217. Bendelac, A. *et al.* CD1 recognition by mouse NK1+ T lymphocytes. *Science* **268,** 863–865 (1995).

218. Hansen, T. H., Huang, S., Arnold, P. L. & Fremont, D. H. Patterns of nonclassical MHC antigen presentation. *Nat. Immunol.* **8,** 563–568 (2007).

219. Martin, E. *et al.* Stepwise development of MAIT cells in mouse and human. *PLoS Biol.* **7,** e54 (2009).

220. Tilloy, F. *et al.* An invariant T cell receptor alpha chain defines a novel TAP-independent major histocompatibility complex class Ib-restricted alpha/beta T cell subpopulation in mammals. *J. Exp. Med.* **189,** 1907–21 (1999).

221. Le Bourhis, L. *et al.* Antimicrobial activity of mucosal-associated invariant T cells. *Nat. Immunol.* **11,** 701–708 (2010).

222. Laroux, F. S. Regulation of chronic colitis in athymic nu/nu (nude) mice. *Int. Immunol.* **16,** 77–89 (2004).

223. Poussier, P. A Unique Subset of Self-specific Intraintestinal T Cells Maintains Gut Integrity. *J. Exp. Med.* **195,** 1491–1497 (2002).

224. Locke, N. R., Stankovic, S., Funda, D. P. & Harrison, L. C. TCR gamma delta intraepithelial lymphocytes are required for self-tolerance. *J. Immunol.* **176,** 6553–9 (2006).

225. Svensson, M. *et al.* CCL25 mediates the localization of recently activated CD8αβ+ lymphocytes to the small-intestinal mucosa. *J. Clin. Invest.* **110,** 1113–1121 (2002).

226. Guy-Grand, D. & Vassalli, P. Gut intraepithelial lymphocyte development. *Curr. Opin. Immunol.* **14,** 255–259 (2002).

227. Rocha, B., Vassalli, P. & Guy-Grand, D. The V beta repertoire of mouse gut homodimeric alpha CD8+ intraepithelial T cell receptor alpha/beta + lymphocytes

reveals a major extrathymic pathway of T cell differentiation. *J. Exp. Med.* **173,** 483–6 (1991).

228. Pobezinsky, L. a *et al.* Clonal deletion and the fate of autoreactive thymocytes that survive negative selection. *Nat. Immunol.* **13,** 569–78 (2012).

229. Rocha, B., Vassalli, P. & Guy-Grand, D. The extrathymic T-cell development pathway. *Immunol. Today* **13,** 449–54 (1992).

230. Guy-Grand, D. *et al.* Two gut intraepithelial CD8+ lymphocyte populations with different T cell receptors: a role for the gut epithelium in T cell differentiation. *J. Exp. Med.* **173,** 471–81 (1991).

231. Bruno, L., Rocha, B., Rolink, A., von Boehmer, H. & Rodewald, H. R. Intra- and extra-thymic expression of the pre-T cell receptor alpha gene. *Eur. J. Immunol.* **25,** 1877–1882 (1995).

232. Lambolez, F. *et al.* Characterization of T cell differentiation in the murine gut. *J. Exp. Med.* **195,** 437–49 (2002).

233. Bandeira, A. *et al.* Extrathymic origin of intestinal intraepithelial lymphocytes bearing T-cell antigen receptor gamma delta. *Proc. Natl. Acad. Sci.* **88,** 43–47 (1991).

234. Lin, T., Matsuzaki, G., Kenai, H., Nakamura, T. & Nomoto, K. Thymus influences the development of extrathymically derived intestinal intraepithelial lymphocytes. *Eur. J. Immunol.* **23,** 1968–74 (1993).

235. Peaudecerf, L. *et al.* The role of the gut as a primary lymphoid organ: CD8αα intraepithelial T lymphocytes in euthymic mice derive from very immature CD44+ thymocyte precursors. *Mucosal Immunol.* **4,** 93–101 (2011).

236. Lambolez, F. *et al.* The thymus exports long-lived fully committed T cell precursors that can colonize primary lymphoid organs. *Nat. Immunol.* **7,** 76–82 (2006).

237. Eberl, G. & Littman, D. R. Thymic origin of intestinal alphabeta T cells revealed by fate mapping of RORgammat+ cells. *Science* **305,** 248–51 (2004).

238. Egawa, T., Kreslavsky, T., Littman, D. R. & von Boehmer, H. Lineage diversion of T cell receptor transgenic thymocytes revealed by lineage fate mapping. *PLoS One* **3,** e1512 (2008).

239. Bäckhed, F., Ley, R. E., Sonnenburg, J. L., Peterson, D. A. & Gordon, J. I. Host-bacterial mutualism in the human intestine. *Science* **307,** 1915–1920 (2005).

240. Chung, H. *et al.* Gut immune maturation depends on colonization with a host-specific microbiota. *Cell* **149,** 1578–93 (2012).

241. Laroux, F. S. & Grisham, M. B. Immunological basis of inflammatory bowel disease: role of the microcirculation. *Microcirculation* **8,** 283–301 (2001).

242. Wehkamp, J. *et al.* Reduced Paneth cell alpha-defensins in ileal Crohn's disease. *Proc. Natl. Acad. Sci. U. S. A.* **102,** 18129–34 (2005).

243. Strober, W. The LTi cell, an immunologic chameleon. *Immunity* **33,** 650–2 (2010).

244. Hill, D. a & Artis, D. Intestinal bacteria and the regulation of immune cell homeostasis. *Annu. Rev. Immunol.* **28,** 623–67 (2010).

245. Kabashima, K. *et al.* The prostaglandin receptor EP4 suppresses colitis, mucosal damage and CD4 cell activation in the gut. *J. Clin. Invest.* **109,** 883–893 (2002).

246. Libioulle, C. *et al.* Novel Crohn disease locus identified by genome-wide association maps to a gene desert on 5p13.1 and modulates expression of PTGER4. *PLoS Genet.* **3,** e58 (2007).

247. Van der Sluis, M. *et al.* Muc2-deficient mice spontaneously develop colitis, indicating that MUC2 is critical for colonic protection. *Gastroenterology* **131,** 117–29 (2006).

248. Barrett, J. C. *et al.* Genome-wide association defines more than 30 distinct susceptibility loci for Crohn's disease. *Nat. Genet.* **40,** 955–62 (2008).

249. Koslowski, M. J., Beisner, J., Stange, E. F. & Wehkamp, J. Innate antimicrobial host defense in small intestinal Crohn's disease. *Int. J. Med. Microbiol.* **300,** 34–40 (2010).

250. Horwitz, D. a, Zheng, S. G. & Gray, J. D. The role of the combination of IL-2 and TGF-beta or IL-10 in the generation and function of CD4+ CD25+ and CD8+ regulatory T cell subsets. *J. Leukoc. Biol.* **74,** 471–8 (2003).

251. Kühn, R., Löhler, J., Rennick, D., Rajewsky, K. & Müller, W. Interleukin-10-deficient mice develop chronic enterocolitis. *Cell* **75,** 263–74 (1993).

252. Davidson, N. J. *et al.* T helper cell 1-type CD4+ T cells, but not B cells, mediate colitis in interleukin 10-deficient mice. *J. Exp. Med.* **184,** 241–51 (1996).

253. Hagenbaugh, a *et al.* Altered immune responses in interleukin 10 transgenic mice. *J. Exp. Med.* **185,** 2101–10 (1997).

254. Powrie, F. *et al.* Inhibition of Th1 responses prevents inflammatory bowel disease in scid mice reconstituted with CD45RBhi CD4+ T cells. *Immunity* **1,** 553–62 (1994).

255. Li, M. O., Sanjabi, S. & Flavell, R. a. Transforming growth factor-beta controls development, homeostasis, and tolerance of T cells by regulatory T cell-dependent and -independent mechanisms. *Immunity* **25,** 455–71 (2006).

256. Marie, J. C., Liggitt, D. & Rudensky, A. Y. Cellular mechanisms of fatal early-onset autoimmunity in mice with the T cell-specific targeting of transforming growth factor-beta receptor. *Immunity* **25,** 441–54 (2006).

257. Hahm, K. B. *et al.* Loss of transforming growth factor beta signalling in the intestine contributes to tissue injury in inflammatory bowel disease. *Gut* **49,** 190–8 (2001).

258. Izcue, A., Coombes, J. L. & Powrie, F. Regulatory lymphocytes and intestinal inflammation. *Annu. Rev. Immunol.* **27,** 313–338 (2009).

259. Elson, C. O. *et al.* Experimental models of inflammatory bowel disease reveal innate, adaptive, and regulatory mechanisms of host dialogue with the microbiota. *Immunol. Rev.* **206,** 260–76 (2005).

260. Rakoff-Nahoum, S., Hao, L. & Medzhitov, R. Role of Toll-like Receptors in Spontaneous Commensal-Dependent Colitis. *Immunity* **25,** 319–329 (2006).

261. Corbeaux, T. *et al.* Thymopoiesis in mice depends on a Foxn1-positive thymic epithelial cell lineage. *Proc. Natl. Acad. Sci. U. S. A.* **107,** 16613–8 (2010).

262. Pham, C. T., MacIvor, D. M., Hug, B. A., Heusel, J. W. & Ley, T. J. Long-range disruption of gene expression by a selectable marker cassette. *Proc. Natl. Acad. Sci. U. S. A.* **93,** 13090–13095 (1996).

263. Nagy, a. Cre recombinase: the universal reagent for genome tailoring. *Genesis* **26,** 99–109 (2000).

264. Farley, F. W., Soriano, P., Steffen, L. S. & Dymecki, S. M. Widespread recombinase expression using FLPeR (flipper) mice. *Genesis* **28,** 106–10 (2000).

265. Köpf-Maier, P. & Mboneko, V. F. Anomalies in the hormonal status of athymic nude mice. *J. Cancer Res. Clin. Oncol.* **116,** 229–231 (1990).

266. Mecklenburg, L., Nakamura, M., Sundberg, J. P. & Paus, R. The nude mouse skin phenotype: the role of Foxn1 in hair follicle development and cycling. *Exp. Mol. Pathol.* **71,** 171–8 (2001).

267. Bennett, A. R. *et al.* Identification and characterization of thymic epithelial progenitor cells. *Immunity* **16,** 803–14 (2002).

268. Ripen, A. M., Nitta, T., Murata, S., Tanaka, K. & Takahama, Y. Ontogeny of thymic cortical epithelial cells expressing the thymoproteasome subunit β5t. *Eur. J. Immunol.* **41,** 1278–87 (2011).

269. Hikosaka, Y. *et al.* The Cytokine RANKL Produced by Positively Selected Thymocytes Fosters Medullary Thymic Epithelial Cells that Express Autoimmune Regulator. *Immunity* **29,** 438–450 (2008).

270. White, A. J. *et al.* Sequential phases in the development of Aire-expressing medullary thymic epithelial cells involve distinct cellular input. *Eur. J. Immunol.* **38,** 942–7 (2008).

271. White, A. J. *et al.* Lymphotoxin signals from positively selected thymocytes regulate the terminal differentiation of medullary thymic epithelial cells. *J. Immunol.* **185,** 4769–76 (2010).

272. Dooley, J., Erickson, M. & Farr, a. G. Alterations of the Medullary Epithelial Compartment in the Aire-Deficient Thymus: Implications for Programs of Thymic Epithelial Differentiation. *J. Immunol.* **181,** 5225–5232 (2008).

273. Akiyama, T. *et al.* The tumor necrosis factor family receptors RANK and CD40 cooperatively establish the thymic medullary microenvironment and self-tolerance. *Immunity* **29,** 423–37 (2008).

274. Takahama, Y. Journey through the thymus: stromal guides for T-cell development and selection. *Nat. Rev. Immunol.* **6,** 127–35 (2006).

275. Starr, T. K., Jameson, S. C. & Hogquist, K. a. Positive and negative selection of T cells. *Annu. Rev. Immunol.* **21,** 139–76 (2003).

276. Kadish, J. L. & Basch, R. S. Hematopoietic thymocyte precursors. I. Assay and kinetics of the appearance of progeny. *J. Exp. Med.* **143,** 1082–99 (1976).

277. Ikuta, K. & Weissman, I. L. Evidence that hematopoietic stem cells express mouse c-kit but do not depend on steel factor for their generation. *Proc. Natl. Acad. Sci. U. S. A.* **89,** 1502–6 (1992).

278. Kondo, M., Weissman, I. L. & Akashi, K. Identification of clonogenic common lymphoid progenitors in mouse bone marrow. *Cell* **91,** 661–72 (1997).

279. Spangrude, G. J., Heimfeld, S. & Weissman, I. L. Purification and characterization of mouse hematopoietic stem cells. *Science* **241,** 58–62 (1988).

280. Perry, S. S., Welner, R. S., Kouro, T., Kincade, P. W. & Sun, X.-H. Primitive lymphoid progenitors in bone marrow with T lineage reconstituting potential. *J. Immunol.* **177,** 2880–7 (2006).

281. Perry, S. S. *et al.* L-selectin defines a bone marrow analog to the thymic early T-lineage progenitor. *Blood* **103,** 2990–6 (2004).

282. Zook, E. C., Zhang, S., Gerstein, R. M., Witte, P. L. & Le, P. T. Enhancing T lineage production in aged mice: a novel function of Foxn1 in the bone marrow niche. *J. Immunol.* **191,** 5583–93 (2013).

283. Maleckar, J. R. & Sherman, L. A. The composition of the T cell receptor repertoire in nude mice. *J. Immunol.* **138,** 3873–6 (1987).

284. MacDonald, H. R., Lees, R. K., Bron, C., Sordat, B. & Miescher, G. T cell antigen receptor expression in athymic (nu/nu) mice. Evidence for an oligoclonal beta chain repertoire. *J. Exp. Med.* **166,** 195–209 (1987).

285. Watts, C. J., Hahn, B. L. & Sohnle, P. G. Resistance of athymic nude mice to experimental cutaneous Bacillus anthracis infection. *J. Infect. Dis.* **199,** 673–9 (2009).

286. Thornton, A. M. *et al.* Expression of Helios, an Ikaros transcription factor family member, differentiates thymic-derived from peripherally induced Foxp3+ T regulatory cells. *J. Immunol.* **184,** 3433–41 (2010).

287. Yadav, M. *et al.* Neuropilin-1 distinguishes natural and inducible regulatory T cells among regulatory T cell subsets in vivo. *J. Exp. Med.* **209,** 1713–22, S1–19 (2012).

288. Weiss, J. M. *et al.* Neuropilin 1 is expressed on thymus-derived natural regulatory T cells, but not mucosa-generated induced Foxp3+ T reg cells. *J. Exp. Med.* **209,** 1723–42, S1 (2012).

289. Gottschalk, R. a, Corse, E. & Allison, J. P. Expression of Helios in peripherally induced Foxp3+ regulatory T cells. *J. Immunol.* **188,** 976–80 (2012).

290. Akimova, T., Beier, U. H., Wang, L., Levine, M. H. & Hancock, W. W. Helios expression is a marker of T cell activation and proliferation. *PLoS One* **6,** e24226 (2011).

291. Kung, J. T. & Thomas, C. a. Athymic nude CD4+8- T cells produce IL-2 but fail to proliferate in response to mitogenic stimuli. *J. Immunol.* **141,** 3691–6 (1988).

292. Grumont, R. *et al.* The mitogen-induced increase in T cell size involves PKC and NFAT activation of Rel/NF-kappaB-dependent c-myc expression. *Immunity* **21,** 19–30 (2004).

293. Ostanin, D. V *et al.* T cell transfer model of chronic colitis: concepts, considerations, and tricks of the trade. *Am. J. Physiol. Gastrointest. Liver Physiol.* **296,** G135–46 (2009).

294. Saleh, M. & Elson, C. O. Experimental inflammatory bowel disease: insights into the host-microbiota dialog. *Immunity* **34,** 293–302 (2011).

295. Asseman, C., Mauze, S., Leach, M. W., Coffman, R. L. & Powrie, F. An essential role for interleukin 10 in the function of regulatory T cells that inhibit intestinal inflammation. *J. Exp. Med.* **190,** 995–1004 (1999).

296. Chinen, T. *et al.* Prostaglandin E2 and SOCS1 have a role in intestinal immune tolerance. *Nat. Commun.* **2,** 190 (2011).

297. Bhan, a K., Mizoguchi, E., Smith, R. N. & Mizoguchi, A. Colitis in transgenic and knockout animals as models of human inflammatory bowel disease. *Immunol. Rev.* **169,** 195–207 (1999).

298. Linterman, M. a *et al.* Follicular helper T cells are required for systemic autoimmunity. *J. Exp. Med.* **206,** 561–76 (2009).

299. Busser, B. W., Adair, B. S., Erikson, J. & Laufer, T. M. Activation of diverse repertoires of autoreactive T cells enhances the loss of anti-dsDNA B cell tolerance. *J. Clin. Invest.* **112,** 1361–1371 (2003).

300. Chinn, I. K., Blackburn, C. C., Manley, N. R. & Sempowski, G. D. Changes in primary lymphoid organs with aging. *Semin. Immunol.* **24,** 309–20 (2012).

301. Bryson, J. L. *et al.* Cell-autonomous defects in thymic epithelial cells disrupt endothelial-perivascular cell interactions in the mouse thymus. *PLoS One* **8,** e65196 (2013).

302. Liu, C. P., Kappler, J. W. & Marrack, P. Thymocytes can become mature T cells without passing through the CD4+ CD8+, double-positive stage. *J. Exp. Med.* **184,** 1619–30 (1996).

303. Goldrath, a W., Bogatzki, L. Y. & Bevan, M. J. Naive T cells transiently acquire a memory-like phenotype during homeostasis-driven proliferation. *J. Exp. Med.* **192,** 557–64 (2000).

304. Cowan, J. E. *et al.* The thymic medulla is required for Foxp3+ regulatory but not conventional CD4+ thymocyte development. *J. Exp. Med.* **210,** 675–81 (2013).

305. Godkin, A. & Gallimore, A. Setting the threshold for extra-thymic differentiation of Foxp3+ Tregs: TGF-β-dependent and T-cell autonomous. *Eur. J. Immunol.* **41,** 1218–1220 (2011).

306. Bosco, N., Agenes, F., Rolink, A. G. & Ceredig, R. Peripheral T cell lymphopenia and concomitant enrichment in naturally arising regulatory T cells: the case of the pre-Talpha gene-deleted mouse. *J. Immunol.* **177,** 5014–5023 (2006).

307. Holländer, G. a *et al.* Severe colitis in mice with aberrant thymic selection. *Immunity* **3,** 27–38 (1995).

308. Trobonjaca, Z. *et al.* MHC-II-independent CD4+ T cells induce colitis in immunodeficient RAG-/- hosts. *J. Immunol.* **166,** 3804–12 (2001).

309. Ablamunits, V., Quintana, F., Reshef, T., Elias, D. & Cohen, I. R. Acceleration of autoimmune diabetes by cyclophosphamide is associated with an enhanced IFN-gamma secretion pathway. *J. Autoimmun.* **13,** 383–92 (1999).

310. Götlind, Y.-Y. C., Raghavan, S., Bland, P. W. & Hörnquist, E. H. CD4+FoxP3+ regulatory T cells from Gαi2-/- mice are functionally active in vitro, but do not prevent colitis. *PLoS One* **6,** e25073 (2011).

311. Abo, T., Tomiyama, C. & Watanabe, H. Biology of autoreactive extrathymic T cells and B-1 cells of the innate immune system. *Immunol. Res.* **52,** 224–30 (2012).

312. Zediak, V. P., Maillard, I. & Bhandoola, A. Multiple prethymic defects underlie age-related loss of T progenitor competence. *Blood* **110,** 1161–7 (2007).

8. Acknowledgment

The presented work was done in the laboratory of Pediatric Immunology at the Department of Biomedicine of University of Basel under the supervision of Prof. Georg A. Holländer. First I would like to thank Georg for giving me the opportunity to work in his lab on this interesting and demanding project, for his patience, constructive criticism and continuous support till the end of my thesis.

Also, I would like to thank Prof. Antonius G. Rolink and Prof. Giulio Spagnoli for taking time to read and evaluate my thesis.

I would further like to thank to all past and present lab members for creating an excellent working atmosphere, for their great support and many funny memories. A special thanks goes to Thomas Barthlott for scientific and practical advices and technical assistance in TEC sorting and to Katrin Hafen, for her assistance and teaching how to handle mice correctly.

Last but not least I would like to thank my family and Patrick for all their patience and support.

9. Appendix

9.1. Figures

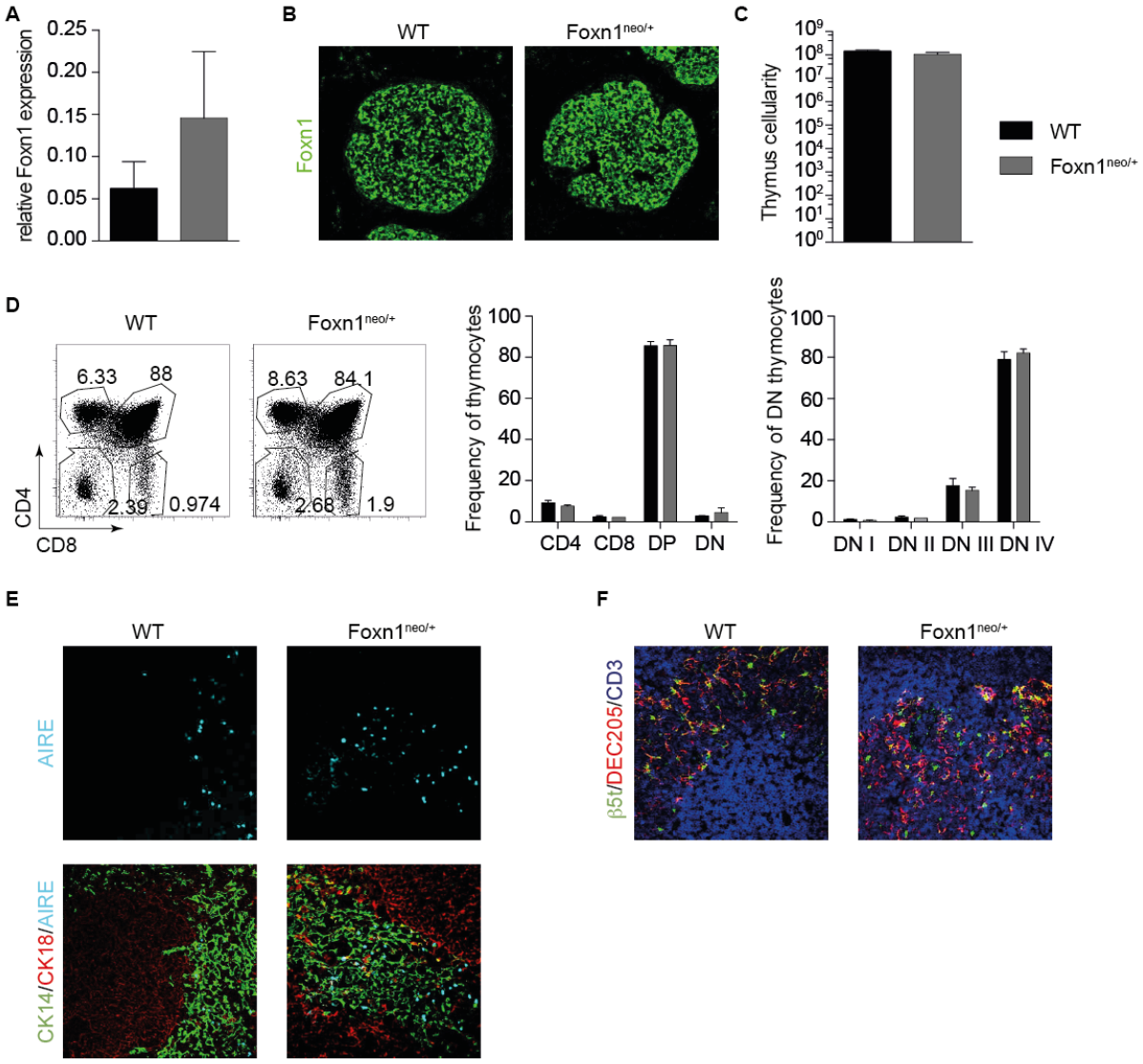

Appendix I: Foxn1$^{neo/+}$ mice did not show any thymus phenotype. (A) Relative Foxn1 expression in TEC isolated from 4 week old wild type (WT) mice. (B) Foxn1$^{neo/+}$ and Foxn1 protein expression on E12.5 thymus section. (C) Thymus cellularity at six week of age. (D) T-cell development in six week old wild type and Foxn1$^{neo/+}$ thymus. (E) Confocal microscopy on thymic sections stained for the medullary marker CK14 (green), the cortical marker CK18 (red) and Aire expression (blue). (F) Confocal microscopy on thymic sections stained for β5t (green), Dec205 (red) and CD3 (blue). n=3 p values were determined using Mann-Whitney test.

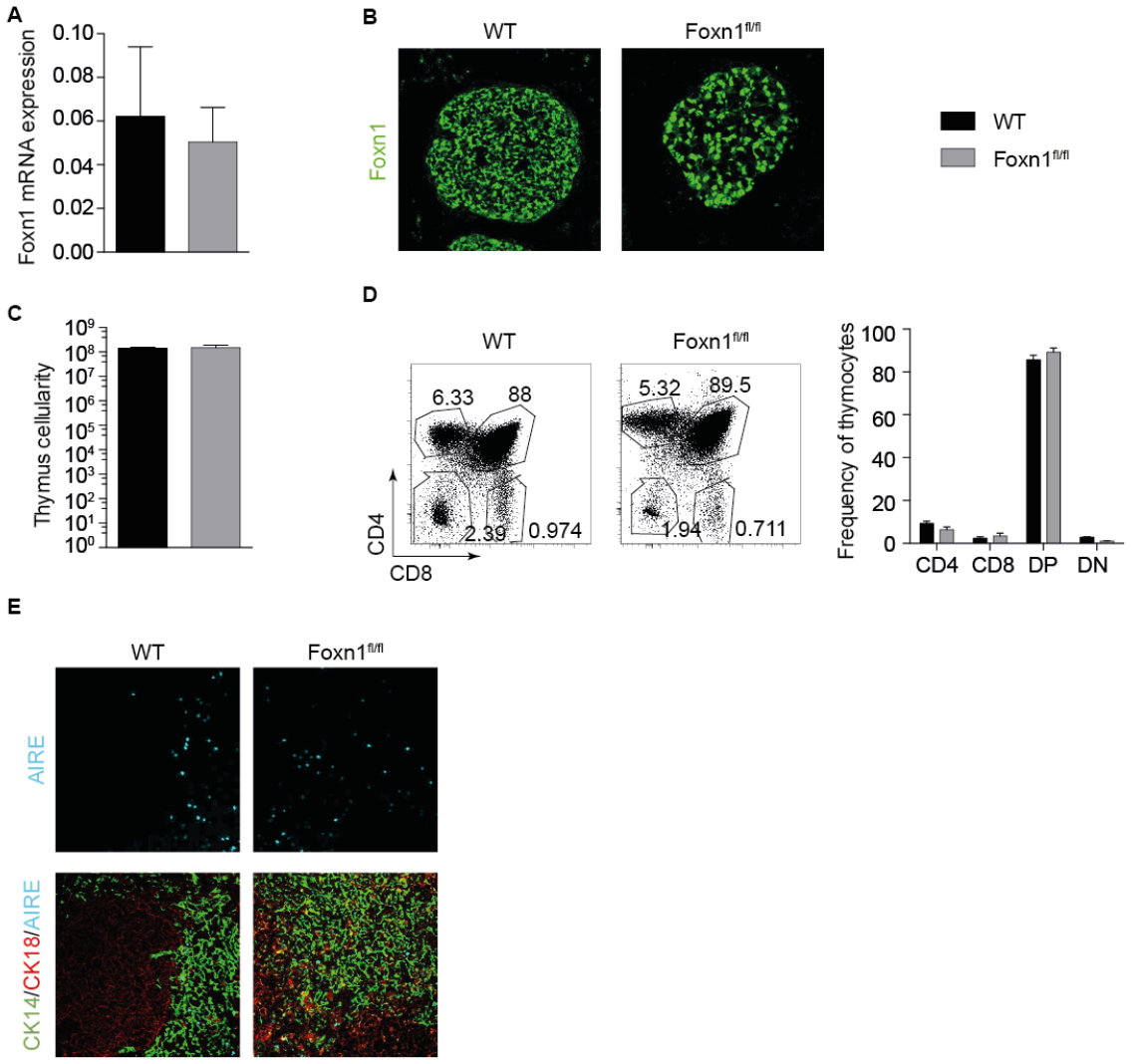

Appendix II: Foxn1$^{fl/fl}$ mice did not show any thymus phenotype. (A) Relative Foxn1 expression in TEC isolated from 4 week old wild type (WT) and Foxn1$^{fl/fl}$ mice (B) Foxn1 protein expression on E12.5 thymus section. (C) Thymus cellularity at six week of age. (D) T-cell development in six week old wild type and Foxn1$^{fl/fl}$ thymus. (E) Confocal microscopy on thymic sections stained for the medullary marker CK14 (green), the cortical marker CK18 (red) and Aire expression (blue) n=3 p values were determined using Mann-Whitney test.

9.2. Statement of my work

I designed, conducted and analysed all the experiments, except the generation of Foxn1$^{neo/neo}$ mice, which was done by Marcel Keller and Thomas Boulay.

9.3. Posters

The role of Foxn1 expression in thymus organogenesis and maintenance

Angela Bosch, Thomas Barthlott, Saulius Zuklys and Georg A. Holländer
Pediatric Immunology, Department of Biomedicine, University of Base and Basel University Children's Hospital, Basel, Switzerland

Background

The transcription factor Foxn1 is essential for thymic epithelial cells (TEC) differentiation since its functional loss constitutes the molecular cause of the nude phenotype characterised by athymia and alopecia. How thymic Foxn1 expression (as opposed to the skin) controls the maintenance of an established and functional thymic microenvironment remains so far unknown, not least because Foxn1 target genes that define the nude phenotype have not yet been identified.
The aim of the project is to define the requirements of Foxn1 expression for regular organogenesis and TEC maintenance.

Methods

Two different mouse models have been generated to test the role of Foxn1 expression for thymus organogenesis. (i) **Foxn1$^{lox/lox}$::Foxn1-Cre mic**e: The DNA binding domain of Foxn1 is deleted once the thymus anlage has normally formed (embryonic day 12.5 [E12.5]). (ii) **Foxn1$^{neo/neo}$ mice**: The introduction of the neo gene into the Foxn1 locus results in a hypomorphic locus.

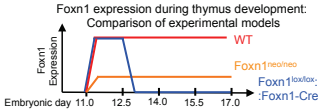

Results

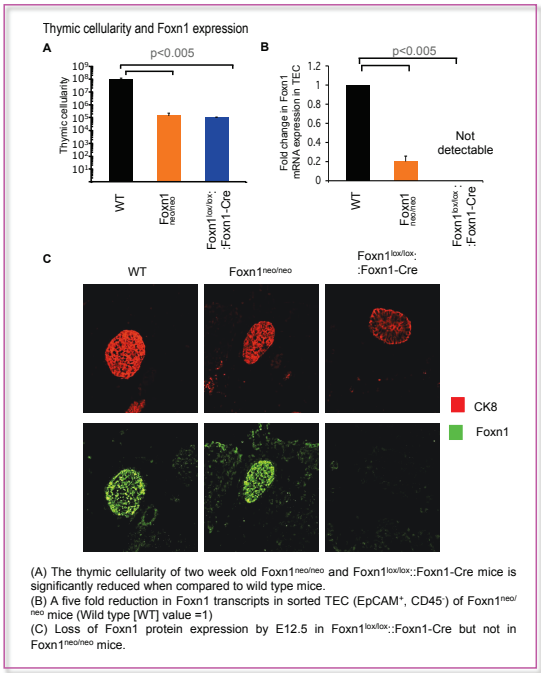

(A) The thymic cellularity of two week old Foxn1$^{neo/neo}$ and Foxn1$^{lox/lox}$::Foxn1-Cre mice is significantly reduced when compared to wild type mice.
(B) A five fold reduction in Foxn1 transcripts in sorted TEC (EpCAM$^+$, CD45$^-$) of Foxn1$^{neo/neo}$ mice (Wild type [WT] value =1)
(C) Loss of Foxn1 protein expression by E12.5 in Foxn1$^{lox/lox}$::Foxn1-Cre but not in Foxn1$^{neo/neo}$ mice.

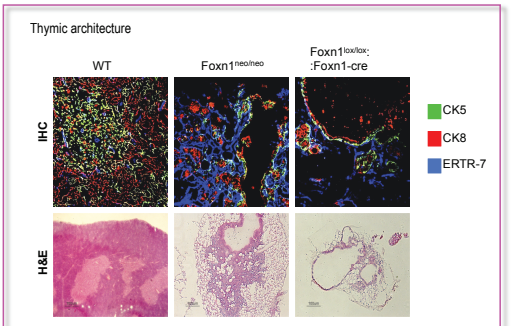

Severely disturbed stromal architecture with a significantly increased frequency of fibroblasts and the formation of cysts.

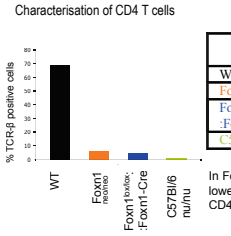

	MFI TCR	MFI CD4
WT	1985	6046
Foxn1$^{neo/neo}$	1461	3243
Foxn1$^{lox/lox}$: :Foxn1-Cre	706	3705
C57Bl/6 nu/nu	730	3752

In Foxn1 mutant mice, peripheral T cells express lower cell surface concentrations of TCR and CD4.

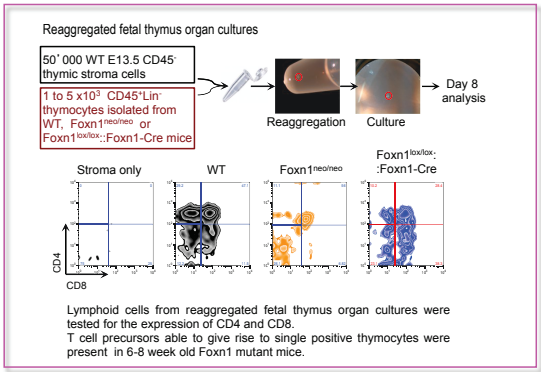

Lymphoid cells from reaggregated fetal thymus organ cultures were tested for the expression of CD4 and CD8.
T cell precursors able to give rise to single positive thymocytes were present in 6-8 week old Foxn1 mutant mice.

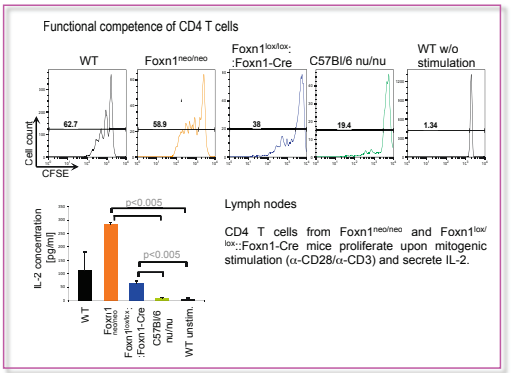

Lymph nodes

CD4 T cells from Foxn1$^{neo/neo}$ and Foxn1$^{lox/lox}$::Foxn1-Cre mice proliferate upon mitogenic stimulation (α-CD28/α-CD3) and secrete IL-2.

Conclusion

TEC differentiation and maintenance are dependent on the sustained presence of Foxn1 expression at adequate cellular concentrations as neither the loss of expression after embryonic day 12.5 nor a largely reduced expression of Foxn1 allow regular thymus architecture and thymopoietic support to occur. However, continued precursor homing to the postnatal thymus and minimal T cell differentiation can occur independent of the continued presence of Foxn1 once development proceeded normally to the E12.5 developmental stage. These results underscore the importance of continuous and sufficient Foxn1 expression for TEC development and maintenance.

Presented at the EUThyme-Rolduc Meeting 2011, 21-24 May 2011, Noordwijkerhout Netherlands

The role of Foxn1 expression in thymus organogenesis and maintenance

Angela Bosch, Thomas Barthlott, Saulius Zuklys and Georg A. Holländer
Pediatric Immunology, Department of Biomedicine, University of Basel and Basel University Children's Hospital, Basel, Switzerland

Universitäts-Kinderspital beider Basel

Background

The transcription factor Foxn1 is essential for thymic epithelial cells (TEC) differentiation since its functional loss constitutes the molecular cause of the nude phenotype characterised by athymia and alopecia. How thymic Foxn1 expression (as opposed to the skin) controls the maintenance of an established and functional thymic microenvironment remains so far unknown, not least because Foxn1 target genes that define the nude phenotype have not yet been identified.
The aim of the project is to define the requirements of Foxn1 expression for regular organogenesis and TEC maintenance.

Methods

Two different mouse models have been generated to test the role of Foxn1 expression for thymus organogenesis. (i) **Foxn1$^{lox/lox}$::Foxn1-Cre mice**: The DNA binding domain of Foxn1 is deleted once the thymus anlage has normally formed (embryonic day 12.5 [E12.5]). (ii) **Foxn1$^{neo/neo}$ mice**: The introduction of the neo gene into the Foxn1 locus results in a hypomorphic locus.

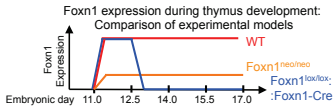

Results

Thymic cellularity and Foxn1 expression

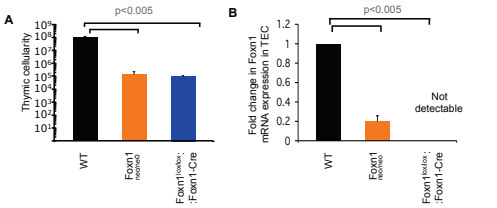

(A) The thymic cellularity of two week old Foxn1$^{neo/neo}$ and Foxn1$^{lox/lox}$::Foxn1-Cre mice is significantly reduced when compared to wild type mice.
(B) A five fold reduction in Foxn1 transcripts in sorted TEC (EpCAM$^+$, CD45$^-$) of Foxn1$^{neo/neo}$ mice (Wild type [WT] value =1)
(C) Loss of Foxn1 protein expression by E12.5 in Foxn1$^{lox/lox}$::Foxn1-Cre but not in Foxn1$^{neo/neo}$ mice.

Thymic architecture

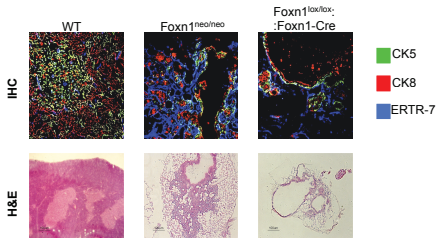

Severely disturbed stromal architecture with a significantly increased frequency of fibroblasts and the formation of cysts.

Functional competence of CD4 T cells

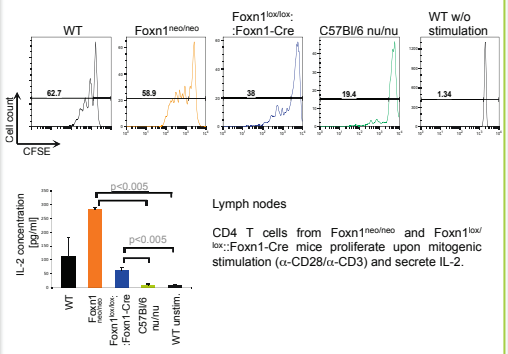

Lymph nodes

CD4 T cells from Foxn1$^{neo/neo}$ and Foxn1$^{lox/lox}$::Foxn1-Cre mice proliferate upon mitogenic stimulation (α-CD28/α-CD3) and secrete IL-2.

Characterisation of CD4 T cells

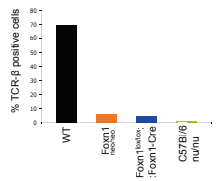

	MFI TCR	MFI CD4
WT	1985	6046
Foxn1$^{neo/neo}$	1461	3243
Foxn1$^{lox/lox}$:Foxn1-Cre	706	3705
C57Bl/6 nu/nu	730	3752

In Foxn1 mutant mice, peripheral T cells express lower cell surface concentrations of TCR and CD4.

Presence of regulatory T cells

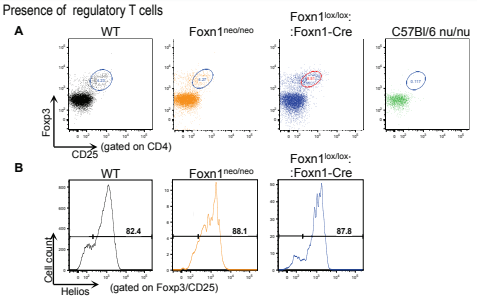

Foxp3$^+$ regulatory T cells could be identified in CD4 T cells of lymph nodes of Foxn1$^{neo/neo}$ and Foxn1$^{lox/lox}$::Foxn1-Cre mice (A). The majority of these regulatory T cells are thymus derived as they express the transcription factor Helios (B).

Reaggregated fetal thymus organ cultures

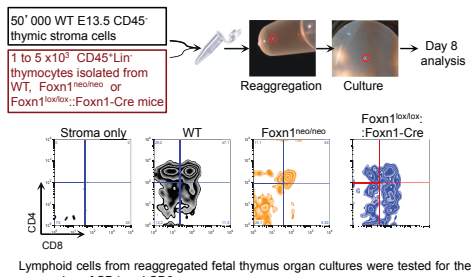

Lymphoid cells from reaggregated fetal thymus organ cultures were tested for the expression of CD4 and CD8.
T cell precursors able to give rise to single positive thymocytes were present in 6-8 week old Foxn1 mutant mice.

Conclusion

TEC differentiation and maintenance are dependent on the sustained presence of Foxn1 expression at adequate cellular concentrations as neither the loss of expression after embryonic day 12.5 nor a largely reduced expression of Foxn1 allow regular thymus architecture and thymopoietic support to occur. However, continued precursor homing to the postnatal thymus and minimal T cell differentiation can occur independent of the continued presence of Foxn1 once development proceeded normally to the E12.5 developmental stage. These results underscore the importance of continuous and sufficient Foxn1 expression for TEC development and maintenance.

Presented at the research Day of the Children's University Hospital Basel 2011, 25 August 2011, Basel, Switzerland

The role of Foxn1 expression in thymus organogenesis and maintenance

Angela Bosch, Thomas Barthlott, Saulius Zuklys and Georg A. Holländer
Pediatric Immunology, Department of Biomedicine, University of Basel and Basel University Children's Hospital, Basel, Switzerland

Background

The transcription factor Foxn1 is essential for thymic epithelial cells (TEC) differentiation since its functional loss constitutes the molecular cause of the nude phenotype characterised by athymia and alopecia. How thymic Foxn1 expression (as opposed to the skin) controls the maintenance of an established and functional thymic microenvironment remains so far unknown, not least because Foxn1 target genes that define the nude phenotype have not yet been identified.
The aim of the project is to define the requirements of Foxn1 expression for regular organogenesis and TEC maintenance.

Methods

Two different mouse models have been generated to test the role of Foxn1 expression for thymus organogenesis. (i) **Foxn1$^{lox/lox}$::Foxn1-Cre mice**: The DNA binding domain of Foxn1 is deleted once the thymus anlage has normally formed (embryonic day 12.5 [E12.5]). (ii) **Foxn1$^{neo/neo}$ mice**: The introduction of the neo gene into the Foxn1 locus results in a hypomorphic locus.

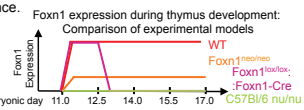

Results

Thymic cellularity and Foxn1 expression

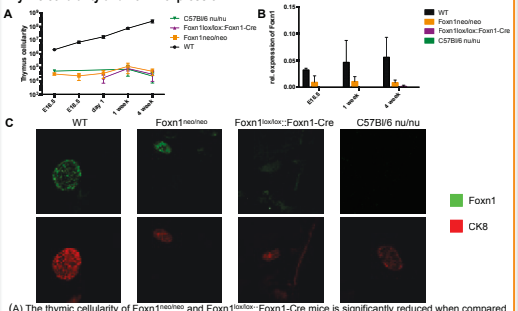

(A) The thymic cellularity of Foxn1$^{neo/neo}$ and Foxn1$^{lox/lox}$::Foxn1-Cre mice is significantly reduced when compared to wild type mice.
(B) Quantification of Foxn1 transcripts in sorted TEC (EpCAM$^+$, CD45$^-$) isolated of wild type and Foxn1 mutant mice.
(C) Loss of Foxn1 protein expression by E12.5 in Foxn1$^{lox/lox}$::Foxn1-Cre but not in Foxn1$^{neo/neo}$ mice.

Thymic architecture and T cell development in adult Thymus of Foxn1 mutant mouse strains

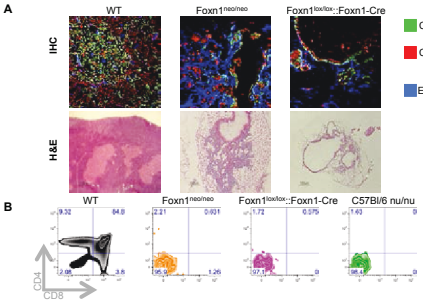

(A) Severely disturbed stromal architecture with a significantly increased frequency of fibroblasts and the formation of cysts.
(B) Thymocyte development in Foxn1 mutant mouse strains compared to wild type.

Both engineered Foxn1 mutant mouse strains display increased peripheral T cell numbers compared to congenital C57Bl/6 nu/nu mice

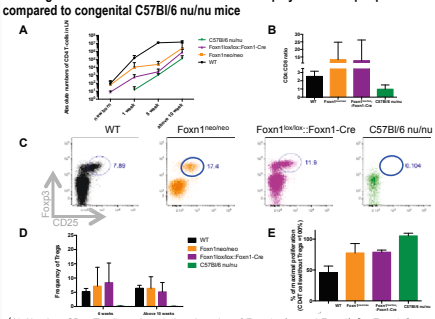

(A) Absolute CD4$^+$ T cell numbers in lymph nodes of Foxn1$^{neo/neo}$ and Foxn1$^{lox/lox}$::Foxn1-Cre compared to wild type and C57Bl/6 nu/nu mice at different time points.
(B) The CD4/CD8 ratio in Foxn1$^{neo/neo}$ and Foxn1$^{lox/lox}$::Foxn1-Cre mice is significantly higher than in C57Bl/6 nu/nu mice.
(C) Regulatory T cells (Tregs) are detectable in the lymph nodes of Foxn1$^{neo/neo}$ and Foxn1$^{lox/lox}$::Foxn1-Cre mice whereas they are absent in C57Bl/6 nu/nu mice.
(D) The frequency of regulatory T-cells in Foxn1$^{neo/neo}$ and Foxn1$^{lox/lox}$::Foxn1-Cre mice is comparable to wild type mice.
(E) Reduced suppressive capacities in Tregs isolated from Foxn1$^{neo/neo}$ and Foxn1$^{lox/lox}$::Foxn1-Cre mice

Colitis is the prominent cause of death in Foxn1$^{neo/neo}$ and Foxn1$^{lox/lox}$::Foxn1-Cre mice

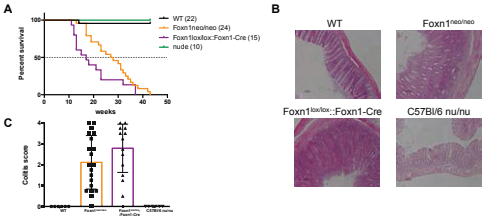

(A) The life-span of Foxn1$^{neo/neo}$ and Foxn1$^{lox/lox}$::Foxn1-Cre mice is reduced when compared to wild type or congenital nude control mice .
(B) Colons isolated from Foxn1$^{neo/neo}$ and Foxn1$^{lox/lox}$::Foxn1-Cre mice show hyperplasia and goblet cell depletion, which were not observed in aged matched wild type or C57Bl/6 nu/nu control mice.
(C) Colitis scores in wild type and Foxn1 mutant mice.

Infiltrating CD4 T cells display a Th1 effector response

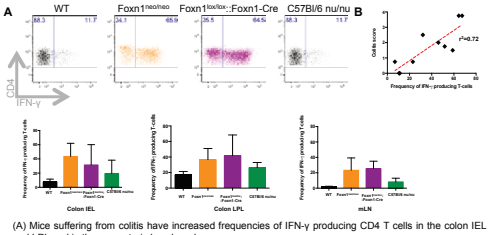

(A) Mice suffering from colitis have increased frequencies of IFN-γ producing CD4 T cells in the colon IEL and LPL and in the mesenteric lymph nodes
(B) Correlation between colitis score and frequency IFN-γ producing CD4 T cells

Colitis correlates with the presence of CD4 T cells in the colon of affected mice

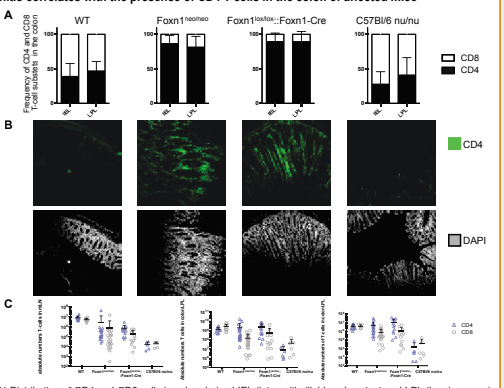

(A) Distribution of CD4 and CD8 cells in colon derived IEL (intraepithelial lymphocytes) and LPL (Lamina propria lymphocytes) αβ- T cells.
(B) Infiltrating CD4 T cells are detected in the colons of Foxn1$^{neo/neo}$ and Foxn1$^{lox/lox}$::Foxn1-Cre mice
(C) Absolute numbers of T-cells in colon IEL, LPL and mesenteric lymph nodes.

Conclusion

TEC differentiation and maintenance are dependent on the sustained presence of Foxn1 expression at adequate cellular concentrations as neither the loss of expression after embryonic day 12.5 nor a largely reduced expression of Foxn1 allow regular thymus architecture and thymopoietic support to occur. Inadequate expression of Foxn1 expression results in a genration of a T cell repertoire that reveals its autoreactivity over time by causing severe colitis.

Preseted at the annual Meeting of the Swiss Society for Paediatrics (Schweizerische Gesellschaft für Pädiatrie) 2013, 21 June 2012, Lucerne, Switzerland

The role of Foxn1 in thymus organogenesis and maintenance

Angela Bosch, Thomas Barthlott, Saulius Zuklys and Georg A. Holländer
Pediatric Immunology, Department of Biomedicine, University of Basel and Basel University Children's Hospital, Basel, Switzerland

Background

The transcription factor Foxn1 is essential for thymic epithelial cell (TEC) differentiation since its functional loss constitutes the molecular cause of the nude phenotype characterised by athymia and alopecia. How thymic Foxn1 expression (as opposed to the skin) controls the maintenance of an established and functional thymic microenvironement remains so far unkown, not least because Foxn1 target genes that define the nude phenotype have not yet been identified.

The aim of this project is to define the requirements of Foxn1 expression for regular organogenesis and TEC maintenance.

Methods

Two different mouse models have been generated to test the role of Foxn1 expression for thymus organogenesis. (i) Foxn1$^{fl/fl}$::Foxn1-Cre mice:The DNA binding domain of Foxn1 is deleted once the thymus anlage has normally formed (embryonic day 12.5 [E12.5]). (ii) Foxn1$^{neo/neo}$ mice: The introduction of the neomycine cassette into the Foxn1 locus results in a hypomorphic locus.

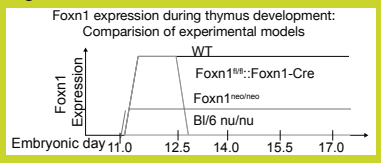

Results

Thymic cellualrity and Foxn1 expression

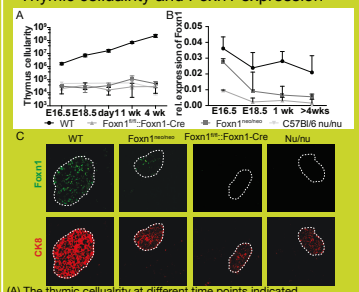

(A) The thymic cellualrity at different time points indicated
(B) Quantification of Foxn1 transcripts in sorted TEC (EpCAM$^+$, CD45$^-$)
(C) Loss of Foxn1 protein expression by E12.5 in Foxn1$^{fl/fl}$::Foxn1-Cre but not in Foxn1$^{neo/neo}$ mice.

Thymic archiecture and T-cell development

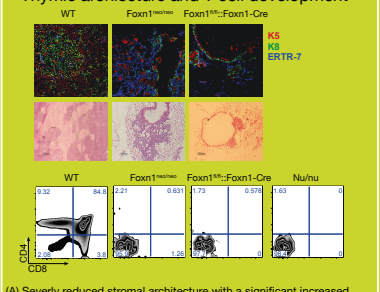

(A) Severly reduced stromal architecture with a significant increased frequency of fibroblasts and the formation of cysts
(B) Thymocyte development in Foxn1 mutant mouse strains compared to wild type mice

T-cell numbers and regulatory T-cells

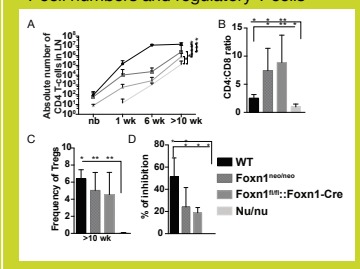

(A) Absolute CD4$^+$ T cell numbers in lymph nodes at different time points
(B) CD4/CD8 ratio at 6 weeks of age
(C) Frequency of regulatory T-cells in lymph nodes
(D) Suppressive capacities of Tregs

Colitis is the prominent cause of death in Foxn1$^{neo/neo}$ and Foxn1$^{fl/fl}$::Foxn1-Cre mice

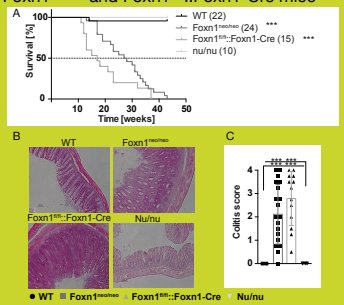

(A) Survival curve of wild type and Foxn1 mutant mice
(B) Colons isolated from wild type and Foxn1 mutant mice
(C) Colitis score in wild type and Foxn1 mutant mice

Colitis correlates with presence of CD4 T cells

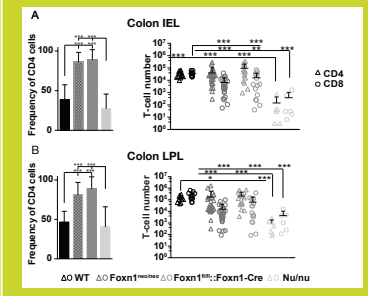

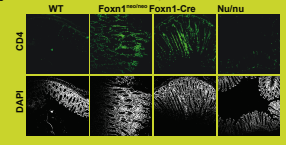

(A) Frequency and absolute numbers of CD4 cells in colon IEL (intraepithelial lymphocytes)
(B) Frequency and absolute numbers of CD4 cells in colon LPL (lamina propria lymphocytes)
(C) Infiltrating CD4 T cells are detected in the colons of Foxn1$^{neo/neo}$ and Foxn1$^{fl/fl}$::Foxn1-Cre mice

Infiltrating CD4 cells display a Th1 effector response

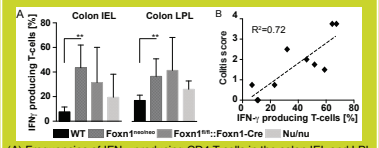

(A) Frequencies of IFN-γ producing CD4 T cells in the colon IEL and LPL and in the mesenteric lymph nodes
(B) Correlation between colitis score and frequency of IFN-γ producing CD4 cells.

Conclusion

TEC differentiation and maintenance are dependent on the sustained presence of Foxn1 expression at adequate cellular concentrations as neither the loss of Foxn1 expression after embryonic day 12.5 nor a largely reduced expression of Foxn1 allow regular thymus architecture and thymopoietic support to occur. Inadequate expression of Foxn1 results in a generation of a T-cell repertoire that reveals its autoreactivity over time by causing severe colitis.

Presented at the annual Meeting of the Swiss Society for Paediatrics (Schweizerische Gesellschaft für Pädiatrie) 2013, 21 June 2013, Geneva Switzerland

9.4. Curriculum Vitae

Personal information

Name	Angela Bosch
Address	Hohenrainring 28, 4133 Pratteln
Phone	+41 61 823 02 00
E-Mail	angela.bosch@unibas.ch
Birth date/-place	23. June 1981, Bern, Switzerland
Citizenship	Swiss
Marital status	Single
Work Address	Pediatric Immunology Center for biomedicine University of Basel Mattenstrasse 28 4058 Basel
Phone	+41 61 695 30 77

Education and Professional Experience

2009-2014	University of Basel and University Childern's Hospital (UKBB), Department of Biomedicien, Basel, Switzerland PhD student in Biomedical Research Research project: The role of the transcription Foxn1 in thymus organogenesis and maintenance In the group of Prof. Georg A. Holländer
2008-2009	University of Basel and University Childern's Hospital (UKBB), Department of Biomedicien, Basel, Switzerland Master of Science in Molecular Biology, Major Immunology Thesis title: "Functional analysis of regulatory T-cell subpopulations" In the group of Prof. Georg A. Holländer
2007-2008	University of Basel Bachelor of Science in Biology, Major in Molecular Biology
2003-2007	University of Basel, Faculty of Natural Sciences, Nanoscience
2000-2002	Gymnasium Muttenz (BL), Matura Type C, Switzerland
1997-2000	Diplom Mittel Schule 3, Muttenz (BL) Switzerland
1993-1997	Secondary School Frenkendorf (BL) Switzerland
1988-1993	Primary School Gerlafingen (SO) and Füllinsdorf (BL) Switzerland

Skills

Technical: Permit to work with animals (LTK Module 1E corresponding to FELASA Cat. B), *in vivo* work, flow cytometry, immunohistochemistry, confocal microscopy, qPCR, single cell PCR, ELISA, cell culture work

IT: MS Office programs (Word, Excell, Powerprint)
Adobe Programs (Illustrator, Photoshop)
Flow jo
Prism
Image J

Languages: German (Mother tongue)
English (fluent, written and orally)
French (good)
Spanish (basic knowledge)

Attendance at conferences

- Third Basel Immunology Focus Symposium (BIFS III), Basel, Switzerland, 29-31 August 2013, Attendance
- Research Day of the Children's University Hospital Basel 2013, 26 September 2013, Basel Switzerland, Poster presentation
- Annual Meeting of the Swiss Society for Paediatrics (Schweizerische Gesellschaft für Pädiatrie) 2013, 21 June 2013, Geneva Switzerland, Poster presentation
- Annual Meeting of the Swiss Society for Paediatrics (Schweizerische Gesellschaft für Pädiatrie) 2013, 21 June 2012, Lucerne, Switzerland, Poster presentation
- Wolfsberg-Immunology-Student Meeting, 2-4 April 2012, Oral presentation
- Research Day of the Children's University Hospital Basel 2011, 25 August 2011, Basel, Switzerland, Poster presentation
- Wolfsberg-Immunology-Student Meeting March, 30 March – 1 April 2011, Oral presentation
- EUThyme-Rolduc Meeting 2011, 21-24 May 2011, Noordwijkerhout Netherlands, Poster presentation
- Research Day of the Children's University Hospital Basel 2011, 25 August 2011, Basel Switzerland, Poster presentation
- Second Basel Immunology Focus Symposium (BIFS II), Basel, Switzerland, September 2009, Attendance